

**T-AM-Sy1** RESOLVING THE ENERGETICS OF COOPERATIVE SITE-SPECIFIC PROTEIN-DNA INTERACTIONS AND THEIR ROLE IN GENETIC REGULATION OF THE BACTERIOPHAGE LAMBDA. G. K. Ackers and M. A. Shea  
Dept. of Biology, The Johns Hopkins University, Baltimore, Maryland 21218

Cooperative, site-specific binding of proteins to DNA plays an important role in genetic regulation; to investigate the underlying physical processes, methods are required which directly analyze the protein-DNA interactions. The technique of DNase protection mapping (footprinting) has previously been used to locate specific protein-DNA binding sites and to determine simple binding constants. We have developed an analysis which extends the technique to make possible the quantitative study of cooperative binding at neighboring DNA sites by assessing the fractional saturation of each site at a series of protein concentrations. Thus we can resolve the free energies of cooperative interaction between DNA-bound proteins in addition to the intrinsic protein-DNA binding constants. These energies can be used along with kinetic and structural factors to predict genomic regulation in particular systems. We have applied these methods to the analysis of interactions at the right operator of the bacteriophage lambda, and have developed a model based on statistical thermodynamic assumptions for the processes which are known (Ptashne *et al.*, Cell (1980) 19:1-11) to control the switchover from the lysogenic to lytic state. The analysis includes the regulatory binding interactions of three proteins: cI repressor, cro, and RNA polymerase, and the degradative action of recA on cI repressor. From independently determined constants, the model predicts known physiological characteristics of the system for both wild-type and mutant phages, including (a) maintenance of the lysogenic state through synthesis of cI repressor and repression of cro, and (b) induction of lysis by turning on the cro gene and shutting off the cI gene.

**T-AM-Sy2** THE MOLECULAR BASIS OF DNA-PROTEIN RECOGNITION SUGGESTED BY THE STRUCTURE OF CRO REPRESSOR PROTEIN. B.W. Matthews\*, D.H. Ohlendorf\*, W.F. Anderson†, R.G. Fisher\* and Y. Takeda† (Introduced by P.H. von Hippel). \*Institute of Molecular Biology, U. of Oregon, Eugene, OR 97403; †MRC Group on Protein Structure and Function, U. of Alberta, Edmonton, Alberta T6G 2A7, Canada; ‡Chemistry Department, U. of Maryland, Baltimore County, MD 21228.

The recent determination of the structure of cro repressor protein from phage λ ("Cro") suggests that the protein binds to its sequence-specific sites on the DNA with a pair of two-fold-related α-helices of the protein located within successive major grooves of right-handed B-form DNA (W.F. Anderson *et al.*, Nature 290, 754-758 (1981)).

From a series of amino acid sequence and gene sequence comparisons, it appears that a number of other DNA-binding proteins have an α-helical DNA-binding region similar to that seen in Cro. In addition, it has also been found that the conformations of part of the presumed DNA-binding regions of CAP activator and Cro repressor proteins are strikingly similar.

The accuracy of the Cro structure determination has been improved by extension of the resolution to 2.2 Å, by molecular averaging and phase extension, and by partial refinement to a crystallographic residual of 27%. Model-building, based on this partially-refined structure, has been used to explore the apparent specific interactions between Cro repressor and its different DNA operators. These studies are consistent with the idea that the specificity of DNA-protein recognition is generated, in large part, by a network of hydrogen bonds between side chains of the protein and the parts of the DNA-base-pairs which are exposed in the grooves (in particular, the major groove) of the DNA.

**T-AM-Sy3** CONTROL OF TRANSCRIPTION INITIATION IN ESCHERICHIA COLI.

William R. McClure, Dept. Biological Sciences, Carnegie-Mellon University, Pittsburgh, PA 15213.

The initiation of RNA synthesis is an important control point in gene expression. Experiments performed *in vitro* with E. coli RNA polymerase have enabled us to identify the rate limiting steps in the initiation reaction. These experiments employ both biochemical and physical techniques for probing the RNA polymerase-promoter interaction. The *in vitro* characterization of several mutant and wild-type promoters has shown a good correlation with *in vivo* RNA chain initiation frequency. In addition, the effect of gene activators and repressors on initiation frequency has revealed several novel features of transcriptional control in E. coli. Recent *in vitro* results on the control of the λ<sub>PR</sub>, λ<sub>PRM</sub> and the E. coli lac operons will be discussed and compared with other mechanistic studies.

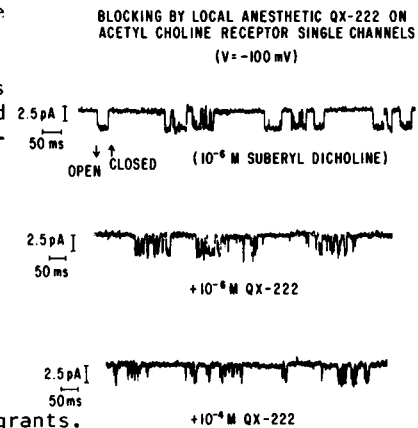
## T-AM-Sy4 AUTOREGULATION OF GENE EXPRESSION: THE T4-CODED GENE 32 PROTEIN SYSTEM.

Peter H. von Hippel\*, Stephen C. Kowalczykowski\*, Nils Lonberg\*, John W. Newport\*, Leland S. Paul\*, Gary D. Stormo\* and Larry Gold\*. \*University of Oregon, Eugene, OR 97403 and +University of Colorado, Boulder, CO 80309.

Bacteriophage T4-coded gene 32 protein is required in stoichiometric amounts to facilitate T4 DNA replication, recombination and repair. This protein binds cooperatively, and with relatively little base sequence specificity, to single-stranded nucleic acid lattices; furthermore it binds with a greater overall affinity to DNA than to RNA. During T4 infection gene 32 protein autoregulates its own synthesis (and thus its free intracellular concentration) by binding preferentially and reversibly to its own mRNA as a translational repressor. The thermodynamic parameters controlling the binding of gene 32 protein to DNA and RNA of varying base composition and sequence have been determined and extrapolated to physiological conditions. These parameters are applied to the T4 system to establish a set of coupled equilibria that describe the distribution of the protein over the various potential intracellular nucleic acid binding sites as a function of free gene 32 protein concentration. On this basis we can describe quantitatively the operation of this autoregulatory system, and predict certain features of the gene 32 mRNA binding site responsible for specific repression. These predictions are compared with the known base sequences and calculated secondary structures of T4 mRNAs. General principles involved in the development of effective binding specificity with intrinsically nonspecific cooperatively binding proteins will be described, and possible molecular mechanisms will be considered. [Supported in part by NIH and NSF research grants].

**T-AM-Min1** STUDIES ON THE PROPERTIES OF THE PURIFIED ACETYLCHOLINE RECEPTOR RECONSTITUTED IN PLANAR LIPID BILAYERS. P. Labarca\*, J. Lindstrom\* and M. Montal\*#, Depts. of Physics\* and Biology#, University of California, San Diego, and Salk Institute\*, La Jolla, CA.

The electrical properties of the purified acetylcholine receptor (AChR) from the electric organ of *Torpedo californica* reconstituted in planar lipid bilayers were studied. Membranes containing AChR display a conductance which depends on agonist concentration. This conductance is inhibited by micromolar concentrations of curare or hexamethonium. Analysis of the fluctuations in membrane conductance due to the opening and closing of single AChR channels shows that the lifetime of the open state ( $\tau_0$ ) depends on the agonist used, following the sequence  $\tau_0$  Suberyldicholine  $>$   $\tau_0$  Acetylcholine  $>$   $\tau_0$  Carbachol.  $\tau_0$  is also a function of the applied voltage, doubling each 80mV of membrane "depolarization". Channel fluctuations occur in "bursts" represented by the sudden appearance of channel activity, followed by quiescent periods. Burst duration depends on the agonist used, being longest in the presence of suberyldicholine. The open state of the AChR channel is blocked by the local anesthetic QX-222, as illustrated in the figure. Thus, the agonist-regulated ion channel of the purified AChR displays the pharmacological specificity expected of this receptor in native membranes. ONR & MDA grants.



**T-AM-Min2** INCORPORATION OF ION CHANNELS FROM BIOLOGICAL MEMBRANES INTO PLANAR LIPID BILAYER MEMBRANES. Ramon Latorre, Cecilia Vergara and Roberto Coronado\*, Department of Physiology & Biophysics, Harvard Medical School, Boston, MA 02115.

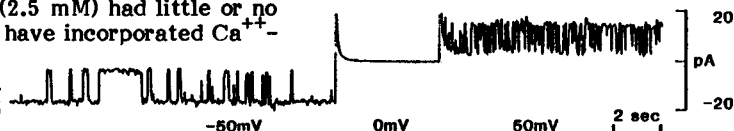
Recently in our laboratory we have been able to study in planar lipid bilayer membranes a  $\text{Ca}^{++}$ -dependent  $\text{K}^+$  channel. The channel has a conductance of 230 pS, is activated by micromolar amounts of  $\text{Ca}^{++}$ , and it appears to be present in transverse tubule membrane vesicles from rabbit skeletal muscle. Furthermore, the channel is sensitive to tetraethylammonium ions and is highly selective to  $\text{K}^+$ , showing a permeability ratio  $P_{\text{K}}/P_{\text{Na}} \approx 7$ . This  $\text{Ca}^{++}$ -dependent channel resembles those recorded with the patch clamp technique by Pallota et al. (*Nature* 293:471, 1981) in rat muscle cell culture. In skeletal muscle fibers, however, the evidence for  $\text{Ca}^{++}$ -dependent  $\text{K}^+$  conductances is only circumstantial. It is possible, therefore, that the method of channel incorporation described here may be useful to reveal and characterize conductance systems that are difficult to study by conventional electrophysiological techniques.

Using a similar incorporation approach, we have been successful in recording channels from a cardiac sarcolemma membrane fraction. Several types of channels were found, most notably one that is potassium selective and one that is chloride selective. Both channels are voltage dependent. These channels await further pharmacological and electrical characterization that will enable us to identify them with conductances found in cardiac muscle.

Supported by NIH grant GM-25277.

**T-AM-Min3** INCORPORATION OF  $\text{Ca}^{++}$ -ACTIVATED  $\text{K}^+$ -CHANNELS, FROM RAT BRAIN, INTO PLANAR LIPID BILAYERS. Bruce K. Krueger, Robert J. French, Marc B. Blaustein\*, and Jennings F. Worley, III\*. Departments of Physiology and Biophysics, Univ. of Maryland School of Medicine, Baltimore, Maryland 21201.

We have observed unitary steps in membrane conductance after exposure of planar bilayers (PE:DPG,4:1) to a suspension of membrane vesicles from rat brain (Krueger et al., *J. Membrane Biol.* 50:287, 1979) in the presence of  $\text{Ca}^{++}$ . Up to 5 discrete levels (integral multiples of the unit step) of conductance have been seen. These steps apparently correspond to opening and closing of single,  $\text{K}^+$ -selective channels incorporated into the bilayers. In symmetric solutions of 100 mM KCl, 0.1 mM  $\text{CaCl}_2$ , pH 7, the unit conductance was 200-260 pS, but was reduced by half when half of the KCl was replaced by NaCl. In asymmetric solutions, the reversal potential for single-channel currents approximated the  $\text{K}^+$ -equilibrium potential. Free  $\text{Ca}^{++}$  on the cis side (side of vesicle addition) was required for the conductance fluctuations: conductance steps ceased when EGTA was added to the cis side. Subsequent addition of  $\text{Ca}^{++}$ , but not of  $\text{Mg}^{++}$ , to the cis side restored the fluctuations; removal of  $\text{Ca}^{++}$  from the trans side had no effect. Fluctuation rates were also modulated by voltage (see figure).  $\text{Cs}^+$  (2-10 mM) blocks the channels only from the trans side with positive voltages (trans minus cis) enhancing the block. Tetrabutylammonium, quinine, and phenylethylamine (.1-1 mM) reduced or abolished the fluctuations while 3,4 diaminopyridine (2.5 mM) had little or no effect. These observations suggest that we have incorporated  $\text{Ca}^{++}$ - and voltage-dependent  $\text{K}^+$ -channels from rat brain into the planar bilayers. Supported by NIH grants NS 16285 and NS 16775 and the Alfred P. Sloan Foundation.



**T-AM-Min4 FUNCTIONAL RECONSTITUTION OF A PURIFIED MAMMALIAN SODIUM CHANNEL INTO LIPID VESICLES.**

J.B. Weigele &amp; R.L. Barchi, University of Pennsylvania, Philadelphia, PA.

The saxitoxin binding component (SBC) of the voltage-dependent sodium channel was purified from rat sarcolemma as previously reported (Barchi et al., PNAS 77, 1306-1310). The purified protein was reconstituted into unilamellar phospholipid vesicles composed of egg PC using detergent/lipid supplementation followed by detergent removal with Bio-beads SM2. 20-60% of  $^3\text{H}$ -STX binding sites were typically recovered in the vesicles and displayed STX binding parameters comparable to those of the native membrane. Thermal stability of toxin binding was enhanced by reconstitution.

The rate of  $^{22}\text{Na}$  influx into vesicles containing the reconstituted SBC could be specifically augmented 100% or more at the earliest time point (10 sec) by  $5\mu\text{M}$  batrachotoxin (BTX). This stimulated influx could be blocked by STX or TTX to an extent which may relate to the fraction of SBC incorporated with STX binding sites oriented outward. Toxin stimulated  $^{22}\text{Na}$  influx was complete in <15 sec at  $36^\circ\text{C}$ . Stimulated  $^{22}\text{Na}$  influx increased hyperbolically with concentration of BTX, with an apparent  $K_{0.5}$  between 0.5 and  $2\mu\text{M}$ . BTX was a more effective agonist than veratridine. Neither veratridine nor BTX altered  $^{22}\text{Na}$  influx into PC vesicles formed in the absence of the SBC protein. Freeze-fracture EM and Sepharose column analysis of the reconstituted vesicles revealed a bimodal size population, with 60% large vesicles  $>1000\text{\AA}$  and the remainder averaging  $\sim 330\text{\AA}$  dia. Following reconstitution, labelled SBC was found in the same ratio to PC in both populations of vesicles. Freeze-fracture EM of reconstituted vesicles revealed intramembranous particles of  $\sim 100\text{\AA}$  not present in vesicles formed in the absence of SBC. The purified SBC represents a functional sodium channel which retains its ability to control Na flux in response to pharmacological activation and block.

**T-AM-Min5 LATERAL MOBILITY AND DISTRIBUTION OF SODIUM CHANNELS IN FROG SKELETAL MUSCLE SARCOLEMMMA. W. Stühmer, P.R. Stanfield and W. Almers. Dept. of Physiology and Biophysics, Univ. of Washington, Seattle, Wash., U.S.A.**

Sodium ( $I_{\text{Na}}$ ) and potassium ( $I_{\text{K}}$ ) currents were recorded from frog sartorius muscles (*Rana temporaria*,  $17^\circ\text{C}$ , Ringer's fluid) using fire-polished glass micropipettes to electrically isolate and voltage-clamp small ( $\sim 10\mu\text{m}$  diameter) patches of sarcolemma. Enzymatic pre-treatment was generally avoided. Two findings suggest that  $\text{Na}^+$ -channels cannot readily re-distribute themselves over the sarcolemma by lateral diffusion. (A) Recording  $I_{\text{Na}}$  and  $I_{\text{K}}$  at several places on the same fiber, we often find that both currents vary 2-5 fold in size over distances of 10-30  $\mu\text{m}$ . Collagenase pretreatment does not abolish this lateral variation.  $I_{\text{Na}}$  and  $I_{\text{K}}$  are not correlated, as spots may have large  $I_{\text{Na}}$  and small  $I_{\text{K}}$  and vice versa. Apparently the concentration of Na and K channels shows steep lateral gradients. (B) Using the pipette as a light guide,  $\text{Na}^+$ -channels in the patch beneath the pipette were irradiated and destroyed by locally applied ultraviolet light (UV, 302 nm). UV was directed through a quartz fiber into the back end of the pipette and emerged from the tip as a fairly well-defined beam. If Na channels could diffuse laterally, one would expect  $I_{\text{Na}}$  from the patch to recover with time, as fresh channels enter from neighboring areas. No recovery was seen during 1 hr post-flash observation. Our results set an upper limit of  $10^{-12}\text{ cm}^2/\text{s}$  for the lateral diffusion coefficient of sodium channels, 100 times less than for ACh receptors in rat myotubes, and 1000 times less than for rhodopsin, a membrane protein in retinal rods. We suggest that most Na channels are anchored in the sarcolemma. Supported by the MDA, USPHS #AM17803, and the Max Kade Foundation.

**T-AM-Min6 GATING CURRENTS AND POTASSIUM CHANNEL ACTIVATION**

M.M. White, F. Bezanilla, and R.E. Taylor, Dept. of Physiology, UCLA CA 90024; Laboratory of Biophysics, NINCDS, NIH, Bethesda, MD 20205.

Measurements of gating currents ( $I_{\text{g}}$ ) in squid giant axons have failed to detect any component of  $I_{\text{g}}$  with kinetics similar to those of  $\text{K}^+$  channel activation. This is not altogether surprising in view of the small amount of charge postulated to move and the slow time course of  $\text{K}^+$  channel activation at the temperatures normally used ( $6-8^\circ\text{C}$ ). We have succeeded in maintaining perfused axons for up to several hours at 20 to  $22^\circ\text{C}$ .  $I_{\text{g}}$  was measured from a holding potential of -60 mV (to inactivate some of the  $\text{Na}^+$  channel gating current) using the P/4 procedure in the absence of permeant ions and the presence of TTX.  $I_{\text{g}}$  associated with  $\text{Na}^+$  channel activation becomes very fast and an extra, slower, component of the charge movement is readily detected. Addition of dibucaine (0.2 mM) to the external solution decreased the fast component of  $I_{\text{g}}$  but not this extra component. The slow component has kinetics similar to those of  $\text{K}^+$  channel activation at the same temperature. The charge ( $Q_{\text{K}}$ ) vs. voltage curve of this extra component follows a sigmoid relation with a maximum value of  $450 \pm 100$  electronic charges/ $\mu\text{m}^2$ . The voltage dependence of  $Q_{\text{K}}$  is similar to that of  $g_{\text{K}}$ , the  $\text{K}^+$  conductance. Finally, this extra charge movement shows a Cole-Moore shift identical to that seen for  $\text{K}^+$  channel activation.  $\text{Na}^+$  channel inactivation, on the other hand, shows no detectable Cole-Moore shift under these conditions. These results strongly suggest that at least a large fraction of the extra component ( $Q_{\text{K}}$ ) represents  $\text{K}^+$  channel gating currents.

Supported by USPHS grant GM 30376 and a training grant 1-T32-NS 07101-03 to M.M.W.

**T-AM-A1** CHLORAMINE-T-CYTOCHROME *c*: CONFORMATIONAL, CONFIGURATIONAL AND MOLECULAR STATE.

Kathleen W. Kinnally, Swatantar Kumar, and Yash P. Myer, Inst. of Hemoproteins, SUNY at Albany, Albany, NY 12222, and Raj Gupta, Cancer Research Institute, Philadelphia, Pa.

The two structurally identical, but functionally distinct, forms of Chloramine-T (CT-) treated cytochromes *c*, F-III and F-II, with modification of methionine to methionine sulfoxide (*Fed. Proc.* (1979) 38, 639; *Biochem. Biophys. Res. Commun.* (1980) 94, 1106), have been further examined. The sedimentation coefficients of F-III and F-II are 0.98 and 1.09 S vs. 1.12 S of native protein. In native gels F-III and F-II exhibit electrophoretic mobility distinct from each other and from monomer or dimer cytochrome *c*. The PMR spectra of ferric F-III and F-II lack the up-field-shifted resonances of Met-80 protons and have partially normalized down-field-shifted resonances of pyrrol 2 and 4 methyl groups and of  $\beta$ -propionic acid protons. The spectrum of the ferrous form contains the up-field-shifted resonances of Met-80 protons, but they are shifted less than those of the native protein. In general, the normalization is greater, and resonances are broader for F-II than F-III. In certain instances, some splitting is observed. The Soret CD spectra of ferric and ferrous CT-cytochromes *c* are more like simple heme *c* systems than the native protein. Both F-III and F-II are reduced with ascorbate, but the kinetics is complex and reflects multiplicity of forms. The reduced forms bind CO and are oxidized with molecular oxygen. These findings confirm earlier conclusions that the ferric and ferrous CT-cytochrome *c* contain altered heme iron coordination and loosened heme crevice. These findings also show that the derivatives are monomeric, but have multiple interconverting conformational forms. (Supported by NIH grant #GM 24854 and NSF grant #PCM 22622)

**T-AM-A2** CYTOCHROME *c*: ASCORBATE REDUCTION AND PROTEIN STRUCTURES. Swatantar Kumar, Kathleen W. Kinnally & Yash P. Myer, Inst. of Hemoproteins, State Univ. of NY at Albany, Albany, NY.

Ascorbate reduction of horse heart cytochrome *c* follows a mechanism involving a binding step with steady state stability constant,  $K_{ss}$  of  $5.9 \text{ M}^{-1}$ , followed by reduction,  $k_3$  of  $2.9 \text{ s}^{-1}$  (Myer et al., *J. Biol. Chem.* (1980) 255, 9666). We have further investigated this reaction and have also studied the reaction of a chemically modified form containing alteration of methionines to methionine sulfoxides, Chloramine-T-cytochrome *c* fraction III (*Fed. Proc.* (1979) 38, 639). Temperature dependence shows the reduction step to have a zero or close to zero activation energy, and the protein-ascorbate complex, a  $\Delta H_{ss}^\circ$  of 8.7 Kcals and  $\Delta S_{ss}^\circ$  of 32.5 eu. Modified cytochrome *c* is reduced by ascorbate through a three-phase reduction profile: two ascorbate-dependent-saturating processes with kinetic parameter,  $k_3$ , of  $4.4 \text{ s}^{-1}$  and  $0.04 \text{ s}^{-1}$ , and stability constant,  $K_{ss}$ , of 10.6 and  $9.1 \text{ M}^{-1}$ , for the fast and middle steps, and a slow ascorbate-independent process with a reversion constant of  $0.003 \text{ s}^{-1}$ . The effect of lowering the temperature is to increase the proportion of the ascorbate-independently reduced form. The activation energies from the limiting second-order reduction constants are 8.5 and 4.6 Kcals, the corresponding value for the native protein being 9.1 Kcals. These findings show that the electron-transfer reaction of the cytochrome *c*-ascorbate system is a near-zero activation energy reaction, possibly non-adiabatic, and the overall reaction is entropy-controlled. The integrity of the Met-80-S-Fe linkage is not critical for ascorbate reduction; however, the modification of Met-80 to methionine sulfoxide results in multiple interconverting conformational forms, none like the native protein. (Supported by NSF grant #PCM 22622 and NIH grant #GM 24854.

**T-AM-A3** A REVERSIBLE HEMICHROME TYPE STRUCTURE OF HORSE METHEMOGLOBIN PRODUCED BY SLOW FREEZING. J. M. Rifkind and A. Levy, National Institute on Aging, Baltimore, MD 21224 and The Johns Hopkins University, Baltimore, MD 21218.

It has generally been assumed that hemichrome formation, which involves the coordination of the distal histidine with Fe(III) heme requires denaturation of the globin to bring the distal histidine closer to the iron. Hemichrome formation has, thus, been found to be only slowly reversible after reduction of the iron or completely irreversible. By Mössbauer and electron spin resonance techniques, we have found that slow freezing of methemoglobin produces a pair of low spin species with *g*-values in the region of that which we found for the imidazole hemoglobin complex. Furthermore, the rhombic and tetragonal splittings obtained from these *g*-values indicate that the sixth ligand is a nitrogen which presumably comes from the distal imidazole. These hemichrome type structures, unlike other reported hemichromes, are, however, readily reversible. Rapid freezing by direct immersion into liquid nitrogen minimizes the formation of these structures, with the extent of formation depending on the rate of cooling, above a temperature of  $\sim 200^\circ\text{K}$  where no further change takes place. These alterations during the freezing process, which depend on the temperature history of the sample, emphasize the need to exert caution in interpreting results of frozen solutions. At the same time the conversion of methemoglobin into a reversible hemichrome structure suggests that the ligand pocket can readily assume a configuration with the distal imidazole close to the Fe and that the distal histidine may actually play a greater role in determining the functioning of hemoglobin.

**T-AM-A4** PROTON NMR STUDIES OF ISONITRILE - HEMOGLOBIN COMPLEXES. Martha P. Mims and John S. Olson, Department of Biochemistry, Rice University and Chien Ho, Irina M. Russu, Thomas E. Cedel and Shigetoshi Miura, Department of Biological Sciences, Carnegie-Mellon University.

Steric interactions between bound ligand molecules and the valine E11 methyl groups of human hemoglobin have been examined directly by high resolution nmr techniques. The  $\gamma$  methyl proton resonances of this amino acid are shifted markedly upfield due to shielding by the induced  $\pi$ -electron currents of the porphyrin ring. For the CO complex of isolated hemoglobin subunits, the  $\gamma$  methyl resonances of  $\beta$  E11 valine are -6.82 and -6.61 ppm. relative to H<sub>2</sub>O, respectively. There is little change in the position of these peaks when either methyl or ethyl isocyanide is bound to the subunits. Significant downfield shifts occur, however, when propyl and butyl ligands are bound, indicating that these larger ligands disrupt the structure of the sixth coordination site. The nmr spectra of the isonitrile forms of hemoglobin also exhibit ring current shifted resonances due to the aliphatic protons of the ligand side chain. In order to resolve these ligand resonances, experiments were carried out with several per-deuterated compounds ( $D_5$ -ethyl,  $D_7$ -isopropyl and  $D_9$ -n-butyl isocyanides). The spectra for the deuterated versus non-deuterated ligand-hemoglobin complexes were compared and any peaks missing in the results for the deuterated samples were assigned to isonitrile protons. For example, the  $\beta$ -methyl proton resonances for ethyl isocyanide bound to  $\alpha$  and  $\beta$  subunits were found at -5.96 and -5.76 ppm., respectively. These results should allow us to construct a rough three-dimensional model of the positions of the bound ligand atoms and any movements of the valine residues which result from this binding. Supported by NIH Grants HL-16093(JSO) and HL-24525(CH), Robert A. Welch Foundation Grant C-612(JSO) and NSF Grant PCM-78-25818(CH).

**T-AM-A5** SPIN LATTICE RELAXATION IN HIGH-SPIN FERRIC HEMEPROTEIN FROZEN SOLUTIONS. R. Thorkildsen, F.G. Fiamingo and A.S. Brill, Dept. of Physics, U. of Virginia, Charlottesville, VA 22901.

The temperature dependence of the spin-lattice relaxation rate was investigated for several high-spin ferric hemeprotein frozen solutions. Development of a microcomputer-based data acquisition and experiment control system, which was interfaced to an existing pulsed microwave power EPR spectrometer, permitted precise determination of spin-lattice relaxation times,  $T_1$ , at many temperatures in the range 2.2° K to 4.0° K. Past experiments in this range show that these protein systems involve relaxation which occurs predominantly through the Orbach process, with a temperature dependence  $1/T_1 = A \exp(-2 D/kT)$  where  $D$  is the zero field splitting of the ground state sextuplet. However, in order to fit data from the experiments reported here, a distribution (taken to be gaussian) in  $D$  was required; e.g. for sperm whale myoglobin, pH 6.3,  $D = 11 \text{ cm}^{-1}$  and  $\sigma_D = 3.0 \text{ cm}^{-1}$ .

The values of  $D$  and  $\sigma_D$  arrived at in this work were used, in conjunction with previous determination of  $E/D$  (rhombic to tetragonal symmetry ratio),  $\sigma_E/D$ ,  $\eta$  (amount of excited state admixture into the ground state), and  $\sigma_\eta$ , arrived at through computer simulations of experimentally observed frozen solution spectra, to calculate the crystal field energy levels (molecular) and their distributions in the 4-level model. An expression for the influence of the normal modes of the heme group upon the lowest electronic states of the ferric ion is proposed, and gives a framework for understanding the relative magnitudes of the energy level fluctuations and their relationship to structural distributions in the ferric ion environment. Supported by the National Science Foundation.

**T-AM-A6** RESONANCE RAMAN INVESTIGATION OF CARBONMONOXIDE BONDING IN CARBONMONOXY HEMOGLOBIN AND MYOGLOBIN: DETECTION OF Fe-CO STRETCHING AND Fe-C-O BENDING VIBRATIONS AND INFLUENCE OF THE QUATERNARY STRUCTURE CHANGE. Nai-Terg Yu, M. Tsubaki and R. B. Srivastav School of Chemistry, Georgia Institute of Technology, Atlanta, GA 30332.

We report for the first time, the identification of the iron-carbon bond in carbon-monoxo hemoglobins (Hb) and myoglobin (Mb) by resonance Raman spectroscopy. The Fe-CO stretching, Fe-C-O bending and bound C-O stretching vibrations have been detected at 507 (512), 578 (577) and 1951 (1944  $\text{cm}^{-1}$ ), respectively, in carbon-monoxo human HbA (or sperm whale Mb) upon excitation at 406.7 nm within the Soret band. These assignments were made on the basis of frequency shifts with the isotopes  $^{13}\text{C}^{16}\text{O}$ ,  $^{12}\text{C}^{18}\text{O}$  and  $^{13}\text{C}^{18}\text{O}$ . Calculated isotope shifts according to the model  $\text{Im-Fe-C-O}$  (but not  $\text{Im-Fe-O-C}$ ) agree well with the observed data. The possible mechanisms of resonance Raman enhancement of these vibrations are discussed in terms of  $d_\pi(\text{Fe})-\pi^*(\text{CO})$  interaction.

Careful examination of the Fe-CO stretching mode at 507  $\text{cm}^{-1}$  in carbonmonoxo HbA and Hb Kansas both with and without inositol hexaphosphate (IHP) reveals no changes in either frequency nor intensity. This implies that no significant change in the Fe-C bond energy is induced by switching the quaternary structure from R- to T-form in ligated COHb Kansas. The absence of bond tension between the iron atom and the proximal imidazole is also suggested, as it has been demonstrated that the  $\nu(\text{Fe-CO})$  frequency is sensitive to a change from l-methylimidazole to l,2-dimethylimidazole (as fifth ligand) in model heme-CO complexes. However, resonance Raman spectrum of carbonmonoxo carp Hb exhibits a broadening of the Fe-CO stretching mode on the lower energy side upon R $\rightarrow$ T conversion with IHP, suggesting the presence of a new conformer (or conformers) with a lesser degree of distortion in CO bonding geometry (supported by NIH GM18894).

**T-AM-A7 RESONANCE RAMAN DETECTION OF STRUCTURAL DYNAMICS AT THE ACTIVE SITE IN HEMOGLOBIN.**

M. R. Ondrias, D. L. Rousseau, Bell Laboratories, Murray Hill, NJ 07974 and S. R. Simon, State University of New York at Stony Brook, Stony Brook, NY 11790

The low frequency ( $100\text{--}500\text{ cm}^{-1}$ ) resonance Raman spectra of various hemoglobins, isolated  $\alpha$  and  $\beta$  subunits, and model 2-methylimidazole heme complexes have been obtained at 77K. All hemoglobin species have nearly equivalent spectra under these conditions suggesting that quaternary structure dependent differences are not maintained at low temperature. The temperature dependence of the deoxyhemoglobin spectrum was examined over the range of 10–300K. Of particular interest is the behavior of the band assigned as the iron-histidine stretching mode. It displays a large change in frequency and width upon lowering the temperature from 300 to 10K. The temperature dependence of the data indicates the presence of dynamic processes. The dynamics of this mode in frozen hemoglobins can be qualitatively and quantitatively described as a vibrational dephasing via anharmonic coupling to other vibrations of the heme-imidazole system. The effects which occur at the melting transition in the low frequency modes cannot be quantitatively addressed at this point but may be indicative of the introduction of additional degrees of freedom predicated on protein influences that reflect differences in protein quaternary structure.

**T-AM-A8 RESONANCE RAMAN STUDIES ON CO AND O<sub>2</sub> BINDING TO ELEPHANT MYOGLOBIN.** Nai-Teng Yu and E.A. Kerr, School of Chemistry, Georgia Institute of Technology, Atlanta, Ga. 30332; D.E. Bartnicki, H. Mizukami and A.E. Romero-Herrera, Dept. of Biological Sciences and Dept. of Anatomy, Wayne State University, Detroit, MI. 48202.

Carbon monoxide and dioxygen were employed as resonance Raman-visible ligand for probing the nature of heme binding site in elephant myoglobin, which has a distal glutamine at E7 instead of the usual histidine. Distal His (E7) residue has been thought to be responsible for weakening the carbon monoxide binding to hemoproteins (detoxification of CO). It is of interest to see how the His (E7)  $\rightarrow$  Gln replacement affects such parameters as  $\nu(\text{Fe-CO})$ ,  $\delta(\text{Fe-C-O})$ ,  $\nu(\text{C-O})$  and  $\nu(\text{Fe-O}_2)$  vibrational frequencies and relative intensities.

Kinetic measurements indicated that elephant Mb has a CO affinity  $\sim 6$  times higher than that for human/sperm whale Mb. If this enhanced affinity were solely due to the removal of some of the steric hindrance that normally tilts the CO off the heme axis, one would have expected the  $\nu(\text{Fe-CO})$  frequency to decrease and the  $\nu(\text{C-O})$  frequency to increase relative to the corresponding values in sperm whale Mb. However, the opposite was found. This may imply that factors such as interaction between the amide oxygen of Gln E7 and the carbon of CO ligand, as well as a hydrogen bonding between the amide hydrogen and the oxygen of the ligand may be responsible for the enhanced CO binding in elephant myoglobin.

The  $\nu(\text{Fe-O}_2)$  stretching vibration in elephant oxymyoglobin consists of two resolved peaks at 561 and  $572\text{ cm}^{-1}$ , which may correspond to two different conformers. (Supported by grants from NIH GM 18894, NSF DEB 7619924 and PCM 7717644.

**T-AM-A9 REPRODUCIBILITY OF ELECTRON DIFFRACTION INTENSITY DATA OBTAINED FROM HYDRATED MICROCRYSTALS OF RAT HEMOGLOBIN,** William F. Tivol, Bun-Woo Bertram Chang\*, and Donald F. Parsons, Ultrastructure Analysis Section, Laboratory Medicine Institute, Division of Laboratories and Research, New York State Department of Health, Albany, New York 12201, U.S.A., and \*Research and Development Department, MRO Associates, Inc., Oil and Gas Exploration, 730 17th Street, Denver, CO 80202, U.S.A.

Analysis of electron diffraction patterns from rat hemoglobin taken at 200 kV on a wet stage yields intensity data to a resolution of 2–3 Å which are as reproducible as those from typical x-ray diffraction. Some crystals were so similar that the differences in measured intensities were insignificant ( $R = 0.056$ ), but in other cases real differences between crystals were observed ( $R = 0.33$ ). Dynamic scattering was insignificant under our diffraction conditions; however, exposures to electron doses as low as  $10^{-2}\text{ e}/\text{\AA}^2$  produced detectable changes in measured intensities. Limits to the reproducibility of the data are set by radiation damage and errors in microdensitometry.

**T-AM-A10** Thermodynamic Characterization of 2,3-Diphosphoglycerate Binding to Human Hemoglobin A<sub>0</sub>. Mitchell K. Hobish and Dennis A. Powers, Department of Biology, The Johns Hopkins University, Baltimore, MD 21218. The apparent association constants for the binding of 2,3-diphosphoglycerate (DPG) to human oxy- and deoxyhemoglobin A<sub>0</sub> as a function of pH were determined at three temperatures using rate equilibrium dialysis. The data were fitted to a thermodynamic model which allows the generation of continuous curves over the range pH 5.0-9.5. Contributions to the enhanced Bohr effect were determined at 21.5° and 30°C. At no pH was there more than one proton taken up during the binding of DPG to deoxyhemoglobin, although two were taken up during the binding of DPG to oxyhemoglobin. Thermodynamic parameters, calculated at 50 pH values, suggest two classes of amino acid residues that are involved in the binding of DPG to deoxyhemoglobin, and one class for oxyhemoglobin. The change in free energy between the binding of DPG to deoxy- and oxyhemoglobin is consistent with the hypothesis that the regulation of hemoglobin function is the result of the summation of numerous small energy changes, rather than a few large changes due to the breaking of specific salt bridges. (Supported by the National Science Foundation via grant number DEB 79-12216)

**T-AM-A11** INCREASE IN THE APPARENT COMPRESSIBILITY OF CYTOCHROME c UPON OXIDATION

James B. Matthew, Don Eden, Joseph J. Rosa, and Frederic M. Richards, Departments of Chemistry and Molecular Biophysics & Biochemistry, Yale University, New Haven, Connecticut 06511 U.S.A.

The apparent molal adiabatic compressibility of both ferri- and ferrocytochrome c have been determined from measurements of density and ultrasonic velocity. The values found were  $+2.99 \times 10^{-8}$  and  $-2.40 \times 10^{-8} \text{ cm}^5 \text{ mol}^{-1} \text{ dyne}^{-1}$  for the ferri and ferro forms respectively. Experiments were performed on identical solutions containing either the oxidized or reduced form of the protein. Solutions of ferricytochrome c were found to have significantly greater adiabatic compressibility than equivalent solutions of ferrocytochrome c at 25°C and pH 7.15. The remarkable similarity of the three-dimensional structures of the ferri and ferro protein (Takano, T. and Dickerson, R. E. [1980] PNAS 77, 6371-6375) strongly suggests that this difference in compressibility is due to an increase in volume fluctuations within ferricytochrome c relative to ferro rather than a change in equilibrium structure or hydration. Such a difference in the dynamic properties of the structures is consistent with both the crystallographic thermal B-factors and with the observed increase in amide hydrogen exchange kinetics when ferrocytochrome c is oxidized. The relative magnitude of the volume fluctuations is approximated from an ideal solution treatment of the compressibility data and yields a ratio of  $\delta V_{\text{rms}}(\text{ferri cyt c})/\delta V_{\text{rms}}(\text{ferro cyt c}) = 1.3$ . Examination of the electrostatic component of protein stability, using the solvent accessibility modified Tanford-Kirkwood model (Matthew, et al. [1981] Biochemistry 20, 571-580) predicts that the tertiary configuration of ferricytochrome c is destabilized by 1.5 kcal/mole with respect to ferrocytochrome c. This value agrees with the 30-fold change in mean rate of hydrogen exchange.

**T-AM-A12** KINETIC PROPERTIES OF THE INTERMEDIATES IN THE ASSEMBLY OF LUMBRICUS HEMOGLOBIN.

J. K. Schreiber and L. J. Parkhurst, Dept. of Chemistry, University of Nebraska, Lincoln, NE 68588.

The hemoglobin of Lumbricus terrestris has a molecular weight of three million. The twelve spherical subunits are organized as a dodecamer in a double hexagonal array, having  $D_{6h}$  symmetry. The subunits, or protomers, each contain 16 hemes. Previous work has shown that the liganded dodecamer dissociates rapidly to hexamers and then more slowly to protomers when the pH is suddenly increased to 10.3 from pH 7. A Hill number for O<sub>2</sub> binding greater than 5 has been reported for this hemoglobin, making it one of the most highly co-operative of all biological macromolecules. An important problem is the assessment of co-operativity in the hexamers and the protomers. These questions cannot be easily answered by making equilibrium measurements because of the transient nature of the intermediates. On the other hand, by carrying out tandem flow experiments, we can trap the hexamers and protomers at pH 7 and probe the ligand kinetics of these species. If, in the first flow experiment, the hemoglobin is rapidly brought to pH 10.3, dissociation occurs in two distinct phases. Analysis of the light-scattering curves gives the concentrations of the dodecamer, the hexamers, and the protomers as a function of time. A second rapid mixing restores the pH to 7 and gives a non-equilibrium, but known, distribution of the three species. The oxygen and CO ligation kinetics of these forms can be studied by laser photolysis. A co-operative assembly is indicated if the fraction of T-state varies with the fraction of photolysis and the functional dependence of this variation gives an indication of the T to R cross-over point in the aggregate. Measurements of O<sub>2</sub> release in the R-state and of overall oxygen release also permit assignments of co-operativity to be made for the 3 Hb forms. Grant support: NIH HL 15,284 and NSF PCM 8003655.



**T-AM-A13** THE INTERACTION OF DIFFERENT HEMOGLOBINS IN CONCENTRATED SOLUTIONS AND IN PRECIPITATES  
ANDREAS ROSENBERG, ROBERT HAIRE AND WILLIAM T TISEL UNIVERSITY OF MINNESOTA MINNEAPOLIS MN 55455

The participation of hemoglobin A and F in the fibres of deoxyhemoglobinS and more general questions of cocrystallization of different forms of hemoglobin has been the object of several recent studies. Experimental difficulties due to the high solubility of hemoglobins and the large corrections in form of activity coefficients have led to considerable ambiguity in interpretation of such data. We have developed a method where we control the solubility of all hemoglobins by presence of polyethyleneglycol (PEG). The solubilities of hemoglobins in such mixed solvent system can be so low that if we define our standard state for PEG water mixtures we can neglect activity coefficients. The resulting phase diagrams where we plot the solubility of different forms as a function of their molefraction in the solid state resemble vapour pressure functions for binary solvent mixtures. Data can be obtained over the whole range of mixtures. We find that all hemoglobins investigated HbA,S,A behave like isomers and participate extensively in mixed solid state. We can distinguish three types of phase diagrams. First mixtures of R forms such as oxyhemoglobin A and methemoglobin A show nearly ideal behavior for solid solution or isomorphous crystals T forms show sharp triple points Mixtures of R and T forms show very extensive incorporation of R form in the T lattice. Thus deoxy A and F molecules are incorporated into deoxyS fibres which retain their structure when studied by electronmicroscopy. Supported by HL 16833-08.

**T-AM-B1** LATERAL MOBILITY OF BAND 3 IN THE HUMAN ERYTHROCYTE MEMBRANE: CONTROL BY ANKYRIN-MEDIATED INTERACTIONS. D.E. Golan and W.R. Veatch. Dept. of Pharmacol., Harvard Medical School, Boston, MA 02115 and Dept. of Mol. Biophys. and Biochem., Yale Medical School, New Haven, CT 06520

Band 3, the major integral protein of the human erythrocyte membrane, was labeled with eosin-5-isothiocyanate and its lateral mobility examined using the fluorescence photobleaching recovery technique. Earlier work (Golan and Veatch (1980) PNAS 77:2537-41) was extended using an improved and recalibrated fluorescence photobleaching apparatus, with these results: 1) Even in the presence of protease inhibitors, low phosphate (14 mM NaPO<sub>4</sub>) and high temperature (37°C) led to 50-fold increases in diffusion coefficient (from 1 to 50 x 10<sup>-11</sup> cm<sup>2</sup>sec<sup>-1</sup>) and large increases in fractional mobility (from 10% to 80%) of band 3, compared to values at high phosphate (40 mM NaPO<sub>4</sub>) and low temperature (21°C). 2) Spectrin was not dissociated from the membrane under low phosphate, high temperature conditions. 3) All increases in fractional mobility and moderate increases in diffusion coefficient were not associated with specific proteolysis of any major membrane component. Extreme increases in diffusion coefficient were associated with the specific proteolysis (>70%) of ankyrin alone. 4) Addition of 320 mM KCl to 42 mM NaPO<sub>4</sub> at 37°C, conditions thought to destabilize specifically ankyrin-band 3 linkages, led to increases in both fractional mobility (90%) and diffusion coefficient (50 x 10<sup>-11</sup> cm<sup>2</sup>sec<sup>-1</sup>) of band 3. 5) Incubation of ghost membranes with a 72000 dalton proteolytic fragment of ankyrin which serves as the high-affinity spectrin attachment site on the membrane led to 2½-3-fold increases in both fractional mobility and diffusion coefficient of band 3. These data confirm that band 3 mobility is severely restricted by the proteins of the erythrocyte cytoskeleton under physiological conditions, and suggest that this restriction is mediated at least in part by the particular cytoskeletal protein ankyrin.

**T-AM-B2** REDUCTIVE METHYLATION OF TWO H<sub>2</sub>DIDS-BINDING LYSINE RESIDUES ON BAND 3, THE HUMAN ERYTHROCYTE ANION TRANSPORT PROTEIN. Michael L. Jennings. Department of Physiology and Biophysics, The University of Iowa, Iowa City, Iowa 52242.

Inorganic anion transport in human erythrocytes is catalyzed by band 3, the major transmembrane protein. The bifunctional inhibitor of anion transport, H<sub>2</sub>DIDS (4,4'-diisothiocyano-dihydrostilbene-2,2'-disulfonate), can react covalently with two lysine residues of band 3. One of these lysines (Lys α) is in the 60,000 dalton chymotryptic peptide; the other (Lys β) is in the complementary 38,000 dalton peptide (Jennings & Passow 1979, Biochim. Biophys. Acta 554:498). Both Lys α and Lys β can be modified irreversibly by reductive methylation of intact cells at 0° with formaldehyde and borohydride, under conditions where only outward facing lysines are modified. The methylated (probably dimethylated) Lys α and Lys β do not react covalently with H<sub>2</sub>DIDS, but the methylation does not lower the affinity of band 3 for the reversibly acting transport inhibitor DNDS (4,4'-dinitrostilbene-2,2'-disulfonate). Methylation of all copies of band 3 at both Lys α and Lys β inhibits <sup>36</sup>Cl-Cl exchange (150 mMCl) by about 75%. Since the methylation does not alter charge and introduces only a minor steric perturbation, the substantial inhibition suggests that Lys α or Lys β has an important role in anion binding or translocation. Preliminary data indicate that much of this inhibition results from methylation of Lys β. The reductive methylation may be used to label Lys β radioactively, with minimal labeling of other residues in the 38,000 dalton chymotryptic peptide. This labeling procedure should make it possible to localize Lys β in the band 3 primary structure.

Supported by USPHS Grant GM26861.

**T-AM-B3** IDENTIFICATION OF HEMOGLOBIN BINDING SITES ON THE INNER SURFACE OF THE ERYTHROCYTE MEMBRANE. P.B. Rauenbuehler\*, K.A. Cordes\* and J.M. Salhany. VA Medical Center and Cardiovascular Center and Dept. of Biomedical Chemistry UNMC Omaha, NE 68105. The hemoglobin (Hb) binding sites were identified by measuring the fraction of Hb released following selective proteolytic or lipolytic enzyme digestion. Binding stoichiometry to and fractional Hb release from inside-out-vesicle (IOV) preparations of human and rabbit erythrocyte membranes were also compared since rabbit membranes differ significantly from human only in that they lack glycophorin. We show that rabbit IOVs bind about 65% less human (or rabbit) Hb under conditions of optimal and stoichiometric binding. Neuraminidase treatment of human membranes did not effect Hb binding. Reconstitution studies with isolated glycophorin incorporated into phosphatidyl choline vesicles further suggests that Hb binds to glycophorin. Hb binding to band 3 protein was confirmed by demonstrating that about 30% of the Hb binding sites were sensitive to chymotrypsin digestion, an enzyme which cleaves the cytoplasmic portion of band 3 protein but not glycophorin. The involvement of phosphatidyl serine in Hb binding was demonstrated by comparing the fraction of Hb released upon digestion with phospholipase C from *B. cereus* versus *C. welchii*. The latter enzyme does not hydrolyze phosphatidyl serine. Approximately 37% of the total Hb binding capacity involved binding to phospholipid with about one-third of that fraction involving phosphatidyl serine. The present results show that the predominant interaction of Hb with the cytoplasmic surface of the erythrocyte membrane involves binding to integral membrane glycoproteins.

**T-AM-B4** SPECIFIC BINDING OF PROGESTERONE TO THE CELL SURFACE OF RANA OOCYTES AND ITS ROLE IN THE MEIOTIC DIVISIONS. Adele B. Kostellow, Steven P. Weinstein, and Gene A. Morrill. Dept. Physiology and Biophysics, Albert Einstein College of Medicine, New York, New York 10461

Progesterone is believed to act at the cell surface to induce the resumption of the meiotic divisions in amphibian oocytes. The large size of *Rana* oocytes (1.8 mm diameter) and the integrity of the vitelline envelope (a meshwork of fibers closely applied to the oocyte surface) make it possible to manually isolate the intact plasma-vitelline membrane complex. In the prophase oocyte, [<sup>3</sup>H]-ouabain uptake is primarily into the plasma-vitelline membrane complex. Ouabain binding is K<sup>+</sup>-dependent and has a K<sub>d</sub> (2.6 x 10<sup>-7</sup> M) and number of binding sites (1,800 per μm<sup>2</sup>) similar to muscle. Analysis of [<sup>14</sup>C]-progesterone uptake and exchange by the plasma-vitelline membrane complex of the isolated prophase oocyte indicates that uptake by the plasma membrane is saturable, specific, temperature-dependent, and has a slow off-rate. More than 90% of the [<sup>14</sup>C] recovered with the membrane complex co-migrated with progesterone on thin-layer chromatography. Estradiol (a non-inducer) did not compete with progesterone whereas testosterone (an inducer) blocked progesterone binding by the membrane complex. Both Hill and Scatchard type plots indicate cooperative binding with an apparent K<sub>d</sub> of 8 x 10<sup>-7</sup> M over the progesterone range (0.3-3 μM) required for induction. Cytoplasmic uptake was apparently non-specific and less temperature-dependent than membrane uptake. Steroid concentrations exceeded water solubility by 30-60 min. Nuclear uptake was saturable and specific but uptake was independent of temperature. Both plasma membrane binding and a physiological response (nuclear breakdown) showed positive cooperativity with only about 6% of the membrane sites being filled to initiate a 50% response. (Supported by HD-10463 & GM-7288)

**T-AM-B5** ADP INTERACTS WITH A LOW AFFINITY SITE ON THE (Na+K) ATPase. M.D. MONE AND J.H. KAPLAN, DEPT. OF PHYSIOLOGY G4, UNIV. OF PENNSYLVANIA, PHILADELPHIA, PA 19104

At physiological levels (mM) of ATP and Mg the addition of K ions to a Na medium containing (Na+K) ATPase enzyme causes a stimulation of Na-ATPase activity. However, at low (μM) levels of ATP the addition of K does not stimulate the activity and at ATP in the range 1-5 μM causes an inhibition of the ATPase activity. The inhibition is apparently due to the formation of an occluded E<sub>2</sub>(K) form of the enzyme from which K slowly dissociates, the rate of K release is stimulated by high (mM) ATP (Post et al J. Biol. Chem. 247:6530, 1972). We have used a purified preparation of (Na+K) ATPase from canine renal outer medulla and confirmed these findings. Furthermore we have shown that if ADP is present along with the low (μM) levels of ATP the addition of K ions always produces a stimulation of ATPase activity. This behaviour suggests that ADP can substitute for ATP at the low affinity substrate site and form an ADP.E<sub>2</sub>.K complex facilitating the release of occluded K. In circumstances where low levels of ATP (μM) and higher levels of ADP are present analysis becomes complex since ADP is also known to interact with the high affinity substrate site on E<sub>1</sub>, causing inhibition. These findings support previous observations on intrinsic fluorescence which showed that ADP stimulated the conversion of E<sub>2</sub>(K) to E<sub>1</sub> forms of the enzyme (Beaugé and Glynn, J. Physiol. 294:367, 1980) and predict that at suitable levels of Pi, ADP should support K:K exchange in resealed red cell ghosts in the absence of ATP. Supported by American Heart Grant in Aid 79787 and NIH HL 28457 to JHK.

**T-AM-B6** INTEGRAL MEMBRANE PARTICLES ARE REDISTRIBUTED INTO CON A CAPS. Holly Bennett and John Condeelis, Dept. of Anatomy, AECOM, Bronx, N.Y. 10461

We have used freeze-fracture electron microscopy to study changes in membrane architecture that occur during lectin induced capping. When vegetative amoebae of *Dictyostelium discoideum* are challenged in suspension with Concanavalin A (Con A) they form Con A caps on their cell surface. The rate at which capping occurs depends on the relative Con A and cell concentration but in all cases occurs within minutes after addition of lectin. Thin section electron microscopy demonstrates that the cap is composed of a discrete tuft of microvilli in one region of the cell cortex and that the cell extends a pseudopod from its surface opposite to that of the cap. These two structures, the microvillar tuft of the cap and the opposing pseudopod, are useful markers for determining the orientation of the cell in freeze-fracture. Cells were freeze-fractured before and after addition of Con A and the size, number, and distribution of integral membrane particles (IMPs) were studied. Although the number and size of IMPs in untreated and capped cells remained the same, the density of IMPs increased by over twofold in the cap as compared to that in the remainder of the cell membrane (P<0.001). This was not due to insertion of new IMPs into the membrane of capped cells since the total number of IMPs in untreated and capped cells remained constant. Hence, the redistribution of Con A into a cap on the cell surface is accompanied by a concomitant redistribution of IMPs into the cap.

Supported by GM25813.

**T-AM-B7** CONCAVALIN A-RECEPTOR REDISTRIBUTION DURING MITOSIS: DIFFUSION VS FLOW. D.E. Koppel, J.M. Oliver and R.D. Berlin; Depts. of Biochemistry and Physiology, Univ. of Connecticut Health Center, Farmington, CT 06032.

The surface distribution of Con A bound to cell membrane receptors varies dramatically as a function of mitotic phase (Berlin *et al.*, 1978. *Cell* 15:327-341). The distribution on cells labeled and observed between mid-prophase and early anaphase is diffuse. However, cells labeled in early anaphase and observed in late anaphase or telophase demonstrate a marked accumulation of Con A-receptor complexes over the developing cleavage furrow, overlying the microfilaments of the contractile ring. Using fluorescently labeled surface ligands, we have characterized the redistribution process on J774.2 macrophages with series of high resolution fluorescence scans with a focused laser beam. Results were analyzed in terms of two simple models: a flow model, in which complexes move unidirectionally at constant velocity; and a diffusion model, in which complexes undergo random lateral diffusion until sticking at the site of accumulation. The observed rate of redistribution of fluorescein labeled succinyl-Con A at 30°C was found to be consistent with either an effective flow velocity of about 1  $\mu\text{m}/\text{min}$  or an effective diffusion coefficient of about  $10^{-9} \text{ cm}^2/\text{sec}$ . However, the lectin-receptor diffusion coefficient measured directly by fluorescence redistribution after photobleaching on metaphase cells was only  $10^{-10} \text{ cm}^2/\text{sec}$ ; and photobleaching experiments during the actual period of accumulation showed that lectin-receptor movement during cleavage is unidirectional. These results rule out a diffusion mechanism, and indicate that ligand-receptor complexes move into the cleavage furrow by a process of oriented flow.

**T-AM-B8** DIFFUSIVE ENCOUNTERS OF RECEPTORS ON THE CELL SURFACE: PROBABILISTIC AND KINETIC CALCULATIONS M. Buas (Intr. by R. Ledley), Dept. of Physiology & Biophysics, Georgetown Univ., Wash. D.C. 20007

Numerous cellular processes are thought to be initiated by the interaction (and, in some cases, crosslinking) of mobile receptors on the cell surface. However, the precise nature of this interaction is not known. For example, in the case of crosslinking, it is not clear whether the crosslink serves to keep receptors together for some (necessary?) minimal amount of time, or whether the crosslink induces some conformational change in the receptors, or whether some other process is occurring. In the hope of throwing light on these matters, we present some simple theoretical calculations exploring the nature of diffusive encounters on the cell surface. We study the idealized situation in which two dimensional discs (receptors) are diffusing through an idealized two dimensional fluid (membrane) on the surface of a sphere, and we derive an expression for the number of receptor pairs,  $T(x)$ , that at any instant are within  $x \text{ \AA}$  of each other, where  $x$  is a small distance typical of chemical interaction (say  $x \approx 1 \text{ \AA}$ ). We derive this expression by two separate approaches. First, we follow a straightforward probabilistic approach which can be justified using either entropic or diffusion-equation calculations. Second, we derive an expression for  $T(x)$  by simple kinetic reasoning. In the kinetic calculation, we derive expressions for the two characteristic times which are relevant: the time between collisions, and the duration of a "close encounter" (i.e. the time during which two colliding receptors stay within  $x \text{ \AA}$  of each other). An apparent paradox arises in that the probabilistic and kinetic approaches appear to yield quite different results (differing by a factor  $\approx d/x$ , where  $d$  is the receptor diameter). And the resolution of this paradox leads to a better understanding of the nature of diffusive encounters in two dimensions. The results of these calculations can be used as an aid in evaluating various hypotheses about the receptor events leading to the initiation of a transmembrane signal; e.g., we can calculate how  $T(x)$ , and close encounter times, change as a result of crosslinking. Examples will be given.

**T-AM-B9** THE CRYSTAL STRUCTURE OF ALAMETHICIN. Robert O. Fox and Frederic M. Richards. Department of Molecular Biophysics and Biochemistry. Yale University, New Haven, Connecticut 06511

Alamethicin is a 20 residue linear peptide antibiotic which partitions into membranes and forms voltage-gated ion channels. Single alamethicin channels appear to be formed by the aggregation of 8 to 10 molecules and to fluctuate among a number of conductance states during a current burst. Crystals of alamethicin which diffract to  $1.0 \text{ \AA}$  resolution were grown from a methanol acetonitrile solvent system. The crystals are of space group  $P2_1$ , and contain three independent molecules per asymmetric unit. The crystal structure was solved by single isomorphous replacement using anomalous scattering to break the phase ambiguity. The molecular model has been refined at  $1.5 \text{ \AA}$  resolution using the geometry restrained least-squares algorithm of Konnert and Hendrickson, resulting in a crystallographic residual of 16% while maintaining covalent bond distances to within  $0.04 \text{ \AA}$  of ideal values on average. The three independent alamethicin molecules are each in a predominantly  $\alpha$ -helical conformation, although they differ in the number and position of several 4-1 hydrogen bonds characteristic of  $3_{10}$  helices. Each  $\alpha$ -helix is bent to a different extent at the Pro-14 residue, leaving two backbone carbonyl oxygen atoms without hydrogen bonds and exposed to solvent. The solvent accessible polar groups of each molecule lie on a narrow strip parallel to the helix axis on the convex side of the helix, resulting in a highly amphipathic molecular surface. A set of possible molecular models of the alamethicin ion conducting channel were constructed from a composite of the molecular conformations seen in the crystal. The channel models are symmetric n-fold funnel-shaped oligomers of 8 to 12 monomers, which exhibit highly complementary helix surface contacts and a polar interior region. A hydrogen bonded annulus of Gln-7 side chains provides the greatest restriction of the channel model interior.

**T-AM-B10** INTERACTIONS OF MEMBRANE ENZYMES (ATPase and AChE) WITH INHIBITORS AND ACTIVATORS. H.D. Brown, Y. Das, and S.K. Chattopadhyay. NJAES-Rutgers University. New Brunswick, New Jersey 08903.

Acetylcholinesterase (AChE) and adenosine triphosphatase (ATPase) reactions and other interactions have been evaluated thermodynamically and kinetically using the reaction (conduction-type) microcalorimeter. Enzyme preparations graded from colloidal sized ghost fragments to purified protein isolates and incomplete chains. Progress curves were deconvoluted by cross correlation to obtain thermodynamic values and equilibrium kinetic parameters. For the AChE reaction with acetylcholine, synthetic substrates (nitrophenyl acetate, acetylthiocholine, propionylcholine, butyrylcholine), inhibitors, and alkylators the events measured were: (a) Complex formation <positioning at anionic subsite, charge relay contribution, approach to esteratic subsite, conformational changes>; (b) Acylation <breaking ester linkage, protonation and departure of leaving group>; (c) Deacylation <addition of hydroxyl, departure of hydrolytic product and restoration of enzyme native state>. A similar series of measurements have been made for the 'transport' ATPase with particular reference to the contributions of activating metal ions. Supported by N.I.H. G.M. 22679 and N.J. Hatch 40102.

**T-AM-B11** REVERSIBLE LOSS OF COOPERATIVE  $\text{Ca}^{2+}$  BINDING BY SR VESICLES. S. Highsmith, Department of Biochemistry and Laboratory of Physiology and Biophysics, U. of the Pacific, San Francisco, CA, 94115.

Intrinsic tryptophan emission, at 335 nm from sarcoplasmic reticulum (SR) vesicles irradiated at 295 nm was used to detect  $\text{Ca}^{2+}$  binding to the Ca-ATPase. At 25°C and pH 7.0, suspensions of SR (1-2  $\mu\text{M}$  protein) in 150 mM MOPS, 50 mM KCl, 5 mM  $\text{MgCl}_2$  and either 1 mM EGTA or 25  $\mu\text{M}$  added  $\text{CaCl}_2$  were incubated for 1 hour and then titrated with  $\text{CaCl}_2$  or EGTA, respectively. The relative fluorescence as a function of free  $\text{Ca}^{2+}$  concentration was determined for each case.

When  $\text{Ca}^{2+}$ -incubated SR was titrated with EGTA, the  $\text{Ca}^{2+}$  dependency of the fluorescence change indicated positive cooperative binding with an apparent Hill coefficient (n) of 1.7 and a transition midpoint of  $-\text{pCa}^{2+}(\text{free}) = 6.7$ . In contrast, when EGTA-incubated SR was titrated with  $\text{Ca}^{2+}$ , no cooperativity of  $\text{Ca}^{2+}$  binding was observed (n = 0.8) and the affinity decreased ( $-\text{pCa}^{2+}(\text{free}) = 5.6$  at the transition midpoint). When the EGTA-incubated SR solution was adjusted to 25  $\mu\text{M}$  free  $\text{Ca}^{2+}$  and then titrated with EGTA, cooperative  $\text{Ca}^{2+}$  binding was reestablished, indicating the EGTA-induced loss of the cooperative binding is reversible under these conditions. The Ca-ATPase activity and  $\text{Ca}^{2+}$  uptake per ATP was not changed significantly by the incubation procedures.

Support: NIH Grant AM25177, NSF Grant CDP-7923045 and an NIH Research Career Development Award.

**T-AM-B12** KINETIC RESONANCE RAMAN SPECTROSCOPY OF CAROTENOIDS: A SENSITIVE KINETIC MONITOR OF BACTERIORHODOPSIN MEDIATED MEMBRANE POTENTIAL CHANGES. A. Lewis, John H. Johnson and G. Gogel, Department of Applied Physics and Section of Biochemistry, Molecular and Cell Biology, Cornell University, Ithaca, New York 14853

A rapid (14-22  $\mu\text{s}$ ) light-induced, bacteriorhodopsin mediated membrane potential has been detected using the technique of kinetic resonance Raman spectroscopy and the model system of  $\beta$ -carotene incorporated into reconstituted vesicles containing bacteriorhodopsin. Our data demonstrate that the kinetic resonance Raman spectrum of  $\beta$ -carotene is an extremely sensitive monitor of kinetic alterations in membrane potential with micron spatial resolution in a highly scattering medium. In addition, our Raman results indicate that the potential sensitivity of  $\beta$ -carotene is an excited state property of the molecule, thus making it an electrochromic monitor of membrane potential. We feel the techniques illustrated in this paper have the advantage of being a native probe of kinetic membrane potential changes and will be applicable to a wide variety of biological systems without the perturbing side-effects which often accompany the use of non-biological, potential-sensitive dyes.

**T-AM-C1** INTRACELLULAR pH CHANGES IN INTERNALLY PERFUSED SNAIL NEURONS. Lou Byerly and W. J. Moody. Dept. of Biol. Sci., U.S.C., and Dept. of Physiology, U.C.L.A., Los Angeles, CA.

We have used a suction pipet method of internally perfusing isolated nerve cell bodies of the freshwater snail *Limnaea stagnalis*. The time course of the change of intracellular pH ( $pH_i$ ) following a step change of the pH of the internal perfusion solution was directly measured using a pH-sensitive microelectrode; the exchange of  $H^+$  was compared to that of  $K^+$  (as measured by K-sensitive electrodes). When the  $[K^+]$  of the internal solution was changed from 74 mM to 0 mM ( $Na^+$  substitution), cytoplasmic  $[K^+]$  fell to 1.0–2.3 mM. When the ratio of cell to suction pipet diameters was 3–4 (our usual value), 90% exchange of  $K^+$  required 1.5–3 min. Exchange of  $H^+$  was considerably slower. When we changed the pH of the internal solution from 7.35 (100 mM HEPES) to 6.35 (100 mM MES), the measured  $pH_i$  changed from  $7.29 \pm 0.04$  to  $6.39 \pm 0.03$  (mean  $\pm$  S.D.;  $n=6$ ). To bring  $pH_i$  within 0.1 unit of the internal solution pH (6.35) required  $10.9 \pm 2.6$  min. Thus the exchange of  $H^+$  was roughly 5 times slower than that of  $K^+$  for a given ratio of cell to suction pipet diameters, even using 100 mM buffer. At 20 mM buffer, the exchange was slower and the steady-state  $pH_i$  further from the pH of the internal solution.

We have begun to study the effects of  $pH_i$  changes on outward K currents measured in Na-free external saline containing 0.1 mM  $Cd^{+2}$ . Preliminary results indicate that a 1.5 unit decrease in  $pH_i$  (from the normal value of 7.35) enhances the magnitude and speeds the activation kinetics of the delayed outward K current, and causes a shift to more negative potentials of the steady-state inactivation curve of the fast-inactivating K current. Further experiments on these effects are in progress. Supported by U.S.P.H.S. NS15341 and an MDA fellowship to W.J.M.

**T-AM-C2** CALCIUM TAIL CURRENTS IN SNAIL NEURONS. Y. Tsuda, D.L. Wilson & A.M. Brown. Department of Physiology & Biophysics, University of Texas Medical Branch, Galveston, Texas 77550

Improvements of the suction pipette-microelectrode voltage clamp system made it possible to measure Ca tail currents in isolated *Helix* nerve cells within 200  $\mu$ sec of their onset. The voltage reached steady levels within 30  $\mu$ sec, and the fast transient capacitative current subsided within 70  $\mu$ sec. A small (8%) slower component of the capacitance had a tau of 1.1 msec.  $R_s$  measured with admittance methods was less than 13 k $\Omega$  giving  $IR_s$  drops of 3 mV or less after the initial fast transient. Ca currents were separated by suppression of Na and K currents and the non-specific outward current was not activated below +50 mV. The results for Ca and Ba currents obtained by substituting Ba for Ca were similar. Tail currents were abolished by Co substitution for Ca ion. The capacitative current transients were cancelled by addition of equal but opposite voltage clamp steps in Co solution. The Ca tail current was biexponential, the fast component having taus as short as 0.2 msec, the slow component having taus as short as 1.5 msec. The relative amplitudes of these two components were approximately 4:1. The taus were independent of prepulse potential but the amplitudes were not. The activation kinetics are therefore not the  $m^2$  type. The instantaneous I-V curve was S-shaped and neither ohmic nor constant field in nature.

(Supported by Grants NS11453 and HL25145)

**T-AM-C3** ACTIVATION OF Ca CHANNELS IN SNAIL NEURONS. D.L. Wilson, Y. Tsuda & A.M. Brown (Intr. by M.C. Andresen). Department of Physiology & Biophysics, University of Texas Medical Branch, Galveston, TX 77550

Activation of Ca currents was studied in isolated snail neurons by the suction pipette method of voltage clamp and internal perfusion. Ca currents were separated from Na, K and non-specific currents. Voltage clamp steps produced an inward Ca current that was preceded by a small outward transient current. When the voltage clamp step was terminated at the peak of the inward current, a large transient Ca tail current was observed. When the Ca channel blocker Cd was added (0.3 to 1.0 mM), the initial outward transient was reduced, inward Ca current was greatly reduced and an inward transient tail current remained that had identical kinetics to the Ca tail current. Ca currents of similar amplitudes in the absence of Cd has smaller amplitude tail currents. The initial outward transient was reduced by cooling from 23°C to 14°C. In Ca solutions turn-on of  $I_{Ca}$  was greatly slowed and the peak current was depressed at 14°C. The amplitude of the Ca tail current transients was reduced at 14°C but the closing rates were unchanged. Co substitution for Ca ion extracellularly completely abolished the outward and inward transients including those that persisted in Cd solutions. It appears that opening of Ca channels involves a temperature sensitive step whereas closing of open channels does not. The results also suggest that Cd blockage of Ca current is voltage dependent and that analysis of Ca asymmetry currents in Cd solution may be complicated. (Supported by Grants NS11453 and HL25145)

**T-AM-C4** INTRACELLULAR  $\text{Ca}^{2+}$  GRADIENT ASSOCIATED WITH  $\text{Ca}^{2+}$  CHANNEL ACTIVATION MEASURED IN A NERVE CELL BODY. S. Levy, D. Tillotson and A.L.F. Gorman. Dept. Physiology, Boston University School of Medicine, Boston MA 02118 and Marine Biological Laboratory, Woods Hole MA 02543

The changes of the absorbance signal during and following voltage dependent  $\text{Ca}^{2+}$  influx (with voltage clamp pulses) in cells injected with arsenazo III has been used as a measure of Ca buffering. Two parameters missing in this analysis are the absolute resting level of  $\text{Ca}^{2+}$  concentration and the spatial gradient of  $\text{Ca}^{2+}$  concentration following  $\text{Ca}^{2+}$  influx. A  $\text{Ca}^{2+}$  sensitive microelectrode was used to obtain this data. The electrode was silanized, the tip was beveled to an outside diameter of 2-4 microns and filled with  $\text{Ca}^{2+}$  neutral ion carrier ETH 1001 (Oehme et al, *Chimia*, 1976, 30, 204). These electrodes were capable of measuring changes in  $P_{\text{Ca}}$  of less than 7.0 and were fast (90% change within 70 ms for a change of  $P_{\text{Ca}}$  from 7.0 to 6.25). Selected *Aplysia* neurons (R15 & L6) were first penetrated with current and voltage electrodes then with the calibrated Ca sensitive electrode. Resting average intracellular  $\text{Ca}^{2+}$  concentration was found to be  $1.8 \times 10^{-7}\text{M}$  in cells held at -50mV. The  $\text{Ca}^{2+}$  electrode was also used to measure transient changes in  $\text{Ca}^{2+}$  concentration and the intracellular  $\text{Ca}^{2+}$  gradient following voltage clamp pulses. The gradient was measured by moving the electrode tip in a step-wise manner relative to the membrane surface. It was found that for a given voltage clamp stimulation (typically multiple 200 msec pulses from -50 to +30mV) the measurement of the rise in  $\text{Ca}^{2+}$  was greatest near the membrane and not measurable within 30-50 microns of the surface. (Supported by NIH Grant NS11429).

**T-AM-C5** Ca-DEPENDENT INACTIVATION OF Ca CONDUCTANCE IN *APLYSIA* NEURONS EXHIBITS VOLTAGE DEPENDENCE. Roger Eckert and Douglas Ewald\*. (Spon: J.A. Conner) Department of Biology, and Ahmanson Laboratory of Neurobiology, UCLA, Los Angeles, CA 90024.

The inactivation of Ca conductance in *Aplysia* neurons, elicited by a prior depolarizing pulse,  $P_1$ , is essentially independent of  $P_1$  voltage, depending primarily on the amount of  $\text{Ca}^{2+}$  remaining from  $I_{\text{Ca}}$  flow during  $P_1$  (Eckert and Tillotson, 1981, *J. Physiol.* 314:265). We now report that the effectiveness of Ca in causing inactivation (seen as a decrease in  $P_2$  current) diminishes as the membrane potential during  $P_2$  ( $V_2$ ) is made increasingly positive. Voltage clamped neurons L2-L6 were bathed in ASW containing 200mM TEA and  $45\mu\text{M}$  TTX at  $14^\circ\text{C}$ .  $P_2$  was 7 ms long, and of variable voltage.  $P_1$  went to +10mV, was 100ms long, and preceded  $P_2$  by 500ms. Each  $V_2$  was delivered once with  $P_1$  "on", and once with  $P_1$  "off". Measurements were made of the Ca deactivation tail current following  $P_2$  as described earlier (Eckert and Ewald, 1981, *Biophys. J.* 33:145a). With  $P_1$  "off",  $I_{\text{tail}}$  increased toward a plateau maximum with increasing amplitude of  $V_2$ . For each value of  $V_2$ ,  $I_{\text{tail}}$  was smaller with  $P_1$  "on". Moreover, the  $I_{\text{tail}}$  amplitude recorded with  $P_1$  "on" relative to the amplitude recorded with  $P_1$  "off" increased as  $V_2$  was made more positive. At  $V_2 = -20$  mV the ratio was typically 0.40, at  $V_2 = +10$  mV the corresponding ratio rose to 0.65, and at +40, to 0.75. Decreased Ca-dependent inactivation at higher positive potentials contrasts with the behavior of the Ca-dependent potassium current,  $I_{\text{K}}(\text{Ca})$ , which shows increased activation by  $\text{Ca}^{2+}$  with increasing positive potential (Gorman and Hermann, 1979, *J. Physiol.* 296:393). Thus these two actions of  $\text{Ca}^{2+}$  on membrane currents, the activation of  $I_{\text{K}}(\text{Ca})$  and the inactivation of  $I_{\text{Ca}}$ , appear to represent different mechanisms. Supported by USPHS NS08364 and the Epilepsy Foundation of America.

**T-AM-C6** CHARACTERISTICS OF Ca CURRENT RECOVERY FROM INACTIVATION IN INTERNALLY PERFUSED SNAIL NEURONS. A. Yatani, Y. Tsuda and A.M. Brown., Department of Physiology and Biophysics, University of Texas Medical Branch, Galveston, TX 77550.

Recovery from inactivation of  $I_{\text{Ca}}$  separated from other membrane currents was examined in voltage-clamped, internally perfused isolated nerve cell bodies of *Helix aspersa*. In this system Ca current-dependent inactivation occurs during perfusion. Cells were stimulated by two depolarizing pulses separated by variable intervals of 1 ms to 20 secs. The duration of the prepulse was 70, 200, 700 or 1000 ms. Long prepulses (>100 ms) produced substantial current inactivation and the rate of recovery followed a bi-exponential time course. The time constant of the faster phase ( $\tau_1$ ) was of the order of several hundred milliseconds and the time constant of the second phase ( $\tau_2$ ) was seconds long. Short prepulses less than 70 ms duration produced less inactivation, and the rate of recovery was a single exponential function. Addition of EGTA intracellularly in doses of 1-10 mM substantially increased the rate of recovery and the amplitude of the initial test current.  $I_{\text{Ba}}$  showed the same fast recovery as  $I_{\text{Ca}}$  with internal EGTA. The intracellular perfusion of ATP ( $10^{-3}\text{M}$ ) accelerated the recovery of both phases of  $I_{\text{Ca}}$ . The Ca-ATPase inhibitor vanadate at  $10^{-4}\text{M}$  slowed the recovery rate. The recovery rate was faster in alkaline solutions (pH 8.5) and slower in acidic solutions (pH 6.5). The rate of recovery was also voltage dependent and accelerated as the membrane potential was changed from -50 to -80 mV, especially for pulse intervals shorter than 200 ms. These results show that recovery from inactivation of the Ca channels is related to regulation of internal Ca concentration and is not a purely voltage-dependent mechanism as for sodium channels involving intracellular metabolic and diffusion processes.

Supported by NIH grants NS11453 and HL25145.

**T-AM-C7 PRIOR Ca ENTRY INDIRECTLY DEPRESSES ACTIVATION OF THE Ca-DEPENDENT K CONDUCTANCE BY INACTIVATING THE Ca CONDUCTANCE.** Roger Eckert and Douglas Ewald\*. Department of Biology, and Ahmanson Laboratory of Neurobiology, UCLA, Los Angeles, CA 90024.

Depression of calcium-activated K current,  $I_K(\text{Ca})$ , recorded during a voltage clamp depolarization ( $P_2$ ) in gastropod neurons is related to Ca entry during a prior condition pulse,  $P_1$  (Eckert and Lux, 1977, *Science* 197:472). Since intracellular  $\text{Ca}^{2+}$  is also reported to mediate inactivation of Ca channels (Eckert and Tillotson, 1981, *J. Physiol.* 314:265), the Ca-dependent depression of  $I_K(\text{Ca})$  could result from reduced entry and accumulation of  $\text{Ca}^{2+}$  during  $P_2$ . Voltage clamp experiments to test this were done on *Aplysia* L6 and R15, injected with TEA to block the voltage-dependent  $I_K(\text{v})$ , leaving  $I_K(\text{Ca})$  (Hermann and Gorman, 1979, *Neurosci. Letters* 12:87). Residual  $I_K(\text{v})$  seen in 0Ca was <10% of total  $I_K$  and exhibited negligible inactivation. A 150ms  $P_2$  to +10mV followed  $P_1$  by 1.0s.  $P_1$  duration was varied from 0 to 500ms to vary  $P_1$  Ca entry. Mixed currents were first recorded in ASW containing 45 $\mu\text{M}$  TTX. The protocol was repeated in 200mM TEA, to isolate  $I_{\text{Ca}}$ , which was then subtracted from the corresponding mixed currents ( $I_{\text{Ca}} + I_K$ ) recorded in ASW. With increasing  $P_1$  duration,  $P_2 I_K$ , consisting primarily of  $I_K(\text{Ca})$ , and  $I_{\text{Ca}}$  both became smaller. The amplitude of  $I_K(\text{Ca})$  was approximately a linear function of the time integral of  $I_{\text{Ca}}$ . The Ca-mediated reduction in  $I_{\text{Ca}}$  and the attending reduction in  $\text{Ca}^{2+}$  accumulation during  $P_2$  can account for diminished activation of  $I_K(\text{Ca})$ . This suggests that a small steady elevation in  $[\text{Ca}]_i$  can interfere with and depress a process that depends on transiently gated  $\text{Ca}^{2+}$  entry. Supported by USPHS NS08364 and the Epilepsy Foundation of America.

**T-AM-C8 RUTHENIUM RED BLOCKS  $\text{Ca}^{2+}$  INWARD CURRENT AND  $\text{Ca}^{2+}$  ACTIVATED OUTWARD  $\text{K}^+$  CURRENT OF MOLLUSCAN NEURONS.** A. Hermann and A.L.F. Gorman (Intr. by M.C. Cornwall) Faculty of Medicine, Univ. of Konstanz, F.R.G. and Dept. of Physiology, Boston Univ. School of Medicine, Boston MA 02118

Ruthenium Red (RuR) is a polycationic dye which binds strongly to negative surface charges and blocks  $\text{Ca}^{2+}$  binding or uptake, or both, in a number of systems. RuR was applied extracellularly or was injected intracellularly by iontophoresis into selected *Aplysia* neurons (R-15 and L cells).  $\text{Ca}^{2+}$  currents were measured with voltage steps after blocking inward  $\text{Na}^+$  currents and most of the outward  $\text{K}^+$  currents. The  $\text{Ca}^{2+}$  activated  $\text{K}^+$  current was activated by a local, internal iontophoretic injection of  $\text{Ca}^{2+}$  ions. RuR blocked the  $\text{Ca}^{2+}$  (or  $\text{Ba}^{2+}$ ) inward current when applied either intercellularly or extracellularly (10 mM). After a transient increase, probably caused by an elevation of internal  $\text{Ca}^{2+}$ , intracellular RuR also blocked the  $\text{Ca}^{2+}$  activated  $\text{K}^+$  current. EGTA was injected internally to keep the  $\text{Ca}^{2+}$  concentration constant and to show that the RuR block was not caused by a change of intracellular  $\text{Ca}^{2+}$ . Extracellular RuR (10 mM) had no obvious effect on the  $\text{Ca}^{2+}$  activated  $\text{K}^+$  current. The effects of RuR on the  $\text{Ca}^{2+}$  and  $\text{Ca}^{2+}$  activated  $\text{K}^+$  currents were almost irreversible. External and internal RuR had no effect on voltage dependent outward  $\text{K}^+$  currents (transient or delayed outward  $\text{K}^+$  currents). Our results suggest that Ruthenium Red occupies  $\text{Ca}^{2+}$  binding sites at the membrane and, therefore, prevents the  $\text{Ca}^{2+}$  inward current and the activation of the  $\text{K}^+$  current by  $\text{Ca}^{2+}$  ions. A possible target of RuR may be the sialic acid moiety of sialoglycoproteins at the inner membrane surface. (Supported by DFG Grant SFB 138 and NIH Grant NS 11429).

**T-AM-C9 REDUCTION OF OUTWARD CURRENTS IN SNAIL NEURONS BY REPLACEMENT OF EXTERNAL POTASSIUM IONS.** D. Junge, UCLA School of Dentistry and Department of Physiology, Los Angeles, CA 90024.

Isolated subesophageal ganglion cells from *Helix aspersa* were studied using the perfusion pipette technique (Lee et al., *J. Gen. Physiol.* 71:489, 1978). Membrane potential was usually measured with a microelectrode, and series resistance compensation was used to obtain flat potential steps. Leak currents were subtracted from total membrane currents electronically. Replacement of the normal 5mM external potassium with sodium caused a reduction and slowing of delayed outward currents. The same result was seen in Na-free solutions if K was replaced with tris. Replacement of potassium had no effect on the leak or series resistance. Addition of 0.5mM cadmium ions to all solutions had no effect. External cesium ions could only partially substitute for potassium in restoring outward currents. If the external K-concentration was raised above 5mM, outward currents were reduced, as predicted by electrodiffusion theory. The zero-current potential measured from instantaneous i-v curves became about 12 mV more negative when  $(\text{K})_o$  went from 5mM to zero. A kinetic model which assumed that two subunits must be in the active form for an outward-current channel to open was fitted to the currents as follows: The rate constants for subunit activation ( $K_1$ ) and inactivation ( $K_2$ ) were incremented from loop statements in the computer, and the minimum least-square difference between theoretical and observed currents determined. From this analysis it was found that  $K_1$  was reduced about 50% by K-replacement at all potentials, and that  $K_2$  was relatively unaffected. This suggests that external potassium ions may be necessary for stabilization of outward-current channels.



**T-AM-C10** INACTIVATION DELAYS AND THE ACTIVATION PROCESS IN MYXICOLA. L. Goldman and J.L. Kenyon, Dept. of Physiology, School of Medicine, Univ. of Maryland, Baltimore, MD. 21201, and Cardiopulmonary Division, Univ. of Texas Health Science Center, Dallas, TX. 75235.

Inactivation time course in *Myxicola* Na channels (two pulse method) proceeds with an initial delay followed by a simple exponential decline of time constant  $\tau_c$  (57 determinations on 27 axons). Delay is not generated by any uncompensated portion of the series resistance,  $R_s$ , (Goldman and Kenyon, *Biophys. J.* 33:209a, 1981), or by contamination from activation development during the conditioning pulse. Inactivation development is preceded by a precursor process. Delay ( $R_s$  compensation, 1/3 or 1/4 Na ASW, 2 mM 3,4-diaminopyridine, 6 ms gap, bracketing procedure, computer controlled pulse protocols) decreases steeply with more positive conditioning potential from -40 mV to about 0 mV (range 130 to 817  $\mu$ s) and tends to saturate beyond 0 mV. Delay increased roughly proportionately with time to peak  $g_{Na}$  of the conditioning pulse as expected if inactivation sequentially follows channel opening. In 10-15% of the determinations the difference between inactivation values for brief conditioning pulses and the extrapolated  $\tau_c$  exponential was sufficiently large in magnitude and low in variance to measure reliably. These difference values could also be described as an exponential of time constant  $\tau_{delay}$ .  $\tau_{delay}$  (V) followed  $\tau_m$  (V).  $\tau_{delay}$  (V) also agreed with activation time constants determined by fitting a sequential, coupled model to clamp data. The whole time course of inactivation could be quantitatively reconstructed by assuming a three state: Rest  $\longleftrightarrow$  Conducting  $\longleftrightarrow$  Inactivated scheme for the gate using the  $\tau_{delay}$  and  $\tau_c$  values determined experimentally. Na channels in *Myxicola* behave as expected if inactivation, at least to some degree, develops sequentially to channel opening. Supported by NIH Grant NS-07734

**T-AM-C11** SIMULATIONS OF MEMBRANE CURRENT AND VOLTAGE CHANGES ASSOCIATED WITH RANDOM OPENINGS AND CLOSINGS OF IONIC CHANNELS IN EXCITABLE MEMBRANES. John R. Clay<sup>1</sup> and Louis J. DeFelice<sup>2</sup> (Intr. by D. L. Alkon), <sup>1</sup>Lab. of Biophysics, NINCDS, MBL, Woods Hole, MA 02543; <sup>2</sup>Department of Anatomy, Emory University, Atlanta, GA 30322.

Recent measurements with the patch voltage clamp technique have demonstrated that ionic channels in excitable membranes have discrete open and closed conducting states and that the durations of openings and closings are random variables (Conti and Neher, 1980; *Nature*, 285: 140-143; Sigworth and Neher, 1980; *Nature*, 287: 447-449). We have simulated the open-close process on a digital computer using a random number generator and the probability density distribution functions of open and closed channel lifetimes, which can be calculated for any model of the ionic conductance process from principles of probability theory. The technique is valid even when the rate constants for transitions between states of the model are functions of time. For example, the rate constants of any traditional kinetic scheme, such as the Hodgkin and Huxley model, are functions of voltage. Consequently, they are essentially functions of time, as well, during a voltage change. We have used the simulation technique to investigate the behavior of small populations of Hodgkin and Huxley model channels during a voltage step and during a voltage clamp action potential. We have also simulated the influence of channel openings and closing on the shape of an action potential from a patch of membrane 1  $\mu$ m<sup>2</sup>, or less, in area. These results are applicable to the analysis of threshold fluctuations. Supported in part by NIH Grant 1-P01-HL27385.

**T-AM-C12** NUMERICAL METHOD FOR OFF-LINE SERIES RESISTANCE ERROR CORRECTION Y. Palti & M. Cohen-Armon Dept. of Physiology & Biophysics, Technion-Medical School, Haifa, Israel.

Current (I) flowing across the voltage clamped membrane generates a potential drop in the resistance in series with the membrane ( $R_s$ ) and thus an error in the potential control. This error, which may be very significant, can only be partially corrected by electronic compensation during the experiment. Subsequent correction by computation is generally believed impossible, even when  $R_s$  is known, for membrane potentials ( $V_m$ ) at which the conductance parameters are voltage dependent. The proposed method, which corrects the error induced by  $R_s$ , in the said  $V_m$  range, is based on the assumption that  $dI/dt$  is a function of the current  $V_m$  only (since  $dm/dt \propto (1-m)g_{Na}$ , etc). The reconstruction of the correct current begins with very small sodium or potassium currents (for which the  $R_s$  error is negligible). Here  $V_m$  and therefore I can be assumed to be errorless. The subsequent I value is calculated using a  $dI/dt$  value obtained under any set of conditions where  $V_m$  is known to have the desired value (as ensured by the extl. protocol) and I equals the initial I value. By iterations the correct I vs  $V_m$  is reconstructed for the chosen potential. It is shown analytically that for squid giant axons, with an uncompensated  $R_s$  of 5  $\Omega$ cm<sup>2</sup>, the maximal error in  $I_{Na}$  (in the said  $V_m$  range) is reduced from about 30% to under 3%. The validity of the reconstruction is demonstrated experimentally by correcting  $I_{Na}$  generated in ASW and comparing  $I_{Na}$  obtained in low [TTX].

**T-AM-D1** EFFECT OF VOLUME (AND INTERFILAMENT SPACING) ON CROSS-BRIDGE MECHANISM IN INTACT SINGLE MUSCLE FIBERS. J. Gulati and A. Babu, A. Einstein College of Medicine, Bronx, N.Y. 10461

The influence of the lateral distance between filaments on the cross-bridge mechanism was evaluated from the contraction properties of frog muscles, at 0°C and sarcomere length 2.2-2.3  $\mu$ , in solutions up to 2.2 times (T) Ringers molarity. Solutions were made hypertonic with either impermeant sucrose or permeant KCl. Fiber diameter, force ( $P_o$ ) and the speed of unloaded shortening ( $V_o$ ) were measured. The fiber was activated by a temp step from 25° to 0°C, in 1-2 mM caffeine.  $P_o$  in 1.4T solution was 0.74, and in 1.8T was 0.45, times the force in 1.0T, irrespective of the solute used for hypertonicity, showing that the quality of solute permeability is not a factor in the force development. In contrast, the fiber diameter, and therefore the cell volume, decreased in sucrose but remained unchanged in KCl. The results show that force is insensitive to change in cell volume. The volume changes in sucrose were similar to the known changes in interfilament separation (Rome, *J. Mol. Biol.* 37, 331, 1968). This is evidence that the force generating mechanism is independent of the decrease in radial separation and that force per cross-bridge is constant at various separations. In isotonic studies, the speed ( $V_o$ ) decreased by a factor of two in 1.4T sucrose, but there was no decrease in KCl. Since, intracellular ionic strength would be roughly the same with the two solutes, this is evidence that ionic strength per se has little effect on  $V_o$  of intact fiber, and invalidates the previous conclusion of Edman et al (*J. Physiol.* 269, 255, 1977). The findings suggest that in hypertonic solutions with sucrose the kinetics of cross-bridge turnover may be modified either (1) directly by decrease in filament separation, and/or (2) by the change in intracellular milieu associated with decrease in separation. (Supported by NIH (AM-26632) and M.D.A.)

**T-AM-D2** THE ONSET OF CONTRACTION IN SKELETAL MUSCLE IS MYOFIBRILLAR, NOT SARCOMERIC.

M. Sharnoff and L.P. Brehm, Dept. Physics, Univ. Delaware, Newark, DE.

We have used holographic methods to construct differential images of the onset of contraction in electrically stimulated single fibers from the frog semi-tendinosus muscle. In such images, inactive portions of the fibers appear dimly if at all, while slight changes in structure or in mechanical condition may be made many times more conspicuous than by any other optical technique. The experiments were performed isometrically in bright field illumination at 18° C and achieved a time resolution of 0.5 msec. We find: 1) in the 0.5 msec interval immediately preceeding the onset of active tension, the fibers are invisibly dark against a dark background; 2) at the onset of tension, a few transversely and longitudinally well-separated, longitudinal regions of myofibrillar diameter and of length ca. 100  $\mu$ m appear against a dark background; 3) during the next 0.5 msec these regions are joined by other similar ones, and their mean transverse spacing is significantly reduced; 4) during the next 10 msec the fibers undergo gross translational motion which complicates the images, but the features which appeared during 2) and 3) persist without significant change in their brightness or increase in their number; 5) these regions appear to occupy less than 25% of the cross section of the fiber.

These results are very different from what might be expected if individual myofibrillar sarcomeres were randomly activated during contraction.

**T-AM-D3** ISOMETRIC CONTRACTION CHANGES THE APPEARANCE OF CROSS-STRIATED MUSCLE FIBERS.

M. Sharnoff and L.P. Brehm, Dept. Physics, Univ. Delaware, Newark, DE.

We have begun to study by direct imaging procedures the structural sources, such as they might be observed at the level of optical microscopy, which may be considered to underlie the enhancement of transparency and the reduction in diffraction efficiency observed to accompany contractile activity in fibers of cross-striated muscle. The reliance upon images, rather than diffraction patterns, permits surveillance of the extent to which the optical changes are homogeneously distributed throughout a fiber. In the experiments reported here, single frog semi-tendinosus fibers held at striation spacing 2.7  $\mu$ m were examined with an objective of N.A. 0.30 under oblique laser illumination, permitting passage of the orders  $\bar{1}$ , 0, 1, and 2 into the microscope. Holographic methods were used to construct images of the difference between the active and the resting states. We have found that the second harmonic of the striation spacing is much more prominent in differential images than in non-differential ones, and that its prominence commences simultaneously with the onset of active tension, appears wherever striation can be observed in the differential images, and persists unchanged for periods of time comparable with the duration of a twitch.

**T-AM-D4 MYOSIN PHOSPHATASE FRACTIONS ENHANCE RELAXATION IN CHEMICALLY SKINNED VASCULAR SMOOTH MUSCLE (VSM).** Richard J. Paul, Joseph DiSalvo and J. Caspar Rüegg.\* Depts. of Physiology, Univ. of Cincinnati, OH 45267, USA, and Univ. Heidelberg, 6901, Federal Republic of Germany.

"Chemically skinned" VSM will develop maximal isometric force at  $10^{-5}$ M  $\text{Ca}^{2+}$  and complete relaxation at  $10^{-8}$ M. The mechanisms underlying this  $\text{Ca}^{2+}$  regulation are controversial.  $\text{Ca}^{2+}$  and calmodulin can activate a myosin light chain kinase increasing the phosphorylation of myosin which appears to be a prerequisite for actin-myosin interaction. Since unphosphorylated smooth muscle myosin is unable to interact with actin, phosphatase-mediated dephosphorylation may be associated with relaxation in intact VSM. Our evidence shows that enriched myosin light chain phosphatase (MLCPase) fractions increase the rate of relaxation in skinned media from hog carotid artery. MLCPase fractions were prepared from bovine aortic muscularis by ion exchange chromatography, precipitation with  $(\text{NH}_4)_2\text{SO}_4$  and affinity chromatography. Following the initial 2 minutes after changing to  $\text{Ca}^{2+}$ -free solution, relaxation of isometric force proceeded along an exponential course. The relaxation half-time ( $t_{1/2}$ ) for the initial contraction in 17 fibers averaged  $4.1 \pm 0.3$  min., comparable to living VSM. The activities (U/ml) of phosphatase fractions and their effects on relaxation were:

MLC Phosphatase Fraction	Protein(mg/ml)	MLC (U/ml)	Myosin	Relaxation (Test $t_{1/2}$ /Control $t_{1/2}$ )
L1	0.04	2.5	0.4	$0.73 \pm 0.03$ (7)
L2	0.41	90.0	17.2	$0.53 \pm 0.02$ (6)
L3	0.10	25	5.4	$0.61 \pm 0.11$ (4)

Heat treatment of the phosphatase resulted in complete loss of both enzymic activity and enhancement of relaxation. VSM phosphatase fractions thus contain a heat labile non-dialyzable factor which, while having little effect on isometric force, strongly enhances relaxation. Supported in part by NIH grants 22619, 23240, 20196; and DFG RU154-14.

**T-AM-D5 TRANSIENT IN PHOSPHAGEN UTILIZATION DURING ISOMETRIC CONTRACTION OF VASCULAR SMOOTH MUSCLE** Joseph M. Krisanda and Richard J. Paul Department of Physiology University of Cincinnati, College of Medicine, OH 45267

The economy of tension maintenance of vascular smooth muscle (VSM) is 300-fold greater than skeletal muscle. Recent evidence (Dillon, Aksoy, Driska & Murphy, *Science* 211:495, 1981) suggests that a phosphorylation-dependent decrease in the cross-bridge cycling rate occurs during the first few minutes of an isometric contraction. We studied the energetics during tension development and maintenance in VSM to: (1) determine whether transients in phosphagen utilization correlate with changes in cross-bridge cycling rate; and (2) assess whether this phenomenon can account for the high economy of tension maintenance. Experiments were conducted on porcine carotid media strips, stimulated with KCl at 37°C. Previous work in our laboratory established that tissue phosphagen (ATP + PCr) concentrations were constant (and equal to baseline levels) as early as 30 seconds after contraction. Thus, the rate of  $\text{O}_2$  consumption ( $\text{J}_{\text{O}_2}$ ) can be directly used to measure phosphagen utilization. Basal  $\text{J}_{\text{O}_2}$  was  $71 \pm 4$  and for steady state contractions  $175 \pm 14$  nmol  $\text{O}_2$ /(gm·min) ( $\pm$ SEM, n=10). The initial suprabasal  $\text{J}_{\text{O}_2}$  (1-4 min) averaged  $1.82 \pm 0.20$  times the steady state suprabasal  $\text{J}_{\text{O}_2}$  ( $\pm 10$  min.). There was no significant change in  $\text{J}_{\text{O}_2}$  during force redevelopment following a quick release at 15-20 minutes after stimulation (n=4). Thus, tension development *per se* is not sufficient to produce the observed metabolic transient. Our data suggest that the metabolic transient and presumably actomyosin ATPase parallel the reported changes in velocity and myosin phosphorylation. However, the maximum change of about 2-fold is not sufficient to account for the high economy of VSM. This suggests that differences in smooth and skeletal actomyosin ATPase are likely to be of greater significance. Supported in part by NIH 23240 and NIH 1 F32 HL06051-01.

**T-AM-D6 THE  $\text{Ca}^{2+}$  TRANSLOCATOR OF THE  $\text{Ca}^{2+}$ - $\text{Mg}^{2+}$ -ATPase OF SKELETAL SARCOPLASMIC RETICULUM IS NEGATIVELY CHARGED.** Duncan H. Haynes, Dept. of Pharmacology, Univ. Miami Medical School, Miami, Fl.

The pH dependence of ATP-driven  $\text{Ca}^{2+}$  uptake by the  $\text{Ca}^{2+}$ - $\text{Mg}^{2+}$ -ATPase pump is reported. Progress curves of the active transport reaction were determined using the fluorescence signal of 1-anilino-8-naphthalenesulfonate as a rapid and continuous monitor of the internal free  $\text{Ca}^{2+}$  concentration,  $[\text{Ca}]_i$ . Experiments were carried out with 100 mM KCl,  $5 \times 10^{-4}$ M Mg-ATP,  $1 \times 10^{-4}$ M  $\text{Mg}^{2+}$ , 10 mM Hepes and 20 mM Tris buffer at 30°C. The external  $\text{Ca}^{2+}$  concentration ( $[\text{Ca}]_o$ ) was varied using a  $\text{Ca}^{2+}$ /EGTA buffer. Progress curves were obtained at variable  $[\text{Ca}]_o$  and the initial rate ( $d[\text{Ca}]_i/dt$ ) and the maximal uptake as steady-state ( $[\text{Ca}]_{i,\text{max}}$ ) were determined. At pH 7.0, Hill plots of  $d[\text{Ca}]_i/dt$  and  $[\text{Ca}]_{i,\text{max}}$  showed identical behavior, with a second order dependence (n=2.0) on  $[\text{Ca}]_o$ . An apparent  $\text{Ca}^{2+}$  binding constant,  $K_{\text{app}}$  ( $=1/K_m$ ) of  $1.8 \times 10^{-7}\text{M}^{-1}$  was determined for both transport parameters. The phenomenon was studied as a function of pH. A plot of  $\log K_{\text{app}}$  vs pH was biphasic. For pH 7.0-8.0 a small dependence on  $[\text{Ca}]_o$  was observed (slope = +0.4). For pH 5.5-7.0 a slope of +1.6 was observed. The data at low pH are interpreted in terms of competition between  $\text{Ca}^{2+}$  and 2  $\text{H}^+$  for occupation of the outwardly-oriented translocator. An apparent  $\text{pK}_a$  of 6.8 is calculated for  $\text{H}^+$  binding. In contrast,  $d[\text{Ca}]_i/dt$  and  $[\text{Ca}]_{i,\text{max}}$  increase with decreasing pH. Analysis shows that this is the result of competition between  $\text{H}^+$  and  $\text{Ca}^{2+}$  for occupation of the inwardly-oriented translocator.  $\text{H}^+$  binding assists in dissociating  $\text{Ca}^{2+}$  from the inwardly-oriented translocator and re-turning it in a charge-compensated fashion. Supported by G.M. 23990 and a grant from the Florida Heart Association.

**T-AM-D7** MECHANISM OF ALLOSTERIC REGULATION OF THE Ca+Mg ATPase OF SARCOPLASMIC RETICULUM: STUDIES WITH ADENYLYL METHYLENE DIPHOSPHONATE. M. Cable, D. Pang, L. Monfalcone, and N. Briggs, Medical College of Virginia, Richmond, VA. 23298.

The Ca+Mg-ATPase of skeletal sarcoplasmic reticulum (SR) shows evidence of allosteric regulation (non-linear Lineweaver-Burk plots) in the 0.5 to 12  $\mu$ M ATP concentration range. Møller, et al. (J. Biol. Chem. 255:1912, 1980) have attributed this to interactions between active sites in an oligomeric enzyme complex. Studies we have carried out with adenylyl methylene diphosphonate (AMPPCP) suggest that both active site coupling and effector sites are involved. At the highest concentration of AMPPCP studied, 2.4 mM, all evidence of negative cooperativity (as judged by Lineweaver-Burk plots) disappeared. Contrary to the report of Taylor and Hattan (J. Biol. Chem. 254:4402, 1979) we found that competition between AMPPCP and ATP for the active site is in part responsible for this apparent loss of cooperativity. Analysis of AMPPCP binding to SR between  $10^{-6}$  and  $10^{-4}$  M showed a complex relationship between binding and  $\text{Ca}^{2+}$  and  $\text{Mg}^{2+}$  concentrations. Except in the presence of 1 mM  $\text{Ca}^{2+}$ , Hill plots were curvilinear. Strong evidence of positive cooperativity in binding was observed in all circumstances except in the presence of 5 mM EDTA. Evidence that AMPPCP between  $10^{-6}$  and  $10^{-4}$  binds to the active as well as the effector sites was obtained.

**T-AM-D8** REGULATION OF CARDIAC  $\text{Ca}^{2+}$ - $\text{Mg}^{2+}$ -ATPase - A POSSIBLE ROLE FOR PHOSPHOLAMBAN, THE 22K DALTON c-AMP DEPENDENT REGULATORY PROTEIN, IN THE CALCIUM TRANSPORT MECHANISM

INDU S. AMBUDKAR AND ADIL E. SHAMOO

Department of Biological Chemistry, University of Maryland School of Medicine, Baltimore, Md. 21201

The regulation of the activity of the  $\text{Ca}^{2+}$ - $\text{Mg}^{2+}$ -ATPase of the cardiac sarcoplasmic reticulum is associated with the phosphorylation of a 22K protein, phospholamban. This protein has been reported to be phosphorylated by both a c-AMP dependent as well as by a  $\text{Ca}^{2+}$ -calmodulin dependent system. We report here a possible interaction between phospholamban and the  $\text{Ca}^{2+}$  transport function of the ATPase. Treatment of the sarcoplasmic reticulum membranes with low concentrations of DOC decreases the c-AMP dependent phosphorylation of the SR. This decrease is accompanied by an 80-90% loss of  $\text{Ca}^{2+}$  transporting activity which is not due to change in  $\text{Ca}^{2+}$ -permeability. This loss is exhibited both as a decrease in levels of uptake as well as in the rates. Phosphorylation of the SR membrane before DOC treatment protects the c-AMP dependent phosphorylation of the membrane as well as the DOC-induced loss of  $\text{Ca}^{2+}$  uptake. ATP hydrolytic rates are not affected by the DOC treatment. This effect of DOC is specific to cardiac sarcoplasmic reticulum since similar treatment of skeletal muscle sarcoplasmic reticulum does not induce any decrease in  $\text{Ca}^{2+}$  transport function. The results suggest a specific role of phospholamban in the  $\text{Ca}^{2+}$ -transporting activity of cardiac sarcoplasmic reticulum.

This work is supported by the Office of Naval Research, Department of Energy, and the Muscular Dystrophy Association.

**T-AM-D9** CHARACTERIZATION OF THE CALMODULIN-DEPENDENT PHOSPHORYLATION OF CARDIAC MUSCLE SARCOPLASMIC RETICULUM. C.F. Louis, M. Maffit, D. Sullivan. Dept. of Vet. Biol., Univ. of Minn., St. Paul, MN 55108

The calmodulin-dependent phosphorylation of phospholamban, a 22,000 dalton protein present in cardiac sarcoplasmic reticulum (SR), has been shown to result in the stimulation of SR Ca uptake (Le Peuch et al. Biochemistry 18, 5150, 1979). To decide whether this phosphorylation occurs at ion concs that are found in the sarcoplasm during normal functioning of the heart, we have investigated the phosphorylation of cardiac SR (0.5 mg/ml) in 40 mM Imidazole, 0.1  $\mu$ M calmodulin, 0.1 mM  $\text{AT}^{32}\text{P}$ , and varying concs of  $\text{K}^{+}$ ,  $\text{Ca}^{2+}$ , and  $\text{H}^{+}$  at 20°C. Phosphorylation increased with pH in the range pH 5.5 to pH 8.5, was inhibited by  $\text{K}^{+}$  concs greater than 100 mM, and was activated by increasing  $\text{Mg}^{2+}$  (max at 8 mM,  $\frac{1}{2}$  max at approx 0.6 mM  $\text{Mg}^{2+}$ ); phosphorylation was inhibited by  $\text{MgCl}_2$  concs greater than 10 mM. The apparent  $K_m$  of this phosphorylation for ATP was 37  $\mu$ M. Phosphorylation increased with increasing  $\text{Ca}^{2+}$  (apparent  $K_m$  for  $\text{Ca}^{2+}$  was 15  $\mu$ M) but was inhibited by  $\text{Ca}^{2+}$  concs greater than approximately 50  $\mu$ M. The apparent  $K_m$  of the Ca-ATPase phosphoprotein intermediate (EP) for  $\text{Ca}^{2+}$  was 4  $\mu$ M. Thus the calmodulin-dependent phosphorylation of cardiac SR could be max activated at sarcoplasmic concs of  $\text{K}^{+}$ ,  $\text{Mg}^{2+}$ , and ATP. The calmodulin-dependent phosphorylation was  $\frac{1}{2}$ -max activated at  $\text{Ca}^{2+}$  concs that were significantly greater than those required to promote SR EP intermediate formation. Thus, the SR Ca pump could be fully activated before any significant calmodulin-dependent SR phosphorylation occurred. Thus, the calmodulin-dependent phosphorylation of cardiac SR may only function when the heart needs to rescue itself from a possibly fatal Ca overload. (Supported by Amer. Heart Assn Minn Aff, HL-25880 from NIH.)

**T-AM-D10 IDENTIFICATION OF CALSEQUESTRIN AND THE INTRINSIC GLYCOPROTEIN IN CANINE CARDIAC SARCOPLASMIC RETICULUM** by Kevin P. Campbell<sup>#</sup>, David H. MacLennan<sup>#</sup> and Annelise O. Jorgensen<sup>\*</sup>.<sup>#</sup>Banting and Best Department of Medical Research; <sup>\*</sup>Department of Anatomy; University of Toronto, 112 College Street, Toronto, Ontario, Canada M5G 1L6.

Sarcoplasmic reticulum vesicles from rabbit skeletal muscle contain three major proteins:  $\text{Ca}^{2+}$  +  $\text{Mg}^{2+}$  ATPase ( $M_r$  105,000), calsequestrin ( $M_r$  63,000) and the intrinsic glycoprotein ( $M_r$  53,000). We have found sarcoplasmic reticulum vesicles from canine cardiac muscle contain a  $M_r$  55,000 protein that shares several chemical and physical characteristics with rabbit skeletal muscle calsequestrin. Both stained blue with "Stains-all", both had anomalous mobility on SDS gels depending on the buffer system and both precipitated in the presence of millimolar  $\text{Ca}^{2+}$ . The  $M_r$  55,000 protein from canine cardiac sarcoplasmic reticulum was extracted from the vesicles with low concentrations of deoxycholate and purified using DEAE-cellulose. The purified  $M_r$  55,000 protein bound approximately 300 nmoles of  $\text{Ca}^{2+}$  per mg protein indicating it was the cardiac form of calsequestrin. An intrinsic glycoprotein was also identified in cardiac sarcoplasmic reticulum by  $^{125}\text{I}$  Con A binding and Endoglycosidase H digestion. It had a molecular weight of 53,000 and its size was reduced to 49,000 daltons by Endo H. Indirect antibody staining with antiserum and  $^{125}\text{I}$  protein-A have shown that an antiserum to the rabbit  $M_r$  53,000 glycoprotein reacts with the cardiac  $M_r$  53,000 glycoprotein but an antiserum to rabbit calsequestrin does not react to cardiac calsequestrin. We have also analyzed sarcoplasmic reticulum vesicles from several other cardiac and skeletal muscles and found calsequestrin and the intrinsic glycoprotein to be invariant components of isolated sarcoplasmic reticulum vesicles. (supported by MRC, MDAC and OHF).

**T-AM-D11 MECHANISMS OF QUINIDINE-INDUCED DECREASES IN MYOCARDIAL CONTRACTILITY: A STUDY ON THE CONTRACTILE PROTEINS AND THE SARCOPLASMIC RETICULUM IN FUNCTIONALLY SKINNED MYOCARDIAL FIBERS FROM RABBITS.** J.Y. Su and R.G. Libao, Dept. of Anesthesiology, Univ. of Washington, Seattle, WA 98195

Quinidine (Q) at concentration greater than 10  $\mu\text{M}$  decreases myocardial contractility in isolated intact cat papillary muscle (JPET, 158:11, 1967). The mechanisms of this depression were studied in functionally skinned myocardial fiber preparation by measuring the  $\text{Ca}^{2+}$ -activated tension development of the contractile proteins (CP), and the  $\text{Ca}^{2+}$  uptake and release from the sarcoplasmic reticulum (SR) using caffeine-induced tension transient (Pflügers Arch., 375:111: 380:29). Rabbit right ventricular papillary muscles were isolated and pieces of the muscles were homogenized (sarcolemma disrupted) in relaxing solution. A fiber bundle was dissected from the homogenate and was mounted on the forceps attached to a photodiode tension transducer. Effect on CP: High [EGTA] (7 mM) was used to control free  $[\text{Ca}^{2+}]$ . The steady-state isometric tension was analyzed. Q (0.3-1 mM) increased the submaximal  $\text{Ca}^{2+}$ -activated tensions (pCa 5.6-5.0) resulting decreases in  $[\text{Ca}^{2+}]$  required to activate 50% of the maximal tension (pCa 5.35 for control vs pCa 5.5-5.7 for Q) in dose-dependent manner. The maximal  $\text{Ca}^{2+}$ -activated tensions were increased by 12% at 0.5-1 mM Q. Effects on SR: The preparations were immersed in solutions to load  $\text{Ca}^{2+}$  (uptake), and to release  $\text{Ca}^{2+}$  (release) from the SR using 25 mM caffeine and a tension transient was generated. The area of the tension transient was used as an estimate of the amount of  $\text{Ca}^{2+}$  released. Q (0.3-1.5 mM) decreased (16-55%) the  $\text{Ca}^{2+}$  uptake and increased (18-131%) the  $\text{Ca}^{2+}$  release from the SR. We conclude that Q decreases myocardial contractility by decreasing  $\text{Ca}^{2+}$  uptake by the SR. (Supported by NIH HL20754 and Am. Heart Assoc. and Univ. of Washington Med. Student Summer Res. Program)

**T-AM-E1** POLYMERIZATION AND STRUCTURE OF *ACANTHAMOEBA* MYOSIN-II FILAMENTS. T.D. Pollard, Dept. of Cell Biology and Anatomy, Johns Hopkins University School of Medicine, Baltimore, MD. 21205.

Myosin-II forms filaments of two different sizes. Thin bipolar filaments 7 nm wide and 200 nm long consist of 16 myosin-II molecules. Thick bipolar filaments of variable width consist of 40 or more myosin-II molecules. Both have a central bare zone ~100 nm long and myosin heads projecting laterally at the ends. The heads are arranged in rows spaced 15 nm apart. In the case of the thin filaments there are 2 molecules per row. The thick filaments are formed rapidly and reversibly in the presence of 6-10 mM  $MgCl_2$  (or any of 8 other different divalent cations tested) by the lateral aggregation of thin filaments. Low pH and low KCl also favor thick filament formation. Neither the myosin-II concentration (50 to 1000  $\mu g/ml$ ) nor ATP has an effect on the morphology of the filaments. The polymerization mechanism was studied quantitatively by measuring the amount of polymer formed (Cp) under various conditions as a function of total myosin-II concentration (Ct). Above a critical concentration of 15 to 40  $\mu g/ml$  Cp was proportional to Ct. However, unlike a classical condensation-polymerization system, the slope of a plot of Cp vs. Ct is not 1.0, but 0.5 to 0.95 depending on conditions. For example, in the presence of 10 mM  $MgCl_2$  this slope was 0.90 to 0.95 in 20 mM KCl and 0.55 in 140 mM KCl. This indicates that the polymerization mechanism is more complex than a simple system like actin. One explanation is that the monomers are not in equivalent positions in filament, giving rise to multiple equilibrium constants. Myosin-II with 0.8 heavy chain phosphates per molecule is more sensitive to depolymerization by KCl than myosin-II with 2.6 phosphates, but phosphorylation has no effect on either the morphology or solution conditions required to form thin and thick filaments. Supported by NIH Grant GM 26338.

**T-AM-E2** PHOSPHORYLATION OF *Dictyostelium* MYOSIN. E.R. Kuczmarski, L.M. Griffith, S.M. Downs, and J.A. Spudich. Department of Structural Biology, Stanford University, Stanford, CA 94305.

We have shown that *Dictyostelium* myosin is phosphorylated in vivo on the 210 Kd heavy chain and the 18 Kd light chain. The site of heavy chain phosphorylation has been localized exclusively to the tail portion of the myosin molecule. Heavy chain phosphorylation inhibits both the assembly of myosin into thick filaments and the actin-activated ATPase activity. This inhibition can be reversibly turned off and on by sequential dephosphorylation and rephosphorylation, respectively (PNAS 77:7292; J. Cell Biol. 89:104). To determine the effect of light chain phosphorylation on myosin assembly and ATPase activity, we have begun isolation of the 18 Kd light chain kinase. Light chain kinase activity is present in the high speed supernate of *Dictyostelium* extracts. The enzyme precipitates between 40-80% ammonium sulfate, elutes as a single peak on Bio-gel A 0.5 m with a  $K_d=0.5$ , and binds to DEAE at pH 7.0. We are currently examining the effect of light chain phosphorylation on myosin function. In addition we have extended our purification and characterization of heavy chain kinase and phosphatase activities. Heavy chain kinase is resolved into three peaks by gel filtration chromatography. All three phosphorylate the tail portion of the myosin molecule. We are using peptide mapping techniques, including reverse phase HPLC, to compare the in vivo and in vitro phosphorylation sites. Heavy chain phosphatase activity elutes from Bio-gel A 0.5 m as a single peak of activity with an apparent M.W. of 60,000. Contaminating alkaline phosphatases are subsequently removed by DE-52 chromatography. This partially purified enzyme appears quite specific for myosin heavy chain, since phospho-histone and phospho-casein are much poorer substrates. NIH GM-25240 (J.A.S.); GM-07781-01 (L.M.G.); Giannini fellowship (E.R.K.).

**T-AM-E3** ORGANIZATION OF  $\alpha$ -ACTININ IN RELAXED AND CONTRACTED SINGLE ISOLATED SMOOTH MUSCLE CELLS.

F.S. Fay, K. Fogarty and K. Fujiwara, Department of Physiology, University of Mass. Medical School, Worcester, MA and Department of Anatomy, Harvard Medical School, Boston, MA.

To probe for organization of the contractile machinery in smooth muscle, we studied the distribution of  $\alpha$ -actinin. Smooth muscle cells, enzymatically disaggregated from the stomach of *Bufo marinus*, were fixed either while relaxed or contracted due to acetylcholine (0.1 mM; 1 min). After treatment with cold acetone, cells were stained with fluorescently labeled antibody specific to  $\alpha$ -actinin either from chicken gizzard or toad stomach. Three dimensional organization of the staining was analyzed from stereo pairs and from computer reconstruction of consecutive optical sections at 0.5  $\mu m$  intervals. Within the cytosol, fusiform bodies (CFBs) are stained by the antibody (axial ratio=4.3; length=1.2  $\mu m$ ; means for relaxed cells). CFBs appear to be principally organized end to end in string-like elements that traverse the cell's interior at shallow angles to its long axis. These strings appear to run into somewhat large irregular stained patches along the cell border. In relaxed cells the mean center to center distance between CFBs is 2.2  $\mu m$ . In contracted cells, this distance decreases to 1.4  $\mu m$  and the string-like elements are more steeply inclined to the long axis of the cell. In all cells, CFBs in 2-5 adjacent strings are in register laterally. These observations provide direct evidence that contraction of the cell is associated with a decrease in the distance between CFBs in these string-like elements. We thus propose that the material between two such CFBs represents the basic unit for contraction of smooth muscle. Finally, we propose that coordinating structures, as yet undetected, exist within smooth muscle to account for the lateral registration of CFBs. (Supported by grants to: FSF from NIH (HL14523) and MDA; KF from NIH (GM25637).)

**T-AM-E4** CAPPING OF OPPOSITE ENDS OF ACTIN FILAMENTS BY TWO DISTINCT MUSCLE PROTEIN PREPARATIONS. S. Lin, J.F. Casella, & M.D. Flanagan. Dept. of Biophysics, Johns Hopkins Univ., Baltimore, MD 21218.

The mechanism by which actin is incorporated into filaments of strikingly uniform length in muscle cells is largely unknown. In this report, we describe two distinct protein preparations derived from the muscle extract described by Maruyama et al. (*J. Biochem.* 81: 215 (1977)), one that inhibits G-actin addition to the "pointed" end of F-actin, and another that has similar activity at the "barbed" end. Actin and tropomyosin-troponin were extracted from acetone powder of rabbit skeletal muscle. The residue was then extracted with 0.6 M KI, 20 mM Na thiosulfate, 5mM  $\beta$ -mercaptoethanol, 10 mM Tris, pH 7.2. After filtration and centrifugation, the supernatant was chromatographed on a DEAE-cellulose column, using a 0.05-0.50 M KCl gradient in 2 M urea. The barbed end inhibitor fraction (BEIF) was eluted at  $\sim 0.1$  M KCl, and the pointed end inhibitor fraction (PEIF) at  $\sim 0.2$  M KCl. PEIF was characterized by its ability to inhibit F-actin elongation under conditions in which "barbed" end growth in 50 mM KCl was retarded by known inhibitors (cytochalasin D or a 90K platelet protein). In addition, this fraction accelerated actin polymerization in the absence of "barbed" end inhibitors, and did not inhibit actin polymerization stimulated by erythrocyte actin-spectrin-band 4.1 complex in 0.4 mM  $MgCl_2$ . BEIF was characterized by its ability to inhibit actin polymerization stimulated by the erythrocyte complex; it enhanced the rate of actin polymerization in the "pointed" end inhibitor assay. We suggest that proteins in the two different inhibitor fractions may cap the opposite ends of actin filaments in muscle, and could theoretically serve as regulators of length, or linkages between filaments and the Z-line. (Supported by ACS grant CD-73, NIH grant GM-22289, and an AHA fellowship).

**T-AM-E5** EFFECTS OF ACTIN-BINDING FACTORS ON THE ASSEMBLY/ DISASSEMBLY OF ACTIN FILAMENTS. Yu-Li Wang and D. Lansing Taylor, Department of Cellular and Developmental Biology, Harvard University, Cambridge, Ma. 02138.

The effects of various actin-binding factors on the assembly/ disassembly of actin filaments are investigated using fluorescence energy transfer assays. The extent of filament assembly is studied by measuring the steady-state energy transfer of the copolymers of donor-and acceptor-labeled subunits. Kinetics of filament assembly, monomer incorporation, and subunit exchange are followed by measuring the change of energy transfer in a solution of donor-and acceptor- labeled subunits mixed in monomeric or filamentous form. Filament depolymerization is followed by diluting preformed donor-acceptor copolymers into excess buffers.  $1\mu M$  cytochalasin B (CB) causes a  $\sim 3\%$  depolymerization of filaments. However, the exchange of subunits among filaments is inhibited by  $>50\%$ . The effect is caused by a combination of reduced rates in monomer incorporation and in depolymerization. At  $10\mu M$  CB, destabilization of filaments is observed without significant depolymerization. The assays have also been used to study the effects of various cytoplasmic actin-binding factors including villin and a factor from *Dictyostelium discoideum*, both factors induce dramatic decreases in the low-shear viscosity of actin filaments. The disassembly is stimulated by villin, but is inhibited by the *Dictyostelium* factor, suggesting that the two factors interact with actin filaments through different mechanisms.

**T-AM-E6** INCORPORATION OF ATP INTO MUSCLE F-ACTIN IN THE PRESENCE OF CYTOCHALASIN D. J.E. ESTES, L.A. SELDEN, L.C. GERSHMAN, Research Service, V.A. Medical Center, Albany and Department of Physiology, Albany Medical College, Albany, NY 12208

It is generally acknowledged that cytochalasin D (CD) stimulates actin ATPase activity in the presence of  $MgCl_2$ . With increasing [actin], the rate of  $P_i$  liberation increases linearly up to the critical actin concentration (CAC) where it tends to a plateau value. The magnitude of the plateau value in 1 mM  $MgCl_2$  is dependent on [CD] and is increased over control about 15-fold with  $1\mu M$  CD and around 20-fold with  $10\mu M$  CD. Concomitant measurement of the incorporation of ATP into the polymer fraction during this ATPase activity shows the initial rate of incorporation to be on the order of 2-fold higher than control with  $1\mu M$  CD and 12-fold higher with  $12\mu M$  CD present. With  $10\mu M$  CD and in the [actin] range of 5-30  $\mu M$ , the initial rates of ATP incorporation were similar in magnitude, suggesting that the number of polymer ends in these solutions was the same. These observations cannot be accounted for by a change in the size of the monomer fraction because the CAC, as determined by both viscosity and the ability of the actin populations to activate myosin ATPase activity, increased only 2- to 3-fold over the [CD] range used (0-10  $\mu M$ ). Thus, the increase in ATP incorporation induced by CD is less compatible with the notion that CD induces actin monomer ATPase activity, but is more in agreement with a mechanism whereby ATP hydrolysis is coupled with actin polymerization. Supported by the Veterans Administration.

**T-AM-E7** FACTORS AFFECTING THE COMPOSITION OF THE PLATELET'S CYTOSKELETON AND THE STATE OF ITS ACTIN. A. Stracher and S. Rosenberg\* (Introduced by Eleanor McGowan). Department of Biochemistry, SUNY-Downstate Medical Center, Brooklyn, N.Y.

Platelets are highly motile cell bodies which contain a large concentration of contractile proteins. When human blood platelets are immersed in an ice cold solution containing 1% Triton X-100, 40 mM KCl, 10mM imidazole-HCl, 10mM EGTA, 2mM  $\text{NaN}_3$ , pH 7.0 a flocculent precipitate appears immediately in the tube. This precipitate can be collected at 3,000 x g and SDS-poly-acrylamide gel analysis shows it to consist mainly of actin,  $\alpha$ -actinin, actin-binding-protein (ABP) and varying amounts of myosin. We have referred to this as the platelets' cytoskeletal structure. Modifications of this Triton solution used to isolate the platelets' cytoskeleton can cause profound changes in the nature of the cytoskeleton isolated. Inclusion of EDTA in the Triton isolation solution results in an increase in the amount of myosin associated with the cytoskeleton, whereas including MgATP decreased the myosin yield. Increasing the KCl concentration or decreasing the EGTA concentration leads to a lower recovery of ABP and actin in the cytoskeletal precipitate. If the cytoskeleton is kept intact during its isolation, ABP and  $\alpha$ -actinin appear to protect the cytoskeletal actin from depolymerization. When platelets are stimulated with thrombin for 2 minutes before the Triton-solution is added, 3-4 time more myosin is found to be associated with the Triton-insoluble cytoskeleton. Since myosin can also confer protection to actin against depolymerization, it may be responsible for the observation that more actin is transformed from G to F and subsequently associated with the activated platelet's cytoskeleton, especially when prepared using high KCl or low EGTA-containing Triton solution as has been demonstrated by others. (Supported by NIH grant HL14020).

**T-AM-E8** A 72,000 MOLECULAR WEIGHT PROTEIN FROM TOMATO DISSOCIATES THE RABBIT ACTO-S-1 COMPLEX. Maryanne T. Vahey and Stylianos P. Scordilis, The Department of Anatomy, Albert Einstein College of Medicine, Bronx, NY and The Department of Biological Sciences, Smith College, Northampton, MA

Tomato actin associating protein (AAP) is a molecule of an apparent molecular weight of 72,000 that co-purifies with tomato actin. In an assay system comprised of rabbit skeletal muscle F actin and rabbit skeletal muscle myosin Subfragment-1 (S-1), the tomato AAP inhibits the actin activation of S-1. At a molar ratio of 1 AAP to 5 F actin, a 50% inhibition is observed. At this same molar ratio, a free calcium ion concentration between pCa 5 and 3.5 restores the actin activated ATPase to 100%. AAP has no effect on the basal  $\text{Mg}^{++}$ ATPase of the myosin S-1 in the absence of F actin. The mechanism by which the tomato AAP inhibits actin activation appears to be by a dissociation of the rabbit acto-S-1 complex. This is suggested by the facts that: (1) when AAP is mixed with F actin, in the absence of ATP, no decoration of the actin with S-1 is observed by electron microscopy and (2) when AAP is mixed with F actin and myosin S-1, analysis of the supernates of high speed centrifugations indicates that the myosin S-1 is dissociated from the F actin even in the absence of ATP.

**T-AM-E9** MAGNESIUM AFFECTS THE NUCLEATION STEP IN ACTIN POLYMERIZATION. J.A. Cooper, T.Y. Tsong, and T.D. Pollard. (Intr. by R. DeVoe) Depts. of Cell Biology and Anatomy and Physiological Chemistry, Johns Hopkins University School of Medicine, Baltimore, MD. 21205.

The polymerization of actin monomers into filaments consists of two steps, nucleation and elongation. Nucleation is slower than elongation, generating a sigmoidal curve for polymer formation vs. time.  $\text{Mg}^{++}$  accelerates actin polymerization. Increasing concentrations of  $\text{Mg}^{++}$  from 1  $\mu\text{M}$  to 10 mM increase the overall rate of actin polymerization in the presence of 0.1 M KCl. The half maximal effect occurs at approximately 50  $\mu\text{M}$   $\text{Mg}^{++}$ .  $\text{Ca}^{++}$  antagonizes the effect of magnesium but has no independent effect of its own. 1 mM  $\text{Mg}^{++}$  markedly accelerates overall polymerization by increasing the nucleation rate without increasing the elongation rate.  $\text{Mg}^{++}$  increases the nucleation rate as shown by 1) an increase in the initial rate of actin polymerization and 2) a decrease in the delay time of polymerization. Plots of log rates vs. log actin concentration have slopes between 1 and 2, indicating that the nucleus may contain two monomers.  $\text{Mg}^{++}$  has little effect on elongation, as assessed in two assays. First, the polymerization of actin to which sheared actin filaments have been added as nuclei is affected little by 1 mM  $\text{Mg}^{++}$ . Second, the elongation rate constants, measured in an electron microscopic assay, change little. At the barbed end, both the association and dissociation rate constants decrease with the addition of 1 mM  $\text{Mg}^{++}$  to 0.1 M KCl but the net rates at various monomer concentrations change little. The rate constants at the pointed end are not accurately measured, but the net rates do not increase to near those for the barbed end.  $\text{Mg}^{++}$ , therefore, likely affects the nucleation step. Supported by NIH grants GM7309 and GM 26132 and GM 26338.



**T-AM-E10** HOW TO BUILD A BEND INTO AN ACTIN BUNDLE. David DeRosier, Rosenstiel Center, Brandeis University, Waltham, MA 02254; Lewis G. Tilney, Department of Biology, University of Pennsylvania, Philadelphia, PA 19104; and Chean Eng Ooi, Graduate Biophysics Program, Brandeis University.

In non-muscle cells, actin filaments are often found assembled into bundles. In the sperm of the horseshoe crab there is a 60 $\mu$  long actin bundle which is coiled about the base of the nucleus. The coiled bundle is polygonal rather than circular with each turn consisting of 14 straight segments, each .7 $\mu$  long and 14 bends each making an angle of about 155°. Isolated from the cell, the coil is a rigid, stable structure. The rigidity and stability are consequences of the crossbridging between filaments which must lock the bends into the structure; otherwise, when the coil is isolated free of cellular constraints, it would straighten out. We will show how the geometry of the bundle determines the angle of the bend and allows such bends to be locked into the structure.

In passing through a bend, different filaments travel different distances. Those on inside tracks (at lower radii of curvature) have a shorter path than those on outside tracks. If we examine neighboring filaments, we find that the difference in path length is equal to the distance between crossbridging sites on a filament. Thus in the straight region, the crossbridging sites on adjacent filaments are exactly in register and crossbridging occurs. As the filaments enter a bend, the path lengths begin to differ and the crossbridging sites fall out of register. At the end of the bend, the path length has increased until the crossbridging sites are again in register and crossbridging between filaments is reestablished and the bend locked in. Given this condition the angle of the bend is equal to the spacing of crossbridging sites divided by the projected interfilament distance. Supported by GM26357 (DJJ) and HD14474 (LGT).

**T-AM-E11** THE 95,000 DALTON ACTIN BINDING PROTEIN FROM *DICTYOSTELIUM DISCOIDEUM*.

Marcus Fechheimer, John Brier, Mark Rockwell, and D.L. Taylor. Cell and Developmental Biology, Harvard University, Cambridge, Massachusetts, 02138.

An actin-binding protein from *D. discoideum* having an apparent molecular weight of 95,000 daltons was originally identified by fractionation of the contracted gel pellet derived from an extract of slime mold amoebae (Hellewell, S.B., and D.L. Taylor, *J. Cell Biol.* 83, 633, 1979). When mixed with purified rabbit skeletal muscle actin, the 95K-containing fraction formed a complex having a high viscosity. This interaction was optimal if the free  $[Ca^{2+}]$  was ca.  $10^{-8}M$ , and the pH was 6.8. More recently, purification of this protein from the extract of *D. discoideum* has been reported (D.L. Taylor, et al., in *CSHSQB XLVI*, 1981). Purified 95K protein is rod-shaped, and has a length of 40 nm when viewed by rotary shadowing techniques. Electrophoretic analysis of this protein in either the presence or absence of sodium dodecyl sulfate following cross-linking with dithiobis(succinimidyl propionate) indicates that the native molecule is a dimer. As judged by falling ball viscometry, slime mold 95K and chicken gizzard filamin are equally competent to form complexes of high viscosity when mixed with actin in the presence of 50 mM KCl,  $10^{-8}M$  free  $[Ca^{2+}]$ , pH 6.8. The activity of 95K, but not filamin, is greatly reduced if tested either in the presence of  $10^{-6}M$  free  $[Ca^{2+}]$ , or at pH 7.5. The binding of 95K to actin, measured by co-sedimentation, is also modulated by the free  $[Ca^{2+}]$ . In contrast to some other calcium-sensitive actin binding proteins, 95K does not dramatically restrict the length of actin filaments in the presence of  $10^{-6}M$  free  $[Ca^{2+}]$ . We suggest that the 95K protein may contribute to regulation by calcium of the structure and contractility of the motile apparatus of *D. discoideum* amoebae.

**T-AM-E12** POLYAMINE-INDUCED POLYMERIZATION OF *PHYSARUM* PLASMODIAL ACTIN. Mark R. Adelman, Department of Anatomy, Uniformed Services University of the Health Sciences, Bethesda, MD 20814.

Studies in this laboratory suggested the polymerization of *Physarum* actin might be regulated by small molecule effectors. Reports of the polymerization of muscle actin by polyamines prompted an analysis of the effects of these compounds on *Physarum* actin, which was prepared as described previously (Biochem. 16, 4862), but with an additional polymerization-depolymerization cycle. The protein was equilibrated with 1mM Pipes, 0.1mM ATP, 1mM  $\beta$ MSH, pH 7.0 by passage over a column of Bio-Gel P6DG immediately prior to use. As judged by viscometry, spermidine (S) caused polymerization to the same extent as did KCl (50-100mM). The rate of S-induced polymerization increased from very slow at low concentrations (<0.1mM) to a maximum (which was  $\approx$  that with KCl) at 0.5mM or above. Putrescine (0.5mM) caused a slower polymerization which reached the same final level as with S. Spermine caused extensive aggregation and flocculation; similar aggregation occurred with S in poorly-buffered solutions. When polymerization was followed by measuring changes in UV absorption, either at  $\lambda = 282$  nm or  $\lambda = 232$  nm, S-polymerization showed a different dependence on ionic strength than did  $Mg^{2+}$ -induced polymerization. When KCl is added to actin polymerizing in the presence of  $Mg^{2+}$  the polymerization rate increases; the same is true when  $Mg^{2+}$  is added to actin containing KCl. In contrast, the addition of KCl to actin, either before or after the addition of S, leads to a polymerization rate characteristic of KCl alone. Similar results were obtained with mammalian skeletal muscle actins. These data suggest that S only causes actin polymerization at non-physiological (low) ionic strength; *in vivo*, S is unlikely to function as an effector of actin polymerization. Supported by USUHS Protocol C07015.

**T-AM-E13** EVALUATION OF *ACANTHAMOEBA* PROFILIN BINDING TO ACTIN AND ACTIN-DNase BY NONEQUILIBRIUM DIALYSIS. M.R. Runge, J.A. Cooper, P. Tseng and T.D. Pollard. (Intr. by R. Williams, Jr.) Dept. of Cell Biology and Anatomy, Johns Hopkins University School of Medicine, Baltimore, MD. 21205.

We used a new non-equilibrium dialysis method to measure the binding of *Acanthamoeba* profilin to skeletal muscle actin monomers. The free profilin concentration was determined from the initial rate of diffusion of profilin across a large pore (MW cutoff: 25,000) dialysis membrane. Nanogram quantities of profilin moving into the buffer compartment were measured by a solid phase antibody binding assay. Actin monomer in the sample compartment reduced the free profilin concentration and the rate of diffusion into the buffer compartment. We calculated the bound profilin by difference. A Scatchard plot of data obtained by this technique was linear over a wide range of profilin concentrations and gave a dissociation constant,  $K_D$ , of  $8.5 \mu\text{M}$  with 2.3 profilin molecules bound to actin at saturation. Profilin also bound to the 1:1 complex of actin and pancreatic DNase-I with a stoichiometry of 0.9 profilin molecules per actin and a  $K_D$  of  $10.4 \mu\text{M}$ . There was little or no binding of profilin to actin filaments or a number of other proteins. The relatively weak binding of profilin to actin, compared with the affinity of actin for the end of actin filaments ( $K_D \sim 1 \mu\text{M}$ ) explains why low concentrations of profilin inhibit nucleation but neither the elongation rate nor the steady state extent of polymerization of actin filaments. Although profilin does not prevent actin polymerization, it could act as an actin monomer buffer in the cell, especially in the suppression of spontaneous nucleation. The nonequilibrium dialysis method is potentially applicable for measuring the binding of any small protein or macromolecule to a larger one. Supported by NIH Grant GM 26338.

**T-AM-E14** MOLECULAR CHARACTERIZATION OF THE MAP 2/PROTEIN KINASE COMPLEX. W.E. Theurkauf\* and R.B. Vallee, Cell Biology Group, Worcester Foundation for Experimental Biology, Shrewsbury, MA

MAP 2 is the major microtubule associated protein in brain. We have found that essentially all of the cyclic AMP dependent protein kinase activity that is found in brain microtubule preparations is associated with MAP 2 (Vallee et al., 1981, J. Cell Biol., 90, 568). Here we report on the molecular characterization of the kinase and the nature of its association with MAP 2. The following results were obtained using calf brain microtubules prepared by 3 cycles of assembly/disassembly purification, or chromatographically purified calf brain MAP 2. 1) The photo-affinity label 8-N<sub>3</sub>-[<sup>32</sup>P]cyclic AMP specifically labeled polypeptide species of  $M_r=54,000$  and  $57,000$  in purified MAP 2 or microtubule preparations. The two peptide species correspond to the dephospho- and phospho- forms of the regulatory subunit of a type II cyclic AMP dependent protein kinase. 2) Chromatography of microtubules on Bio-Gel A-15m or DEAE-Sephadex in the presence of  $10 \mu\text{M}$  cyclic AMP led to the total dissociation of protein kinase catalytic activity from MAP 2. Catalytic activity cochromatographed with a minor protein species of  $M_r=39,000$ , corresponding to the catalytic subunit of cyclic AMP dependent protein kinase. 3) Cyclic AMP binding activity, as determined using [<sup>3</sup>H]-cyclic AMP, cochromatographed with MAP 2 in the presence or absence of cyclic AMP. 4) Using cAMP binding activity as an assay we have found that one third of the cAMP dependent protein kinase in brain cytosol is associated with MAP 2. In light of recent evidence indicating that MAP 2 is localized in the dendritic portion of neurons, we propose that the MAP 2/protein kinase complex represents a major cAMP activated phosphorylation system in dendrites. Supported by grant GM 26701 to R.V.

**T-AM-F1** AMPLIFIED EXCHANGE OF ATP FOR BOUND ADP DURING RHODOPSIN-META II TRANSITION IN INTACT ROD OUTER SEGMENTS. Ralph Zuckerman, Stan M. Dacko, and Geoffrey J. Schmidt (Intr. by Alice Adler), Eye Res. Inst. of Ret. Found., Boston, MA 02114

We report a rapid, light-initiated exchange of ATP for bound ADP in intact rod outer segments (ROS) of the frog. Assay of nucleotide levels was performed with a purified luciferin-luciferase reagent which is virtually unreactive ( $<0.7\%$  of ATP response) to other nucleoside mono-, di- and triphosphates. Bound and unbound phases of the preparation are resolved and assayed separately, enabling us to distinguish between hydrolysis and binding. The unbound phase is assayed directly while bound nucleotides are released by a mild acid treatment (10% TCA). Upon illumination of the ROS, ATP is rapidly removed from the soluble phase of ROS, accompanied by the concomitant release of ADP. Acid extraction reveals little change in total (bound + unbound) ATP and ADP levels, ruling out substantial light-activated hydrolysis of these nucleotides. The exchange process involves the binding of  $\sim 0.5$  mM ATP ROS $^{-1}$  to a saturating flash. At light levels well below saturation ( $<0.001\%$  bleach) the exchange process is highly amplified, with  $2.45 \pm 0.98 \times 10^3$  ATP bound photon $^{-1}$  ROS $^{-1}$ . Rapid time-resolution techniques reveal that ATP-binding is rapid, occurring within 250 msec of a saturating flash. Bleaching rhodopsin to meta II results in ATP exchange for bound ADP, whereas photoreversal of meta II by a blue flash dissociates ATP from its binding site. The photoreversibility of ATP-binding during the rhodopsin to meta II transition establishes, for the first time, a direct link between the state of an early intermediate of photolyzed rhodopsin and the state of a nucleoside triphosphate in intact ROS. This light-activated ATP binding may be the first experimental evidence of the event that has been postulated to inactivate phosphodiesterase.

**T-AM-F2** ATPase MEDIATED PUMPING OF PROTONS INTO RETINAL ROD DISKS AND THEIR PHOTO-EJECTION

T. Borys, R. Uhl and E.W. ABRAHAMSON

Guelph-Waterloo Centre for Graduate Work in Chemistry

Guelph, Ontario

When fresh bovine rod outer segments (ROS) with broken plasma membranes are treated with exogenous Mg-ATP an ATPase mediated dark pumping of protons accompanied by anion symport into the disk lumen occurs which can be monitored by scattered light intensity changes that accompany the swelling of the disks. Flash photolysis of the rhodopsin in the proton loaded disks results in rapid ejection of the protons without anion symport in times  $<50$  msec. in a ratio of approximately 1 proton to 1 photolyzed rhodopsin molecule. This photolysis, in turn, stimulates a renewed, rate enhanced, ATPase proton pumping which is further increased by the presence of exogenous cGMP. A separate GTPase activity leading to swelling of the disks is also observed concurrent with the renewed ATPase activity but this GTPase activity is about 1/80th that of the ATPase. As this same proton pumping and photo-ejection can also be observed with plasma membrane intact ROS containing endogenous Mg-ATP it is suggested that these processes play a role in visual transduction.

**T-AM-F3** ATP-INDUCED RELEASE OF CALCIUM FROM ROS DISCS. H. Gilbert Smith and Peter M. Capalbo, Advance Technology Laboratory, GTE Laboratories Inc., Waltham, MA 02254

Addition of 1 mM ATP or 1 mM GTP to the buffer flowing past 45-Ca-loaded discs supported by controlled pore glass (PG-2000-400) or Celite-545 in a flow system causes a release of calcium from the discs into the buffer in the dark. 3',5'-cyclic GMP has either no effect or an extremely small effect. Combinations of cGMP, ATP and/or GTP are no more effective than ATP or GTP alone. There is considerable variation in the ATP- or GTP-induced calcium release. Most experiments show a release of about one calcium per rhodopsin, but some show releases as high as 3.4 calcium per rhodopsin or as low as 0.1 calcium per rhodopsin. The ATP-induced release was observed even when the external buffer contained 1 mM CaCl $_2$  and 1 mM MgCl $_2$  in addition to 1 mM ATP. This indicates that the observed release is not due simply to chelation by ATP of calcium bound to the external disc surface. Pretreatment of the Ca-loaded discs with the ionophor, A23187, abolished the ATP-induced release and further suggests that the released calcium comes from within the discs.

The bovine ROS discs, isolated by Ficoll flotation, were loaded with 45-calcium by overnight incubation in the refrigerator in a pH 8 solution containing 0.1 M imidazole, 0.1 M KCl, 15 mM CaCl $_2$  and 0.5 mM DTT. After removal of external calcium in the flow system, 4 to 6 mole calcium remained associated with the discs for each mole rhodopsin in the sample. Addition of ATP or GTP to the solution in which the discs were incubated caused an approximately 70% reduction in the amount of calcium accumulated by the discs.

**T-AM-F4** SIMPLE BUFFER MODEL EXPLAINS LOW  $[Ca^{2+}]_0$  EFFECTS ON TOAD ROD PHOTORESPONSE. Richard E. Greenblatt, Jules Stein Eye Institute, University of California, Los Angeles, CA 90024.

Lowered  $[Ca^{2+}]_0$  in the range  $10^{-6}$ - $10^{-9}$ M affected sensitivity and flash response waveform in *Bufo marinus* photoreceptors. Sensitivity decreased in a concentration-dependent manner by up to 10,000 fold. Changes in flash response waveform due to low  $[Ca^{2+}]_0$  included increased apparent latency, increased time-to-peak, and decreased time-to-decay. These waveform changes differed significantly from those caused by adapting lights which produced comparable desensitizations. In addition, the effects of adapting lights and low  $[Ca^{2+}]_0$  were not additive, suggesting that low  $[Ca^{2+}]_0$  and adapting lights desensitize the photoresponse by differing mechanisms.

Flash response and adaptation kinetics measured in normal (1.8mM)  $[Ca^{2+}]_0$  were modelled by simple algebraic functions. Assuming that calcium is the internal transmitter for transduction, the effect of lowering  $[Ca^{2+}]_0$  could be modelled on the assumption that decreasing  $[Ca^{2+}]_0$  acted to increase the concentration of an endogenous  $Ca^{2+}$ -buffer. With buffer concentration and  $V_{max}$  as the only free parameters, good agreement was obtained between experimental data and model calculations. In particular, the calcium buffer hypothesis provides generally accurate predictions of the effects of low  $[Ca^{2+}]_0$  on the shape of the intensity/response function, the dark adapted sensitivity, the changes in sensitivity in background lights, the results of two flash experiments, and the alterations in waveform both under dark-adapted and light-adapted conditions.

**T-AM-F5** CALCIUM-INDUCED CHANGES IN PHOTORECEPTOR LIGHT-DEPENDENT PERMEABILITY NOT CORRELATED TO CYCLIC GMP. Woodruff, Michael L. and Gordon L. Fain. Jules Stein Eye Institute, UCLA Medical Center, Los Angeles, CA 90024.

We have measured the levels of 3',5'-guanosine monophosphate (cyclic GMP) in isolated retinas from toad to investigate their correlation to the opening and closing of the light-dependent permeability of photoreceptors. When  $Ca^{2+}$ -induced changes in cyclic GMP concentration are compared to the  $Ca^{2+}$ -induced changes in the permeability of photoreceptor light-dependent conductance, four quantitative dissimilarities are noted. First, when extracellular  $Ca^{2+}$  ( $[Ca^{2+}]_0$ ) is reduced from normal physiological levels to  $10^{-7}$  M, the light-dependent permeability is increased, but cyclic GMP levels are not significantly changed. We find that cyclic GMP levels are increased only when  $[Ca^{2+}]_0$  is lowered below  $10^{-7}$  M, with a maximum increase from a mean of 56.2 pmoles/mg protein in normal Ringer to over 1000 pmoles/mg protein when  $[Ca^{2+}]_0 \leq 10^{-8}$  M. Second, when  $[Ca^{2+}]_0$  is increased from 1.8 mM to 20 mM, the light-dependent permeability is suppressed, but cyclic GMP levels are decreased by only 10-15%, about one-quarter the decrease that can be obtained with bright illumination. Third, when  $[Ca^{2+}]_0$  is increased from  $10^{-8}$  M to 20 mM, the light-dependent permeability is closed rapidly, but the time course of cyclic GMP decrease is much slower. Fourth, when  $[Ca^{2+}]_0$  is lowered to  $10^{-8}$  M, the sensitivity of the light-dependent permeability to steady illumination is decreased by 3 to 4 orders of magnitude, but the sensitivity of the light-dependent decrease in cyclic GMP is not significantly affected. These observations indicate that there is no simple correlation between cyclic GMP in rods and the opening and closing of the light-dependent conductance. They also show that  $Ca^{2+}$  can affect the conductance without changes in cyclic GMP content.

**T-AM-F6** LIGHT REGULATES GTPase AND KINASE ACTIVITIES IN SQUID PHOTORECEPTORS. Carol A. Vandenberg and M. Montal, Depts. of Neurosciences, Physics and Biology, UCSD, La Jolla, CA 92093

The central regulatory role of a GTP-binding protein has been established in hormone-activated adenylate cyclase, protein chain elongation, and light-activated phosphodiesterase of vertebrate rods. Recent observations suggest that guanosine triphosphates may also participate in *Limulus*<sup>1</sup> and octopus<sup>2</sup> photoexcitation.

In squid, GTPase and kinase activities are stimulated on illumination. Squid (*Loligo opalescens*) rhabdomes purified by sucrose density centrifugation have a GTPase whose activity is increased >4 fold by illumination. Half maximal GTPase activity is observed when less than 1% of the rhodopsin has been photo-converted to metarhodopsin. The  $k_m$  of the light-regulated enzyme is  $\sim 1 \mu$ M GTP. Dithiothreitol preserves the light-regulated activity of the GTPase. Binding of Gpp(NH)p, a non-hydrolyzable analog of GTP, to membranes is enhanced >10 times by illumination.

Illumination of rhabdomes from gently shaken squid retinas (*L. opalescens* or *L. pealei*) results in phosphorylation of several proteins. In the presence of  $Mg$ - $[\gamma^{32}P]ATP$ , rhodopsin phosphorylation is increased 15-20 fold by light, to an average of 1-1.5 phosphates incorporated per rhodopsin. After illumination, delay of addition of ATP in the dark causes a loss of phosphate incorporation within 1 hr. Light also causes phosphate incorporation into 2 bands on SDS-polyacrylamide gels of apparent molecular weights 55,000 and <15,000 daltons. A low molecular weight component is phosphorylated in the dark, and to a lesser extent in the light. This component appears to be lipid. Supported by USPHS EY 02084 and the Grass Foundation.

<sup>1</sup>Fein & Corson (1981) Science 212:555. <sup>2</sup>Calhoon et al. (1980) Biochem. Biophys. Res. Commun. 94:1452

**T-AM-F7** INTRACELLULAR FREE  $Mg^{2+}$  IN BALANUS PHOTORECEPTORS ESTIMATED WITH ERIochrome BLUE. H. Mack Brown and Bo Rydqvist. Dept. of Physiology, University of Utah College of Medicine, Salt Lake City, Utah, 84108; Dept. of Physiology, Karolinska Institutet, Stockholm, Sweden.

Intracellular free  $Mg^{2+}$  ( $Mg_f^i$ ) in Balanus eburneus photoreceptors was estimated by measuring absorbance changes of eriochrome blue (EB) during injection into the cells. It has been shown that EB absorbance is virtually unaffected by  $Ca_f^i$  at suitable wavelength pairs (Scarpa, A., *Biochem.* 13: 2789, 1974). The values obtained for  $Mg_f^i$  were used to correct basal values of  $Ca_f^i$  obtained from  $Ca^{2+}$  ion-sensitive electrodes and Arsenazo III absorbance changes, since both techniques have finite sensitivity to  $Ca^{2+}$ . Absorbance changes were measured in a dual wavelength microspectrophotometer. Absorbance changes at 570 nm were used to monitor EB concentration and the wavelength pair 600-720 nm was used to determine the Mg-EB complex. The mean value of  $Mg_f^i$  from 5 cells was 0.6 mM. There was no absorbance change at 600-720 nm during illumination of EB injected cells indicating that  $Mg_f^i$  does not change appreciably. Cells injected with Arsenazo III yielded a mean value of  $2.3 \times 10^{-7}M$  Ca in darkness (corrected for 0.6 mM  $Mg_f^i$ ) and illumination of the cell raised this value to  $9.9 \times 10^{-7}M$   $Ca_f^i$ . Comparable measurements with  $Ca^{2+}$  ion-sensitive electrodes (Brown, Pemberton, Owen, *Anal. Chim. Acta* 85: 261, 1976) yielded a resting value of  $2 \times 10^{-7}M$  in dark adapted cells (corrected for 0.6 mM  $Mg_f^i$ ) and  $1.1 \times 10^{-6}M$   $Ca_f^i$  during illumination. These measurements indicate that (a)  $Mg_f^i$  in this photoreceptor is comparable to that found in some other tissues, (b) that  $Mg_f^i$  does not change appreciably with light and (c) that  $Ca_f^i$  measurements obtained with AIII and Ca-ISE are in good agreement when corrected for  $Mg_f^i$ . (NIH Grant #EY00762)

**T-AM-F8** ALKALINE PHOSPHATASE AND PROTEIN KINASE INHIBITOR DIALYZED INTO LIMULUS VENTRAL PHOTORECEPTORS. J. Stern and J. Lisman Brandeis Univ. Waltham Mass.

When alkaline phosphatase (MW 68,000) or protein kinase inhibitor (MW 26,000) were dialyzed into ventral photoreceptors, quantum bumps, ordinarily the response to single photons, were observed in the dark. A criterion 20X increase in quantum bump rate occurring within 10 min, was induced by 10 Units/ml alk. phosphatase or 50 U/ml protein kinase inhibitor. Cooperation was apparent, for example, 2 U/ml alk. phosphatase dialyzed with 10 U/ml kinase inhibitor caused bump rate to exceed the criterion.

The following observations weaken the possibility that bumps were produced by two cooperative, contaminant activities in the commercial preparations (Sigma). The similar effect of *E. coli* or bovine alk. phosphatase and rabbit or bovine kinase inhibitor depended on the extent to which the activity had been purified and not on total protein content. Conventional dialysis using a 14,000 MW cutoff membrane to remove low MW contaminants did not alter the proteins ability to cause bumps.

This is the first report that proteins can be introduced into functional cells by the internal dialysis technique. The results suggest that dephosphorylation, most probably protein dephosphorylation, can regulate an early step in visual transduction. Experiments with purer enzyme preparations will be needed to confirm this suggestion.

**T-AM-F9** DYE LABELING OF PATENT ROD OUTER SEGMENT DISKS SHOWS THAT LIGHT-CYCLE DEPENDENT BIREFRINGENCE BANDS CORRESPOND TO DAILY DISK SYNTHESIS. Michael W. Kaplan, Dept. of Ophthalmology, Good Samaritan Hospital & Medical Center, Portland, OR 97210.

Rod outer segments from amphibians maintained on cyclic light and dark cycles exhibit periodic birefringence bands normal to the cell axis (1). The band period of 1.3  $\mu m$  for Rana pipiens and 2.2  $\mu m$  for Xenopus laevis maintained on a 14 hr light-10 hr dark cycle at 21°C suggests that each band corresponds to the amount of disk membrane synthesized and displaced distally along the ROS axis in one day. To confirm that this is the case, adult Xenopus laevis were injected intraocularly with 5  $\mu l$  of a Ringer solution containing 4% (by wt.) lucifer yellow. The dye penetrated and bound to the patent disk membranes near their synthesis site at the basal end of the outer segment. Dye trapped when the open disks sealed was transported distally in a distinct fluorescent band (2). A second dye injection 4-6 days later produced a second fluorescent band, and unambiguously marked the distance occupied by disks synthesized between injections. Outer segments were observed in a microscope fitted with both polarizing and fluorescence optics. The number of birefringence bands between the fluorescent dye bands was invariably equal to the number of days between dye injections. It is concluded that the birefringence bands reliably define the daily synthesis of new disks.

Supported by USPHS EYO1779 and the Oregon Lions Sight & Hearing Foundation.

1. M. W. Kaplan, *Investig. Ophthalmol. Vis. Sci.*, 21 395 (1981).
2. A. M. Laties, D. Bok & P. A. Liebman, *Exp. Eye Res.* 23 139 (1976).

**T-AM-F10** LIGHT-INDUCED VOLTAGE FLUCTUATIONS IN THE PHOTORECEPTORS OF BARNACLES AND THE HONEYBEE DRONE. A. Mauro, E. Kaplan and S. Poitry, The Rockefeller University, New York, N.Y. 10021.

The membrane potential of various invertebrate photoreceptors (e.g.: horseshoe 'crab', locust, and fruit fly) exhibit discrete waves ('quantal bumps') under dim illumination. It has been hypothesized that the summation of these waves gives rise to the receptor potential. With increasing light intensity the mean frequency of the waves increases, but the amplitude decreases. Several investigators have noted briefly that some arthropod photoreceptors (*B. eburneus*, Shaw, J. Physiol., 72; *B. nubilus*, Hudspeth and Stuart, J. Physiol. 77) do not show discrete waves.

We have studied in greater detail the photoreceptors of the lateral eye of the *B. eburneus*, the median eye of *B. nubilus* and the lateral eye of the honeybee drone. None of these receptors showed discrete waves even when the eyes were fully dark adapted, confirming the reports cited above. However, dim light induced small (<1mv) fluctuations, which increased with light intensity up to moderate levels. We have measured the spectral density of the voltage fluctuations, and, in the case of *B. nubilus*, the current fluctuations under voltage clamp. Possible explanations to account for the inability to observe discrete waves will be discussed.

**T-AM-F11** PROLONGATION OF FLASH RESPONSES IN LIMULUS PHOTORECEPTORS BY VANADATE AND GTP- $\gamma$ -S. D. Wesley Corson and Alan Fein, Marine Biological Laboratory

Recently vanadate and GTP- $\gamma$ -S (guanosine-5'-O- $\gamma$ -thio triphosphate) have been shown to induce the production of discrete waves similar to those normally elicited by light in *Limulus* ventral photoreceptors. In preliminary experiments, it sometimes appeared that these compounds prolonged the response to a test flash and thus interfered with the normal response to light. To assess prolongation, we stimulated cells at 10 second intervals with a series of fifty 20 msec test flashes which were just sufficiently bright to elicit a reliable response. Response currents elicited under voltage-clamp were sampled at 2 msec intervals for 2 seconds following the onset of the test flash and averaged over the fifty flash sequence.

Five cells exposed to 5mM vanadate in 1mM  $\text{Ca}^{++}$  ASW for 20 to 30 minutes showed pronounced prolongation on the falling phase of the average response waveforms compared to control averages taken before and after exposure. Cells bathed in 10mM  $\text{Ca}^{++}$  ASW and injected with GTP- $\gamma$ -S sometimes exhibited response prolongation similar to that seen with vanadate.

Prolongation of the average response waveform can be induced by exposure to vanadate or injection of GTP- $\gamma$ -S but does not necessarily accompany induction of discrete waves by these agents. For the 5 cells examined in vanadate, prolongation was not accompanied by a consistent reduction in average amplitude indicating that prolongation was not simply the result of a change in the latency distribution of evoked waves. Some individual records suggest that prolongation results from extra discrete waves late in the light response while others reveal long-lasting complex waveforms which cannot easily be resolved into discrete waves.

**T-AM-Po1** THE SUBTRANSITION IN DPPC: DILATOMETRIC STUDIES OF THE KINETICS OF FORMATION AND DETERMINATION OF THE TRANSITION TEMPERATURE. D.A. Wilkinson & J.F. Nagle, Carnegie-Mellon University, Pittsburgh, PA 15213

The low temperature subgel phase of DPPC (Chen, Sturtevant, & Gaffney, 1980, PNAS 77, 5060) forms very slowly and the transition has a remarkable amount of hysteresis which has precluded precise determination of the transition temperature. Equilibrium measurements performed on our dilatometer show that the subtransition upon heating is centered at 13.5°C, has a half-width of 0.6°C, and comprises a specific volume change of 0.009 ml/g (about 1/4 the size of the main chain melting transition). Upon cooling, the subtransition does not occur until below 6°C, and then the rate of formation of the subgel phase increases as the temperature is lowered, although it is still less than 0.00025 ml/gm.hr. at 1°C. The rate of formation as a function of temperature does not appear to follow simple theories based upon homogeneous nucleation. However, temperature jump experiments suggest that multiple homogeneous nucleation is present since once the subgel phase has begun to form, it will continue to grow in the range 6°C < T < 13°C. Therefore, the true transition temperature lies between 13 and 13.5°C. The large hysteresis upon cooling is presumably due to severe retardation of the formation of subgel phase nuclei above 6°C.

This work was supported by NIH Grant GM 21128.

**T-AM-Po2** THERMODYNAMICS AND KINETICS OF SPONTANEOUS LECITHIN TRANSFER. D.L. Hickson, J.B. Massey, J.T. Sparrow, and H.J. Pownall. Baylor College of Medicine and The Methodist Hospital, 6565 Fannin, Houston, Texas 77030.

We have synthesized lecithins with 9-(3-pyrenyl)nonanoic acid in the SN-2 position and lauric, myristic, palmitic, oleic or linoleic acid at SN-1. We have measured their retention time by high pressure hydrophobic chromatography through a Waters C<sub>18</sub> column eluted with 75% isopropanol and 25% triethylammonium phosphate. In addition, we have measured the rate constant,  $k$ , for the spontaneous transfer of these lecithins between reassembled lipid-protein complexes. The logarithm of the retention time ( $\log rt$ ) increases linearly with the number of methylene units in the lecithin.  $\log rt$  decreases linearly with the number of double bonds. Furthermore, the logarithm of the rate of transfer of pyrene labeled lecithins between lipid-protein complexes decreases linearly with the number of methylenes and increases linearly with the number of double bonds. Therefore, a log-log plot of  $k$  vs  $rt$  is linear. The transfer rate of pyrene labeled lecithins can be predicted from the equation

$$K = C \exp (0.3 d - 0.15 m)$$

where  $C$  is a constant,  $d$  is the number of double bonds and  $m$  is the number of methylene units. The relationship between the rate of transfer and retention time is given by

$$\log k = C' \log rt$$

These results suggest that the rate of desorption of lecithins from lipoproteins and vesicles is controlled by the hydrophobic effect and that these rates can be predicted from retention times obtained from hydrophobic chromatography. (Supported by grants HL 17269, HL 26250, and HL 19459).

**T-AM-Po3** OPTICAL MICROSCOPY OF MULTILAMELLAR PHOSPHOLIPID DISPERSIONS UNDERGOING PHASE TRANSITIONS Paul Yager and James P. Sheridan; Optical Probes Branch, Optical Sciences Division, Washington, D. C. 20375 USA, and Warner L. Peticolas; Department of Chemistry, University of Oregon, Eugene, OR 97403 USA

The changes in shape and size which accompany the endothermic phase transitions of aqueous dispersions of phosphatidylcholines have been monitored by light microscopy. The sharp chain melting phase transition of the liposomes can be clearly observed as the dimensions of some of the liposomes alter by as much as 40%. Liposomes of complex form show a remarkable "shape memory" which persists through several cycles of heating and cooling. The origin of this phenomenon is discussed, as is the relationship of the shape changes to the microscopic changes in the plane of the bilayer. This type of optical microscopic observation is a simple method for monitoring the dependence of the size of large liposomes on temperature, and provides a new method for estimating changes in area per lipid head group.

**T-AM-Po4** DEUTERIUM NMR OBSERVATIONS OF PHASE-TRANSITIONS IN LECITHIN-GRAMICIDIN BILAYER MEMBRANES.

P.W. Westerman, M.J. Vaz, L.M. Strenk and J.W. Doane. Northeastern Ohio Universities College of Medicine, Rootstown, Ohio 44272 and Liquid Crystal Institute and Department of Physics, Kent State University, Kent, Ohio 44242.

The polymorphism of aqueous multilamellar dispersions of 1-myristoyl-2-(14', 14', 14'-<sup>2</sup>H<sub>3</sub>)-myristoyl-sn-glycero-3-phosphocholine (DMPC-d<sub>3</sub>) with gramicidin, has been examined by <sup>2</sup>H NMR spectroscopy. The results obtained by D. Rice and E. Oldfield, *Biochemistry*, **18**, 3272 (1979), for this system at 30°C, have been duplicated. Their data have been extended by recording the spectra as a function of temperature for various lipid to protein ratios. The addition of small amounts of gramicidin to the lipid bilayer has little effect on the pretransition, but raises the sub-transition temperature. At higher protein to lipid ratios, (≥1:10), however, and for temperatures between the main phase temperature (24°C) and 30°C, an additional motionally restricted component is observed in the spectrum. This second powder-pattern spectrum may indicate the presence of a lipid annulus around the peptide, or it could arise from entrapment of lipid molecules by aggregation of the gramicidin in the bilayer.

(Supported in part by the National Institute of General Medical Sciences under Grant No. GM 27127-02).

**T-AM-Po5** THE EFFECT OF TETRACAINE ON THE PHYSICAL STATE OF DIPALMITOYLPHOSPHATIDYLCHOLINE SMALL UNILAMELLAR VESICLES AND THEIR SUSCEPTIBILITY TO PHOSPHOLIPASE A<sub>2</sub> ACTIVITY. M. Menashe, C.F. Schmidt T.G. Conley and R.L. Biltonen, Departments of Biochemistry and Pharmacology, University of Virginia School of Medicine, Charlottesville, Virginia 22908.

The effects of the local anesthetic tetracaine on the hydrolytic activity of pancreatic phospholipase A<sub>2</sub> was investigated using small unilamellar vesicles prepared from dipalmitoylphosphatidylcholine (DPPC) as substrate. At temperatures below the phase transition temperature a low anesthetic-to-lipid ratio (5 mole % tetracaine) enhances enzymatic activity, while at a higher anesthetic concentration (30 mole %) there is inhibition of phospholipase A<sub>2</sub> activity. Light scattering, nuclear magnetic resonance, electron microscopy, and high sensitivity differential scanning calorimetry (DSC) data suggest that tetracaine causes a concentration-dependent fusion of small unilamellar DPPC vesicles to larger unilamellar vesicles. DSC experiments show that at the lower anesthetic concentration the DPPC phase transition is broadened toward higher temperature but that the transition temperature remains essentially unchanged, while at the higher concentration the transition temperature is lowered by 3°C. We suggest that low concentrations of tetracaine enhance the initial activity of pancreatic phospholipase A<sub>2</sub> by inducing local volume fluctuations which allow the protein to penetrate the substrate vesicles more readily, whereas at high anesthetic concentrations the small vesicles fuse rapidly into large unilamellar vesicles which are poor substrates for the enzyme, and an apparent inhibition of enzymatic activity is observed. (Supported by grants from the NIH and NSF).

**T-AM-Po6** CHARACTERIZATION OF THE PRE-TRANSITION IN SMALL UNILAMELLAR DIPALMITOYL PHOSPHATIDYLCHOLINE VESICLES. M. Menashe, D. Lichtenberg, R.L. Biltonen, Departments of Biochemistry and Pharmacology, University of Virginia School of Medicine, Charlottesville, Virginia 22908.

Large multilamellar dipalmitoyl phosphatidylcholine (DPPC) liposomes undergo a gel-liquid crystalline transition at 41.3°C. This transition is preceded by a pretransition at about 34°C. It has previously been shown that small (~250Å) unilamellar DPPC vesicles exhibit a gel-liquid crystalline transition at about 37°C but no pretransition was noted. We now show that high sensitivity differential scanning calorimetry reveals the existence of a pre-phase transition in the small unilamellar vesicles at ~28°C. This transition is relatively slow (t<sub>1/2</sub> ≈ 1 min) and has an enthalpy change of about 0.2 kcal/mole. It has been shown previously that these small vesicles fuse into vesicles of an average size of about 700Å. This transformation in size is accompanied by an apparent 6°C increase in the pre-transition melting temperature. The main transition of the fused vesicles is similar to that of large multilamellar liposomes, but the enthalpy change of the pretransition is markedly smaller in the large unilamellar vesicles than in the multibilayers. (Supported by a grant from the NSF).



**T-AM-Po7** A DIFFERENTIAL SCANNING CALORIMETRIC STUDY OF THE INTERACTION OF  $\text{Ca}^{2+}$  ON MIXTURES OF DIMYRISTOYLPHOSPHATIDYL SERINE AND DIPALMITOYLPHOSPHATIDYLCHOLINE. T.G. Conley and E. Freire, Dept. of Pharmacology, Univ. of Virginia, Charlottesville, VA 22908 and Dept. of Biochemistry, Univ. of Tennessee, Knoxville, TN 37916.

The thermotropic behavior of dimyristoylphosphatidylserine (DMPS) and mixtures containing DMPS and dipalmitoylphosphatidylcholine (DPPC) at a constant pH of 7.4 have been investigated as a function of  $\text{Ca}^{2+}$  concentration using high sensitivity differential scanning calorimetry. In the absence of  $\text{Ca}^{2+}$  the heat capacity function of DMPS has a pronounced maximum at 36.2°C; however, this curve is assymetrical towards the high temperature end of the transition suggesting the presence of a second smaller peak at ~36.7°C. Addition of  $\text{Ca}^{2+}$  separates these two peaks. The area under the first peak decreases dramatically until it completely disappears at ~2 mM  $\text{Ca}^{2+}$ , whereas the area under the second peak is independent of the  $\text{Ca}^{2+}$  concentration. Both peaks are shifted to higher temperatures upon addition of  $\text{Ca}^{2+}$ . We have also obtained the phase diagrams for DMPS-DPPC mixtures in the presence and absence of  $\text{Ca}^{2+}$ . These phase diagrams are very sensitive to the concentration of  $\text{Ca}^{2+}$  and strongly non-ideal under all sets of conditions. In the absence of  $\text{Ca}^{2+}$  the transition temperatures of the mixtures are lower than those of either of the pure component lipids. The addition of low concentrations of  $\text{Ca}^{2+}$  causes phase separation of the two components and an upward shift in the transition temperature, while addition of higher concentrations of  $\text{Ca}^{2+}$  results in very broad and complex heat capacity profiles. These calorimetric studies indicate a very complex interaction between  $\text{Ca}^{2+}$  and DMPS and DMPS-DPPC mixtures.

**T-AM-Po8** CHARACTERIZATION OF THE SUB-TRANSITION OF HYDRATED DIPALMITOYL-PHOSPHATIDYLCHOLINE BILAYERS: X-RAY DIFFRACTION STUDY M.J. Ruocco and G.G. Shipley, Biophysics Institute, Depts. of Med. and Biochem., Boston Univ. Schl. of Med., Boston, Mass.

The structural changes accompanying the recently described sub-transition of hydrated dipalmitoyl phosphatidylcholine (Chen, S.C., Sturtevant, J.M., and Gaffney, B.J. (1980) *Proc. Nat. Acad. Sci. USA* 77, 5060-5063) have been defined using x-ray diffraction methods. Following prolonged storage at -4°C the usual  $\text{L}\beta'$  gel form of hydrated dipalmitoyl phosphatidylcholine (DPPC) is converted into a more ordered stable "crystal" form. The bilayer periodicity is 59.1 Å and the most striking feature is the presence of a number of x-ray reflections in the wide angle region. The most prominent of these are a sharp reflection at  $1/4.4 \text{ Å}^{-1}$  and a broader reflection at  $1/3.9 \text{ Å}^{-1}$ . This diffraction pattern is indicative of more ordered molecular and hydrocarbon chain packing modes in this low temperature "crystal" bilayer form. At the sub-transition ( $T_{\text{sub}} = 15 - 20^\circ\text{C}$ ) an increase in the bilayer periodicity occurs ( $d = 63.6 \text{ Å}$ ) and a strong reflection at  $\sim 1/4.2 \text{ Å}^{-1}$  with a shoulder at  $\sim 1/4.1 \text{ Å}^{-1}$  is observed. This diffraction pattern is identical to that of the bilayer gel ( $\text{L}\beta'$ ) form of hydrated DPPC. Thus, the sub-transition corresponds to a bilayer "crystal"  $\rightarrow$  bilayer  $\text{L}\beta'$  gel structural rearrangement accompanied by a decrease in the lateral hydrocarbon chain interactions. Differential scanning calorimetry and x-ray diffraction show that on further heating the usual structural changes  $\text{L}\beta' \rightarrow \text{P}\beta'$  and  $\text{P}\beta' \rightarrow \text{L}\alpha$  occur at the pre- and main transitions,  $\sim 35^\circ\text{C}$  and  $41^\circ\text{C}$ , respectively.

**T-AM-Po9** PHASE BEHAVIOR OF LARGE, UNILAMELLAR VESICLES PREPARED FROM SYNTHETIC PHOSPHATIDYLCHOLINES. R.A. Parente, B.R. Lentz, M. Hoehli, Biochem. & Anat. Depts., UNC, Chapel Hill, NC 27514.

Dimyristoyl, dipentadecanoyl, and dipalmitoyl phosphatidylcholine large, unilamellar vesicles (LUV's) (800-1000 Å diam.) were prepared by dilution of octyl glucoside-lipid mixtures with subsequent dialysis to less than .03 mole % detergent. Dialysates were fractionated by differential sedimentation and filtration. Vesicles were virtually free of oligolamellar contamination as determined by negative staining and freeze fracture electron microscopy. The phase behavior of these vesicles has been studied by differential scanning calorimetry, fluorescence depolarization of membrane associated 1,6-diphenyl-1,3,5-hexatriene, and freeze fracture electron microscopy. We have also investigated the phase behavior of huge, unilamellar vesicles (HUV's) (10,000-15,000 Å diam.) prepared by dialysis of sodium deoxycholate from solubilized lipids. From calorimetric and fluorometric measurements the pre- and main phase transitions of the two types of unilamellar vesicle populations were similar to those of large, multilamellar vesicles (LMV's). Significant differences were that the unilamellar vesicle transitions were broader and involved slightly larger enthalpy changes when compared with LMV's. Freeze fracture electron micrographs revealed a weakly banded fracture face morphology in HUV's below their main phase transition ( $T_m$ ) similar to- but less distinct than- that observed in LMV's in the same temperature range. No banding was observed at similar temperatures in LUV's, even though the pre-transition was seen calorimetrically. Instead, LUV's displayed faceted fracture faces below their  $T_m$ . These results demonstrate that the banded  $\text{P}\beta'$  phase in synthetic phosphatidylcholines does not require the bilayer juxtaposition found in LMV's. Also LUV's can undergo a pre-transition to a faceted phase that is probably analogous to the banded  $\text{P}\beta'$  phase. Work supported by NSF PPM79-22733.

**T-AM-Po10 PHASE BEHAVIOR OF MIXED PHOSPHATIDYLGLYCEROL-PHOSPHATIDYLCHOLINE MULTILAMELLAR AND UNILAMELLAR VESICLES;** B.R.Lentz, D.R.Alford, M.Hoechli, Biochem.& Anat.Depts., UNC,Chapel Hill,NC 27514.

The phase behavior of dipentadecanoylphosphatidylglycerol (DC<sub>15</sub>PG)/dimyristoylphosphatidylcholine (DMPC) mixtures has been studied in small, unilamellar vesicles and large, multilamellar vesicles. We have used the steady-state fluorescence polarization of DPH and high-sensitivity differential scanning calorimetry to detect temperature-induced changes in membrane structure. Electron microscopy has demonstrated different fracture face morphologies for large, multilamellar vesicles depending on their compositions and the temperatures from which they were "jet-frozen". These data have been interpreted in terms of proposed phase diagrams, whose shapes have led us to conclude that DMPC and DC<sub>15</sub>PG mix freely at all ratios in ordered phases but in the fluid phase only at less than 50 mol % DC<sub>15</sub>PG. In addition, small vesicles containing greater than 50 mol % DC<sub>15</sub>PG demonstrated hysteresis in their order-to-disorder phase transition. Irreversible changes in membrane structure can account only in part for the observed hysteresis, making it necessary to postulate the existence of a metastable gel or liquidus phase. Finally, the anisotropy of DPH fluorescence was found to be invariant with DC<sub>15</sub>PG content at temperatures just above the liquidus phase line in small vesicles. This demonstrated that inclusion of negatively-charged phosphatidylglycerol does not affect the order within the acyl chain region of the bilayer.

Supported by NSF PCM79-22733 and USPHS HL 22771. BRL is an Established Investigator of the American Heart Association.

**T-AM-Po11 A STUDY OF THE PHASE CHARACTERISTICS AND INTERACTIVE FORCES OF DIOLEOYLPHOSPHATIDYLCHOLINE-CEREBROSIDE MIXTURES.** J.M. Collins and L.J. Lis, Department of Physics, Illinois Institute of Technology, Chicago, Illinois 60616.

We have used x-ray diffraction to study the phase characteristics of dioleoylphosphatidylcholine (DOPC)-cerebroside mixtures in ionic solutions. It was found that cerebroside bilayers show minimal swelling in CaCl<sub>2</sub> and NaCl at pH>7. The application of the osmotic force technique of Rand and Parsegian (Biophys. J. 18 (1977) 209-230) on mixtures of DOPC-cerebrosides with molar ratios of 1:1, 3:1, 10:1, and 30:1 in CaCl<sub>2</sub> and NaCl solutions provided information about both the phases present and the forces between bilayers. Preliminary x-ray diffraction results show no phase separation of DOPC and cerebroside in these mixtures. Only one lamellar phase was observed in all cases. In addition, bilayer swelling appears limited to 10-15 Å in all cases. This result indicates that cerebroside acts to stabilize the bilayer phase while providing a large attractive force between bilayers.

**T-AM-Po12 POISSON-BOLTZMANN ANALYSIS OF LIPID BILAYERS AND APPLICATIONS TO ORDER-DISORDER PHASE TRANSITIONS,** Laura L. Unger, Charles F. Anderson, M. Thomas Record, Jr. (Intr. by Paul Kaesberg), Department of Chemistry, University of Wisconsin, Madison, Wisconsin 53706.

The interaction of simple electrolytes and protons with phospholipid bilayers depends upon the bilayer surface charge density. Conformational transitions and ligand binding interactions which alter this charge density are affected by the concentrations of protons and electrolyte ions. We have interpreted these effects using methods analogous to those previously employed to interpret electrostatic effects on phase transitions and ligand binding of DNA. The planar, nonlinearized Poisson-Boltzmann equation is solved in the limit of excess added symmetric salt using a novel approach which emphasizes the significance of the parameter  $\Lambda = \alpha |\sigma| / 2\pi e / \epsilon \kappa T$ , where  $\alpha \sigma$  is the planar surface charge density after specific binding of counterions, and  $\kappa$  is the Debye screening parameter. Complete expressions for thermodynamic quantities including the thermodynamic degree of counterion dissociation and the excess electrostatic free energy as a function of  $\Lambda$  are derived using the relationships of Marcus (J. Chem. Phys. 23 (1955) 1057-1068). The surface concentration of counterions (CIV) is found to be governed by the value of  $\Lambda$ ; the CIV is independent of salt concentration and remains finite in the limit of infinite dilution for  $\Lambda^2 \gg 1$ . We have applied this analysis to data on the salt and pH dependence of order-disorder phase transitions of methylphosphatidic acid bilayers, obtaining satisfactory agreement with the experimental data of Träuble et al. (Biophys. J. 4 (76) 319-342), including the observed linearity of the transition temperature with  $[\text{NaCl}]^{1/2}$  over a wide range of pH and salt and the magnitude of this slope.

**T-AM-Po13** CHARACTERISTICS OF A  $\text{Ca}^{++}$ -DEPENDENT  $\text{K}^+$  CONDUCTANCE RECONSTITUTED IN LIPID BILAYER MEMBRANES. Cecilia Vergara, Dept. Physiol. & Biophys., Harvard Medical School, Boston, MA 02115.

A  $\text{Ca}^{++}$ -activated  $\text{K}^+$  channel was found when purified transverse-tubule (TT) membrane vesicles from rabbit skeletal muscle were incorporated into planar lipid bilayers. TT vesicles were made according to Roseblatt et al. (*JBC* 256:8140, 1981). Lipid bilayers were formed across two compartments of identical composition (.1 M KCl, 1 mM  $\text{Ca}^{++}$ , 10 mM Mops-Tris, pH 7). Addition of TT vesicles to one of the aqueous solutions bathing the bilayer (*cis* side) causes a stepwise increase in membrane conductance, indicative of the incorporation of individual channels into the membrane. This conductance is both voltage and  $\text{Ca}^{++}$  dependent. At +50 mV (*cis* side positive), the concentration of  $\text{Ca}^{++}$  required for half maximal activation of the conductance is  $3.5 \times 10^{-5}$  M.

From single-channel recordings, we found that the channel presents three states: one open and two closed states. In phosphatidylethanolamine-phosphatidylserine membranes, the single channel conductance is 230 pS and is independent of voltage and  $[\text{Ca}^{++}]$ . However, the time spent in the open state is modified by voltage and  $\text{Ca}^{++}$ .  $\text{Ca}^{++}$  activates this conductance only from the *cis* side.  $\text{Mg}^{++}$ ,  $\text{Ba}^{++}$  or  $\text{Cd}^{++}$  cannot replace  $\text{Ca}^{++}$  on its activating role. Tetraethylammonium (TEA) addition to the *trans* side blocks this conductance ~30 times more effectively than addition to the *cis* side. The large channel conductance, the sidedness of action of  $\text{Ca}^{++}$  and TEA, and the voltage dependence of this conductance reflect a channel "polarity" that is in agreement with what has been described for other  $\text{Ca}^{++}$ -activated  $\text{K}^+$  conductances in biological membranes.

This work was supported by NIH grant GM-25277.

**T-AM-Po14** THERMODYNAMICS OF INTERACTION OF PHOSPHOLIPIDS WITH RETINALS. Pierre Tancrede, S. Robert, L. Parent and R.M. Leblanc, University of Québec, Photophysics Research Centre, Trois-Rivières (Québec), Canada G9A 5H7.

The surface pressure isotherms of mixed monolayers of some phospholipids with 11-*cis* and all-*trans* retinal have been measured on a phosphate buffer ( $10^{-3}$  M, pH 7.2) at  $20.5 \pm 0.5^\circ \text{C}$  at the air-water interface. The following mixtures, covering the whole range of mole fractions, were studied: dioleoyl-1-phosphatidylcholine (PC(18:1)) with all-*trans* retinal and 11-*cis* retinal, distearoyl-1-phosphatidylethanolamine (PE(18:0)) and phosphatidylethanolamine extracted from bovine disk membranes (PE(ROS)) with all-*trans* retinal. The results for the four series of mixtures have been analyzed in terms of the surface phase rule and the additivity rule. Furthermore, the excess free energies of mixing have been calculated from the surface pressure isotherms of the mixtures and the pure components. It is shown that 11-*cis* and all-*trans* retinal have about the same thermodynamics of interaction with PC(18:1), the concentration dependence of the negative excess free energy of interactions being symmetrical with respect to the mole fraction. However, with PE(ROS) or PE(18:0) the concentration dependence assumes an S-shape, intercepting the mole fraction axis at about 0.50. These results are analyzed in terms of a Schiff-base formation between the aldehyde group of the retinal molecules and the amino group of PE. The possible consequences of this difference in behaviour between PE and PC with respect to the retinal molecules are discussed, particularly in relation with the ultrastructure of the disk membrane and its function.

**T-AM-Po15 TIME-RESOLUTION OF SPECTRA ASSOCIATED WITH DIFFERENTLY ROTATING FLUOROPHORES: DPH IN LIPID BILAYERS.** Jay R. Knutson, Lesley Davenport and Ludwig Brand, The Johns Hopkins Univ., Balt., MD 21218.

The fluorescence emission anisotropy of the hydrophobic 'microviscosity' probe DPH is known to decay toward a non-zero asymptote ( $r_\infty$ ) in lipid bilayers. This 'persistent' anisotropy has been reported for other fluorophores imbedded in bilayers, and numerous theories explain  $r_\infty$  in terms of hindered rotation. Most of these models assume rotational homogeneity; i.e., that  $r_\infty$  does not arise from a distinct 'immobilized' subpopulation of probe. This assumption has been supported by the inability to link total intensity decay rates with specific anisotropy decay terms. Thus, if there is a distinct 'immobilizing environment,' it is not revealed by an obvious lifetime change.

We have developed a new tool for studying microheterogeneity of probe location. Nanosecond Time-Resolved Emission Spectroscopy has been extended to polarized difference spectra. By combining spectra taken through relatively late electronic 'time windows' (after pulsed excitation), a spectrum associated with 'immobile' probe molecules can be computed. If this spectrum differs from the total spectrum, then rotational heterogeneity is indicated. Further, such a spectrum can yield information regarding the character of the heterogeneous sites.

As a test, a known heterogeneous system (DPH imbedded in two different lipid vesicle types, DML and DPL, prior to mixing) was studied. At 29°C, DPH within pure DML vesicles rotates rapidly, with a small  $r_\infty$ ; while DPH in DPL vesicles is strongly hindered, with a large resulting  $r_\infty$ . Spectra for DPH imbedded in the separate lipids have small but significant differences, and the spectrum in the mixture lies between these characteristic component spectra. The spectrum extracted for 'immobilized' probes in the mixture resembles the DPL spectrum, as might be expected. The application of this technique to other rotationally heterogeneous systems will be described, along with the theoretical basis for time, phase, and lifetime resolution of such spectra. (Supported by USPHS GM11632. JRK is a fellow of the Pharmaceutical Manufacturers' Association Foundation).

**T-AM-Po16 RAMAN SPECTROSCOPIC STUDIES OF PHOSPHOLIPID POLYMORPHISM: CHARACTERIZATION OF DIOLEOYL AND 1-PALMITOYL-2-OLEOYL PHOSPHATIDYL ETHANOLAMINE DISPERSIONS.** Jeffrey R. Lapidés and Ira W. Levin, Laboratory of Chemical Physics, NIADDK, NIH, Bethesda, Maryland 20205.

Both natural and synthetic unsaturated phosphatidyl ethanolamine (PE) dispersions have been observed to adopt non-bilayer structures at temperatures above the gel  $\leftrightarrow$  liquid crystalline phase transition.<sup>1</sup> A variety of techniques have been employed, including x-ray diffraction, <sup>31</sup>P- and <sup>2</sup>H-NMR, EPR and infrared spectroscopies, freeze fracture electron microscopy and calorimetry. In the present study the vibrational Raman spectra of dioleoyl PE and 1-palmitoyl-2-oleoyl PE lipid dispersions were obtained as a function of temperature to ascertain specifically the hydrocarbon interchain disorder. Total integrated intensities of several bands, as well as appropriate intensity ratios were used to monitor lipid interactions. These vibrational transitions include the acyl chain CH<sub>2</sub> deformation modes (1440 cm<sup>-1</sup>), the CH<sub>2</sub> twisting modes (1296 cm<sup>-1</sup>) and the double bond C-H in-plane wagging mode (1275 cm<sup>-1</sup>). All of these vibrational probes suggest the occurrence of, at least, two distinct physical structures at temperatures above the gel  $\leftrightarrow$  liquid crystalline phase transition. Our differential scanning calorimetry partially confirms the Raman observations. The additional structures may correspond to the non-bilayer arrangements observed by <sup>31</sup>P-NMR and freeze fracture studies in other PE systems.<sup>2</sup> One order-disorder phase transition determined by the Raman spectroscopic parameters is tentatively correlated with the formation of the hexagonal II phase. Because of the sensitivity of the Raman spectroscopic technique additional lipid polymorphic structures cannot be ruled out at this time.

<sup>1</sup>See, for example, Cullis, P. R., et al. (1980) Can. J. Biochem. 58, 1091-1100.

<sup>2</sup>Hui, S. W., et al. (1981) Arch. Biochem. Biophys. 207, 227-240.

**T-AM-Po17 EFFECTS OF POLYMYXIN-PHOSPHOLIPID INTERACTIONS ON BILAYER ORGANIZATION DETERMINED BY RAMAN SPECTROSCOPY.** Ernest Mushayakarara and Ira W. Levin, Laboratory of Chemical Physics, NIADDK, National Institutes of Health, Bethesda, Maryland 20205.

For assessing the binding properties of polymyxin, a cyclic polycationic polypeptide antibiotic containing a branched acyl side chain, the vibrational Raman spectra of DMPC (1,2-dimyristoyl phosphatidylcholine), 1,3-DPPC (1,3-dipalmitoyl phosphatidylcholine), DMPA (1,2-dimyristoyl phosphatidic acid), and DPPG (1,2-dipalmitoyl phosphatidylglycerol) bilayers were examined for a range of lipid:peptide mole fractions. Temperature profiles were constructed using the peak height intensity ratios I<sub>1088</sub>/I<sub>1125</sub> (C-C stretching mode region) and I<sub>2940</sub>/I<sub>2885</sub> (C-H stretching mode region) for reflecting changes in the hydrocarbon chain intramolecular (trans/gauche) and lattice intermolecular disorder parameters, respectively. For example, for DMPC bilayers containing the antibiotic the temperature profiles determined from the C-H stretching region parameters indicate a broadening of the phase transition with an increase in T<sub>c</sub> by ~2.5-3.0°C. On increasing the peptide concentrations, the gel state disorder increases, relative to pure DMPC bilayers; while the liquid crystalline order increases. Temperature profiles based upon the intramolecular C-C stretching mode intensities reflect the same general conclusions noted for the intermolecular parameters, except that the gel state trans/gauche isomerization ratios are not significantly altered for increasing peptide mole fractions. For the temperature profile reflecting the 10:1 lipid:peptide mole ratio, however, two order-disorder transitions are observed at 27° and 38°C. The second transition is associated with the disordering of a polymyxin complex in which 2-3 lipid molecules are bound to the cluster.

**T-AM-Po18** IONIZATION BEHAVIOR OF AQUEOUS CARBOXYLIC ACIDS STUDIED BY  $^{13}\text{C}$  NMR SPECTROSCOPY.

David P. Cistola, Donald M. Small, and James A. Hamilton

Biophysics Institute, Boston University School of Medicine, Boston, MA 02118

As a basis for understanding the complex phase behavior of free fatty acids in lipid systems, we have studied the ionization behavior of short-chain water-miscible carboxylic acids (acetic, propionic, and butyric) and slightly water-soluble medium-chain acids (valeric and octanoic). Dilute ( $\leq 4\%$  w/v) aqueous solutions of each acid were titrated with KOH, and  $^{13}\text{C}$  NMR spectra at 50.3 MHz were recorded at intervals along the titration curve. Because of the very low solubility of octanoic acid, 90% isotopically enriched  $[1-^{13}\text{C}]$  octanoic acid was used. The chemical shift ( $\delta$ ) of each carbon resonance increased linearly with added equivalents of base up to the equivalence point, after which no change in  $\delta$  occurred. The magnitude of the  $\delta$  difference between the ionized and unionized forms of each acid ("titration shift") was largest for the carboxyl resonance and decreased for each successive carbon away from the carboxyl. Plots of  $\delta$  for the carboxyl,  $\alpha$ , or  $\beta$  carbon resonances as a function of pH were sigmoidal and yielded  $\text{pK}_a$  values which agreed closely with values obtained by potentiometric titration.

Linewidths ( $\nu_{1/2}$ ) for all resonances of the water-miscible acids were narrow ( $< 3$  Hz) and were unaffected by pH changes. However, the  $\nu_{1/2}$ 's for the carboxyl resonance of valeric acid and octanoic acid and the  $\alpha$  carbon resonance of valeric acid were narrow ( $< 3$  Hz) at low and high pH values but markedly broader (up to 3-fold) at pH values near the  $\text{pK}_a$  of each acid. This is explained by the formation of lamellar aggregates of acid-soap units which restrict the motions of carbon atoms in the carboxyl and  $\alpha$  carbon region.

**T-AM-Po19** RAMAN SPECTROSCOPIC STUDIES OF SATURATED SYMMETRIC-CHAIN PHOSPHOLIPIDS: COMPARISON BETWEEN MICELLAR AND LAMELLAR STRUCTURES. C. Huang,<sup>†</sup> J. Lapidus and I. W. Levin,

Laboratory of Chemical Physics, NIADDK, National Institutes of Health, Bethesda, Maryland 20205.

The conformational order and disorder of phospholipid dispersions of an homologous series of saturated symmetric phosphatidylcholines (PCs), such as diC<sub>6</sub>, diC<sub>8</sub>, diC<sub>10</sub>, diC<sub>12</sub>, diC<sub>14</sub>, diC<sub>16</sub>, diC<sub>18</sub> and diC<sub>20</sub> in excess water are investigated as a function of temperature by vibrational Raman spectroscopy. Both the intrachain and the interchain order/disorder parameters, obtained from the 1000-1150  $\text{cm}^{-1}$  C-C and 2800-3100  $\text{cm}^{-1}$  C-H stretching mode regions, respectively, are compared for the various phospholipid systems. The hydrocarbon chains of symmetric PCs with shorter chains are highly disordered; spectral characteristics of the lamellar gel  $\leftrightarrow$  liquid crystalline phase transition are observed only for dispersions of saturated symmetric PCs with longer chains. Molecular interpretations which may explain the spectral differences will be discussed. Raman spectra of lysoPC and sodium dodecylsulfate micelles will also be presented. <sup>†</sup>On sabbatical leave from the Department of Biochemistry, University of Virginia School of Medicine.

**T-AM-Po20** LIFETIME HETEROGENEITY STUDIES LATERAL PHASE SEPARATION IN LIPID BILAYERS. W. J. Pjura and A. M. Kleinfeld, Biophysical Laboratory, Harvard Medical School, Boston, MA 02115

To characterize lateral phase separation in membranes, we have measured the fluorescence decay of 1,3 diphenylhexatriene (DPH) in lipid bilayers. Multilamellar liposomes were prepared from egg phosphatidylcholine (PC), dipalmitoyl PC (DPPC), dimyristoyl PC (DMPC), distearoyl PC (DSPC) and mixtures of these with cholesterol. DPH was added and the fluorescence decay was measured using the phase-modulation technique at 6, 18 and 30 MHz. The measured phase and modulation lifetimes were analyzed using a two component fit to determine the respective fractional intensities ( $\alpha_i$ ) and lifetimes (ns.) ( $\tau_i$ ). In single component systems measured at several temperatures we find that the decay is homogeneous above or below the main phase transition with  $\tau = 9.7$  and 8.0 for DSPC and DMPC, respectively, at 35°C. We find that very close to the phase transition, the solution is unstable and is generally consistent with heterogeneity. Mixtures of phospholipid and 0, 10, 20, 30 and 40 mole % cholesterol were measured at several temperatures. All mixtures exhibited the same behavior. At temperatures above  $T_m$  the lifetime increased with increasing cholesterol up to 20 mole % and was constant thereafter; at temperatures below  $T_m$  with the addition of up to 20 mole % cholesterol the lifetime decreased and was constant thereafter. In mixtures of DSPC/DMPC, either 1/1 or 3/1, the decay at 35°C was heterogeneous and the component intensities and lifetimes were  $\alpha_1 = 0.33$ ,  $\tau_1 = 12.0$ ,  $\alpha_2 = 0.67$ ,  $\tau_2 = 7.4$  and  $\alpha_1 = 0.76$ ,  $\tau_1 = 10.5$ ,  $\alpha_2 = 0.24$ ,  $\tau_2 = 5.5$ , respectively. These results suggest that the decay heterogeneity correctly reflects the gel/fluid mix. Furthermore, since the  $\tau_2$  is shorter than observed in any single component system the decay is probably best described in terms of 3 components. Work supported by grant GM-26350 NIH and JRFA-15 Am. Can. Soc.

**T-AM-Po21** AN OXYGEN TRANSPORT PARAMETER IN MEMBRANES AS DEDUCED BY SATURATION RECOVERY MEASUREMENTS OF SPIN-LATTICE RELAXATION TIME OF SPIN LABELS. Akihiro Kusumi, Witold K. Subczynski and James S. Hyde. National Biomedical ESR Center, The Medical College of Wisconsin, Milwaukee, WI. 53226.

Spin-lattice relaxation time ( $T_1$ ) measurements of nitroxide radical spin labels in membranes have been made using the saturation-recovery technique. Stearic acid and sterol-type labels were used as probes of dimyristoylphosphatidylcholine (DMPC) liposomes from 0 to 36°C. In the absence of oxygen, the range of variation of  $T_1$  over all samples and conditions is about a factor of 3. Heisenberg exchange between oxygen and spin labels is an effective  $T_1$  mechanism for the spin labels. The full range of variation of  $T_1$  in the presence of air is about a factor of 100. It is suggested that the oxygen transport parameter  $W = T_1^{-1}(\text{air}) - T_1^{-1}(\text{N}_2)$  is a useful new monitor of membrane fluidity that reports on translational diffusion of small molecules. The values of  $W$  change at the pre- and main phase transitions and vary in complex ways. Arguments are advanced that the data are indicative of anisotropic translational diffusion of oxygen. (Supported by NIH grants GM-27665, GM-22923, and RR-01008).

**T-AM-Po22** A COMPARISON OF ESTER- AND ETHER-LINKED LIPIDS IN A  $^{14}\text{N}$  NMR STUDY OF DPPC ANALOGS. David J. Siminovich and Kenneth R. Jeffrey, Univ. of Guelph, Guelph, Ontario, Canada N1G 2W1.

Through the use of synthetic analogs of DPPC, we have modulated the dynamical structure of the polar headgroup. This modulation was accomplished by changing the  $\text{PO}_4^-$  to  $\text{N}^+(\text{CH}_3)_3$  distance and/or substituting alkyl ether linkages for the corresponding diester linkages to the 16:0/16:0 hydrocarbon chains. Previous  $^{31}\text{P}$ ,  $^{13}\text{C}$  and  $^{14}\text{N}$  NMR studies suggest that each headgroup has its own characteristic set of NMR spectroscopic parameters which are independent of the length and degree of unsaturation of the hydrocarbon chains. Do alterations in bonding at the glycerol backbone, which serves as an anchor point for both the hydrocarbon chains and the headgroup, also exert no influence on the dynamical structure of the headgroup? We present  $^{14}\text{N}$  NMR evidence for a change in the orientational order of the headgroup as a direct result of replacing diester linkages with diether. In the case of the phosphatidylcholine (PC) headgroup, the  $^{14}\text{N}$  quadrupolar splittings in diether-PC are 20% larger than those of its diester counterpart, while in the case of the phosphoryl-N,N,N-trimethylhexanolamine (PN6) headgroup ( $\text{PO}_4^--(\text{CH}_2)_6-\text{N}^+(\text{CH}_3)_3$ ), the splittings of diether-PN6 are double those of its diester counterpart. For ester- or ether-linked lipids, the splittings from lipids with a PN6 headgroup are greatly reduced in comparison to those from lipids with a PC headgroup. Although  $^{31}\text{P}$  NMR spectra of these analogs show a substantial reduction in the chemical shift anisotropy (CSA) when the headgroup is changed from PC to PN6, the values of the CSA are identical for lipids which have the same headgroup, irrespective of the type of linkage. [We gratefully acknowledge Dr. Hansjörg Eibl, of the Max Planck Institute at Göttingen, for supplying us with the PN6 lipids.]

**T-AM-Po23** FLUORESCENCE ENERGY TRANSFER IN TWO DIMENSIONS: AN EXACT NUMERICAL SOLUTION FOR RANDOM AND NONRANDOM DISTRIBUTIONS. Brian Snyder and Ernesto Freire, Dpts. of Biochemistry, University of Virginia, Charlottesville, VA 22908 and University of Tennessee, Knoxville, TN 37916

An exact determination of the functional dependence between lateral organization and quantum transfer efficiencies in two dimensions has been obtained using Forster's inductive resonance theory in conjunction with computer generated distribution ensembles. The generality of these results allows calculation of quenching and depolarization curves for both random and nonrandom distributions of fluorophores in membrane systems, and precise estimates of the effects of 1) membrane composition, 2) lateral distribution of protein and lipid molecules, 3) specific protein-protein associations, 4) excluded volume interactions, 5) molecular packing and lattice structure, 6) location of the fluorophores within the bilayer, 7) partitioning of the lipid probes, etc. The accuracy of these numerical calculations has been checked against the quenching curves obtained for those special cases in which exact analytical solutions exist and for all cases the results are identical. The present numerical method also permits evaluation of the validity of the approximate solutions existing in the literature. In this communication we present the general protocol for data analysis and specific applications to protein-lipid mixtures in which the donor groups are covalently linked to the protein molecules and the acceptor molecules are uniformly distributed within the lipid bilayer. The effects of protein aggregation, location of the donor group inside the protein and depth within the bilayer are examined. These studies indicate that fluorescence energy transfer measurements can be utilized to obtain organizational parameters of lipid and protein molecules within the membrane bilayer. (Supported by NIH grants GM-27244 and GM-26894)

**T-AM-Po24** CUBIC, HEXAGONAL, BILAYER PHASES AND LIPIDIC PARTICLES IN PHOSPHATIDYLETHANOLAMINE-PHOSPHATIDYLCHOLINE MIXTURES. S. W. Hui, T. P. Stewart and L. T. Boni, Roswell Park Memorial Institute, Buffalo, New York 14263.

Polymorphic phase transitions in mixtures of unsaturated phosphatidylethanolamines (PE) and egg phosphatidylcholines (PC) were monitored by x-ray diffraction,  $^{31}\text{P}$  NMR and freeze fracture electron microscopy. An inverted cubic ( $\text{C}_{\text{II}}$ ) phase in mixtures containing dilinoleoyl PE was observed by all three techniques. The  $\text{C}_{\text{II}}$  phase has a unit cell dimension of  $178\text{\AA}$ . Regularly spaced lipid particles (LIP) were seen during the transition from bilayer  $\text{L}_{\alpha}$  to  $\text{C}_{\text{II}}$  phases.  $^{31}\text{P}$  NMR spectra of the  $\text{C}_{\text{II}}$  phase consisted entirely of an isotropic resonance, consistent with isotropic molecular motion over the unit spheres. Mixtures containing dioleoyl PE showed  $\text{L}_{\alpha}$ -inverted hexagonal ( $\text{H}_{\text{II}}$ ) transition without the presence of LIP. No isotropic  $^{31}\text{P}$  NMR was detected during the transition. The  $\text{H}_{\text{II}}$  phase has a unit cell dimension of  $72\text{\AA}$ . We believe that lipidic particles as interlamellar attachment sites are instrumental in the  $\text{L}_{\alpha}$ - $\text{C}_{\text{II}}$  transition but are not a unique intermediate structure in the  $\text{L}_{\alpha}$ - $\text{H}_{\text{II}}$  transition. Models of intermediate stages of both phase transitions will be presented.

**T-AM-Po25** THE EFFECTS OF CHOLESTEROL ON LIPID BILAYER STRUCTURE IN EGG LECITHIN MULTILAYER VESICLES. Laura H. Chandler, George B. Zavoico, and Howard Kutchai. Department of Physiology & Biophysics Program, University of Virginia, Charlottesville, VA 22908

The effects of cholesterol on lipid bilayer structure in egg lecithin (PC) multi-lamellar vesicles (MLV) was studied with anthroyloxy-stearic acid (AS) probes. Probes with the anthroyloxy moiety located at the 2,7,9, and 12 carbons of the stearic acid were used. Changes in the polarization of fluorescence of the AS probes were produced when cholesterol was added to the egg PC. Changes in the fluorescence lifetimes of the AS probes were estimated with phase fluorometry. In the absence of cholesterol the fluorescence anisotropy ( $r$ ) decreases from the phospholipid headgroups toward the bilayer center. The profile of  $r$  is biphasic with a small decrease in  $r$  from 2AS to 7AS and larger decreases from 7AS to 9AS and from 9AS to 12AS. The addition of cholesterol (10,20,30,40, or 50 mole%) results in an increase in the  $r$  values of all the AS probes. The increases in  $r$  are roughly proportional to the cholesterol concentration for each probe. The largest increases in  $r$  are reported by 7AS. Somewhat smaller increases in  $r$  of 9AS were produced by adding cholesterol. The smallest increases in  $r$  with added cholesterol were reported by 2AS and 12AS. The results suggest that the structuring influence of cholesterol on the egg PC bilayer is more strongly felt near the middle of the acyl chain region of each monolayer than at the bilayer center or in the polar headgroup region. Studies are underway with MLV of dipalmitoyl PC, dioleoyl PC, and palmitoleyl PC to inquire into the influence of the acyl chain composition of the phospholipids on the ordering effects of cholesterol. (Supported by grant GM 24168 from the NIH.)

**T-AM-Po26** A MULTINUCLEAR NMR STUDY OF BACTERIAL LIPOPOLYSACCHARIDES: STRUCTURAL DETERMINATIONS AND THE INTERACTION OF DIVALENT CATIONS. S. Michael Strain, Stephen W. Fesik, and Ian M. Armitage, Department of Molecular Biophysics and Biochemistry, Yale University, New Haven, Connecticut 06510.

Lipopolysaccharides (LPS) from the outer membrane of gram-negative bacteria play an important role in the protective function against the action of surface active agents, enzymes, and drugs. This property is dependent upon the presence of  $\text{Ca}^{2+}$  and other multivalent cations which have been postulated to form ionic bridges between neighboring LPS molecules. Although the structure of LPS has been studied for many years, these studies have failed to clearly define the position and stereochemistry of all of the sugar linkages and the binding sites of the divalent cations. In this study, the structures of the lipopolysaccharides from Re mutants of *Escherichia coli* and *Salmonella typhimurium* were determined and compared using  $^{13}\text{C}$  and  $^{31}\text{P}$  NMR spectroscopy at high magnetic fields (4.7 and 11.7 T). Resonances have been assigned by comparison with model compounds and degradation products. Differences in the structure of LPS from the different strains of bacteria were found as well as heterogeneity in LPS obtained from the same bacterial source. This is the first reported  $^{13}\text{C}$ -NMR study of the lipid A and 3-deoxyoctulosonate moieties of intact Re mutant LPS. As a non-destructive technique NMR has permitted direct observation and characterization of naturally occurring structural variants of LPS and the tightly bound coisolating molecules which have often confused the results of previous degradative studies. The interaction of  $\text{Ca}^{2+}$ ,  $\text{Mg}^{2+}$  and  $\text{Cd}^{2+}$  with LPS has also been examined directly by NMR observation of the metal ion. In these investigations LPS was studied in bilayers composed of LPS alone and in the presence of SDS and phospholipids. (Supported by NIH Grants AM 18778 and NSF Grant PCM 77-18941).

**T-AM-Po27** RAMAN SPECTROSCOPY AND X-RAY DIFFRACTION STUDIES ON PHOSPHATIDYLETHANOLAMINE DISPERSIONS AS A FUNCTION OF TEMPERATURE AND  $\text{Ca}^{2+}$ . S.Y.K.Wen\*, J.W. Kauffman, J. M. Collins and L. J. Lis, Department of Materials Science and Engineering, Northwestern University, Evanston, Illinois 60201, and Department of Physics, Illinois Institute of Technology, Chicago, Illinois 60616.

Raman Spectroscopy and x-ray diffraction were used to study dimyristoylphosphatidylethanolamine (DMPE) dispersions as a function of heat treatment and  $\text{CaCl}_2$  concentration (0, 1, 10, and 50 mM), DMPE bilayers need to be heat treated before hydration will occur. However, even after heat treatment, DMPE dispersions in  $\text{CaCl}_2$  solutions do not show the dramatic ( $>150 \text{ \AA}$ ) swelling observed with the same acyl chain analog of phosphatidylcholine (Lis, et al (1981) *Biochemistry* **20**, 1761-1770), nor the change in the Raman phosphate stretch mode observed in dipalmitoylphosphatidylcholine dispersions (D.Hess, et al (1980) *Biophys. J.* **33**, 157a). These results indicate that saturated chain PE's provide a large attractive force between bilayers, and that there is little, if any, binding of  $\text{Ca}^{2+}$  to PE head groups.

**T-AM-Po28** A FLUORESCENT STUDY OF THE PERTURBING EFFECT OF n-ALKANOLS ON EGG- AND DIPALMITOYL-LECITHIN MULTI-LAMELLAR VESICLE STRUCTURE. G.B. Zavoico\*, H. Kutchai, and L. Chandler. Dept. of Physiology, Univ. of Virginia Med. School, Charlottesville, VA, 22908 and \*Dept. of Pharmacology, Univ. of Connecticut Health Ctr., Farmington, CT, 06032.

The fluorescence behavior of the lipid soluble probes 2-, 7-, and 12-(9-anthroyloxy) stearic acids, diphenylhexatriene, and 1-(4'-trimethylaminophenyl)-6-phenyl-hexa-1,3,5-triene partitioned into egg- and dipalmitoyl-lecithin multi-lamellar vesicles were studied by differential polarized phase fluorometry with and without the perturbing effects of pentanol, decanol or tetradecanol. The aim of this study is to examine the motional behavior of the probes (described by the limiting hindered anisotropy ( $r_{\infty}$ ) and the rotational rate (R)) when n-alkanols are partitioned into the membrane. Each of the probes used is localized to a distinct, but fairly well defined depth in the membrane. As n-alkanol alkyl chain length increases, the chain penetrates deeper into the membrane. Consequently, the effect of an alkanol on probe motion depends on the degree of overlap between the alkyl chain of the n-alkanol and the fluorescent moiety of the probe. The results support the following conclusions: 1) Since there is a "fluidity" gradient in membranes, a single probe cannot characterize membrane order; 2) The measured parameters that describe probe motion depend on probe structure, orientation and location in the membrane; 3) The same n-alkanol can simultaneously produce an ordering, disordering, or no effect at different depths of the membrane. This differential effect can only be detected by using different probes that localize at different depths in the membrane. (Supported by NIH Grant GM-24168).

**T-AM-Po29** THERMODYNAMICS OF INTERACTION OF PHOSPHOLIPIDS WITH RETINALS. Pierre Tancrede, S. Robert, L. Parent and R.M. Leblanc, University of Québec, Photophysics Research Centre, Trois-Rivières (Québec), Canada G9A 5H7.

The surface pressure isotherms of mixed monolayers of some phospholipids with 11-cis and all-trans retinal have been measured on a phosphate buffer ( $10^{-3} \text{ M}$ , pH 7.2) at  $20.5 \pm 0.5^\circ \text{ C}$  at the air-water interface. The following mixtures, covering the whole range of mole fractions, were studied: dioleoyl-1-phosphatidylcholine (PC(18:1)) with all-trans retinal and 11-cis retinal, distearyl-1-phosphatidylethanolamine (PE(18:0)) and phosphatidylethanolamine extracted from bovine disk membranes (PE(ROS)) with all-trans retinal. The results for the four series of mixtures have been analyzed in terms of the surface phase rule and the additivity rule. Furthermore, the excess free energies of mixing have been calculated from the surface pressure isotherms of the mixtures and the pure components. It is shown that 11-cis and all-trans retinal have about the same thermodynamics of interaction with PC(18:1), the concentration dependence of the negative excess free energy of interactions being symmetrical with respect to the mole fraction. However, with PE(ROS) or PE(18:0) the concentration dependence assumes an S-shape, intercepting the mole fraction axis at about 0.50. These results are analyzed in terms of a Schiff-base formation between the aldehyde group of the retinal molecules and the amino group of PE. The possible consequences of this difference in behaviour between PE and PC with respect to the retinal molecules are discussed, particularly in relation with the ultrastructure of the disk membrane and its function.



**T-AM-Po30 BILAYER DIELECTRIC STRUCTURE: AN ELECTRO-OPTICAL STUDY.** Ron Waldbillig, Department of Physiology and Biophysics, University of Texas Medical Branch, Galveston, TX. 77550 USA

The dielectric constant ( $\epsilon$ ) and thickness of planar bilayers of known composition has been studied using light reflectance (R) and specific capacitance methods. Monoolein bilayers formed with and without solvents were examined in electrolyte and nonelectrolyte solutions of known refractive index (n). Plots of  $\sqrt{R}$  vs  $n-\Delta$  were used to determine the bilayer optical thickness ( $d_o$ ) and refractive index ( $n_b$ ).

It is found that the bilayer optical thickness is greater than its electrical thickness ( $d_e$ ). For example for solvent enriched (10 mg/ml) monoolein/decane bilayers  $d_e = 46\text{\AA}$  whereas  $d_o$  is 62, 60, 54 and 52\AA in aqueous solutions of sucrose, glycerol,  $\text{CaCl}_2$  and  $\text{LiCl}$  respectively. Solvent depletion (225 mg/ml) decreases  $d_e$  to 36\AA while decreasing the  $d_o$  to 50, 48, 45 and 44\AA. The electro-optic difference is less for lens-free monoolein/squalene bilayers where  $d_e = 25\text{\AA}$  and the  $d_o$  values are 30, 33, 32 and 29\AA respectively. Solvent-free pure lipid bilayers from monoolein/triolein mixtures show  $d_e = 22\text{\AA}$  while  $d_o$  is 35, 32, 28 and 30\AA in the different aqueous phases. Thus electrolytes decrease  $d_o$  whereas solvents and nonelectrolytes increase  $d_o$ .

The bilayer dielectric constant was estimated from the relationship  $\epsilon = n_b^2$ . At optical frequencies the monoolein bilayer  $\epsilon$  ranges from 2.051 to 2.107 with decane; from 2.152 to 2.203 with squalene; and from 2.115 to 2.191 with triolein. It is found that  $\epsilon$  changes with the composition of both the oil and water phases. The role of 'thick' microlenses and lipid headgroup layers are considered in a model system.

Supported by NIH grant # GM 26980.

**T-AM-Po31 PHOTO-ELECTRIC EFFECTS FROM AROMATIC AMINO ACIDS IN BILAYER MEMBRANES.**

Rodolfo T. Arrieta<sup>@</sup>, Jay S. Huebner<sup>@</sup> and David B. Millar<sup>\*</sup>, @ University of North Florida, Jacksonville, FL 32216, and \* National Naval Medical Center, Bethesda, MD 20014.

Ultraviolet light flashes induced voltage transients across lipid bilayer membranes when aromatic amino acids (aa) were absorbed to one side of the membrane<sup>1</sup>. The photo-voltages varied with aa structure, aqueous solution salt concentration (sc), pH and oxygen partial pressure, and are attributed to the migration of electrically charged photo-chemical intermediates in the membrane following illumination. The fastest parts of the photo-voltage waveforms are believed to result from photo-ionization of sorbed aa. Variations in the photo-voltage amplitude with sc provided information on the aa sorption sites, a result previously reported with azo<sup>2</sup>, cyanine<sup>3</sup> and xanthene<sup>4</sup> dyes. Preliminary results also showed photo-voltages result from UV light and sorbed proteins; aldolase, chymotrypsinogen and ribonuclease<sup>1</sup>. The apparatus and procedures used, which will be described in the presentation, thus provide a convenient method and model systems for studying the effects of UV irradiation on the membrane components of biological systems.

Support from the Office of Naval Research/American Society for Engineering Education Summer Faculty Research Program, Naval Medical Research and Development work unit MF 58525015.0044 & National Institutes of Health grant GM 23250 is acknowledged.

1. J. S. Huebner, R. T. Arrieta and D. B. Millar, *Photochem. Photobiol.*, in press.
2. J. R. Duchek and J. S. Huebner, *Biophys. J.* **27** (1979) 317-321. 3. J. A. Baker, J. R. Duchek, R. L. Hooper, R. J. Koftan and J. S. Huebner, *Biochim. Biophys. Acta* **553** (1979) 1-10.
4. W. E. Varnadore, R. T. Arrieta, J. R. Duchek and J. S. Huebner, *J. Membrane Biol.*, in press.

**T-AM-Po32 CHANNELS FORMED BY THE KILLER TOXIN OF THE YEAST *PICHIA KLUYVERI*** by Bruce L. Kagan and Alan Finkelstein, Departments of Physiology and Biophysics, and Neuroscience, Albert Einstein College of Medicine, 1300 Morris Park Avenue, Bronx, N.Y. 10461.

The glycoprotein "killer toxins" of various yeast species are thought to act at the plasma membrane of sensitive cells. Physiologic effects reported include leakage of  $\text{K}^+$ , decrease of intracellular pH, depletion of cellular ATP, and inhibition of amino acid transport. We report here that partially purified preparations of killer toxin from *Pichia kluyveri* cause dramatic increases in the conductance of lipid bilayer membranes. These conductance increases result from the formation of ion-permeable channels large enough to account for the *in vivo* physiology of killer action. The channels are permeable to  $\text{K}^+$ ,  $\text{Na}^+$ ,  $\text{Ca}^{++}$  and  $\text{Cl}^-$ . A voltage is not needed to insert the channels into the membrane. The instantaneous and steady-state current-voltage curves are non-ohmic. The *in vivo* physiologic effects of certain channel forming bacterial toxins (colicins E1, K, Ia, etc.) are remarkably similar to the *in vivo* effects of killer toxin. We propose that the lethal action of killer toxin is also due to channel formation in the target cell membrane.

(We thank G.D. Vogels and E. Middelbeek for samples of *Pichia kluyveri* killer toxin. Supported by NIH grant 5T32GM7288.)

**T-AM-Po33** MULTIVALENT ANION EFFECTS ON THE ANION PORE OF MITOCHONDRIA. Eil  en C. Lynch and Meryl S. Rubin, Albert Einstein College of Medicine, Bronx, NY 10461.

VDAC, the voltage-dependent anion-selective channel from the outer mitochondrial membrane inserts into artificial planar bilayer membranes and exhibits a large unit channel conductance ( $\sim 500$  p-siemens) in 0.1 M symmetrical monovalent chloride salt solutions and an anion selectivity which depends on the cation identity (permeability of cation in the anion channel  $K > Na > Li > TEA$ ). In all monovalent chloride gradients permselectivity is a function of both salt concentration and gradient magnitude. When NaCl gradients were imposed across films of VDAC in diphytanoyl phosphatidylcholine, addition of mM  $Na_3ATP$  to the high activity NaCl side instantaneously decreased membrane conductance as measured by  $I=g(V-E)$ , while the fraction of current carried through the pore by  $Na^+$  increased. In identical gradient and pH (5.5-6.0) conditions  $Na_3citrate$  required 15-fold higher concentrations added to the high NaCl side to produce a corresponding decrease in reversal potential (a measure of permselectivity) but overall membrane conductance actually increased. Thus, 2.6 mM  $Na_3ATP$  decreased membrane conductance by 50% and reduced the  $Cl^-:Na^+$  selectivity ratio from 9.2 to 2.3, whereas 41 mM  $Na_3citrate$  decreased the  $Cl^-:Na^+$  permselectivity ratio from 6.0 to 2.3 as the conductance increased appropriately. Channels retained voltage dependence after addition of  $Na_3ATP$  or  $Na_3citrate$ . Our data indicate that in the anion-selective mitochondrial pore ATP decreases ion permselectivity and conductance in a different way from the permselectivity decrease imposed on the channel by citrate. In the artificial membrane, conductance and ion-permeability can be regulated by a specific channel-ATP interaction, but permselectivity itself may be altered by non-specific channel-screening in the presence of high concentrations of multivalent anions like citrate. Supported by NIH T32-GM 7288 (E.C.L.) and AM-18128 (M.S.R.).

**T-AM-Po34** HIGH AFFINITY CALCIUM BINDING TO GANGLIOSIDE IN PHOSPHOLIPID BILAYERS. P. Felgner, T.E. Thompson, J. Beach, Y. Barenholz and M. Wong, introduced by D. Kupke, Departments of Biochemistry and Physiology, University of Virginia, Charlottesville, VA 22908.

A sensitive calcium selective electrode was constructed following the design of G.H. Gold and J.I. Korenbrot (Proc. Natl. Acad. Sci. 77, 5557-5561 (1980)). The electrode exhibits 29 mV per decade change in  $Ca^{+2}$  concentration, down to  $< 1 \mu M$   $Ca^{+2}$  and can be used to monitor calcium concentrations in samples less than 0.25 ml volume. Using this electrode, free calcium concentrations were measured in samples containing dipalmitoyl phosphatidylcholine (DPPC) large unilamellar vesicles with and without purified gangliosides incorporated into them. It was determined by a simple Scatchard type analysis that at 22°C (below the phase transition of DPPC) and in the presence of 0.05 M KCl, calcium binds to ganglioside-containing vesicles with a stoichiometry of about 1 calcium molecule per every 2 sialic acid residues and with a dissociation constant of 0.1 mM. These results were confirmed by equilibrium dialysis using  $^{45}Ca$ . Mono, di and tri sialylated gangliosides show the same binding affinities and stoichiometries. Under these same conditions ganglioside micelles, as well as phospholipid vesicles without ganglioside bind calcium very weakly ( $K_d$ 's  $\gg 10$  mM). Upon raising the temperature of the sample, a phase transition temperature dependent release of calcium is observed. At 45°C the  $K_d$  is approximately 1 mM while the stoichiometry remains unchanged. Calcium binding to cell surface ganglioside may be important in modulating cell surface properties and the size of the extracellular pool of calcium in brain. (Supported by USPHS, NIH grants GM-14628 and GM-23573.)

**T-AM-Po35** THE EFFECTS OF CHOLERA TOXIN  $\pm$  RECEPTOR ON DIMYRISTOYLPHOSPHATIDYLCHOLINE (DMPC) LIPOSOME PERMEABILITY AS FUNCTIONS OF TEMPERATURE AND CHOLESTEROL CONTENT. W.V. Kraske and D.B. Mountcastle, Departments of Physics and Biochemistry, University of Maine, Orono, Maine 04469.

The release over 30 minutes of glucose from DMPC liposomes containing cholesterol and dicetyl phosphate was measured using a standard spectrophotometric glucose assay. Passive permeability, with and without the cholera toxin receptor ganglioside  $G_{M1}$ , and the measured cholera toxin induced permeability agree with the findings of others for 40 mol% cholesterol liposomes at room temperature.<sup>1</sup> Passive glucose permeability as a function of temperature for liposomes of 20 to 30 mol% cholesterol showed the characteristic maximum efflux near the lipid phase transition ( $T_m = 24^\circ C$ ), rather than the monotonic increase with temperature reported by Inoue.<sup>2</sup> The addition of 5 mol% ganglioside  $G_{M1}$  to the liposome preparation has only a small effect on the characteristic temperature profile of the passive glucose release. In 40 mol% cholesterol liposomes, cholera toxin (12mg/ml) increases the maximal glucose release over 30 minutes from 3% to ca. 10%, in agreement with Moss, et.al.<sup>1</sup> When the cholesterol level is reduced to 30 mol%, cholera toxin increases the maximal glucose release from 3% to 18-20%. These findings are consistent with the hypothesis that perturbation of the bilayer state caused by the multivalent toxin-receptor binding may allow local enhancement of the bilayer permeability. Thus the mechanism for membrane translocation of the toxin active sub-unit may be a local transient membrane phenomenon. (Supported by NIH grant # GM 28338, and UMO Faculty Research Awards).

1. J. Moss, P. Fishman, R. Richards, C. Alving, M. Vaughan, and R. Brady (1976) P.N.A.S. 73, 3480.
2. K. Inoue (1974) Biochim. Biophys. Acta 339, 390.

**T-AM-Po36**  $\text{SCN}^-$  AND HSCN TRANSPORT THROUGH LIPID BILAYER MEMBRANES: A MODEL FOR  $\text{SCN}^-$  INHIBITION OF GASTRIC ACID SECRETION. John Gutknecht and Anne Walter, Physiology Department, Duke University, and Duke Marine Laboratory, Beaufort, N.C. 28516.

Diffusion of thiocyanate ( $\text{SCN}^-$ ) and thiocyanic acid (HSCN) ( $\text{pK} = -1.8$ ) through lipid bilayer membranes was studied as a function of pH. Membranes were made of egg phosphatidylcholine or phosphatidylcholine plus cholesterol (1:1 mol ratio) dissolved in tetradecane. Tracer fluxes and electrical conductances were used to estimate the permeabilities to HSCN and  $\text{SCN}^-$ . Over the pH range 1.0 to 3.3 only HSCN crosses the membrane at a significant rate. The relation between the total  $\text{SCN}^-$  flux (J), concentrations and permeabilities is:  $1/J = 1/P_{\text{un}}^{\text{u}} ([\text{A}^-] + [\text{HA}]) + 1/P_{\text{m}}^{\text{m}} [\text{HA}]$ , where  $[\text{A}^-]$  and  $[\text{HA}]$  are the concentrations of  $\text{SCN}^-$  and HSCN,  $P_{\text{un}}^{\text{u}}$  is permeability coefficient of the unstirred layer, and  $P_{\text{m}}^{\text{m}}$  is the membrane permeability to HSCN. By fitting this equation to the data we find that  $P_{\text{m}}^{\text{m}} = 2.6 \text{ cm/sec}$  and  $P_{\text{un}}^{\text{u}} = 9.0 \times 10^{-4} \text{ cm/sec}$ . Conductance measurements indicate that  $\text{SCN}^-$  permeability is  $5 \times 10^{-9} \text{ cm/sec}$ . Addition of cholesterol to phosphatidylcholine (1:1 mol ratio) reduces  $P_{\text{m}}^{\text{m}}$  by a factor of 0.4.

$\text{SCN}^-$  is a potent inhibitor of acid secretion in gastric mucosa, but the mechanism of  $\text{SCN}^-$  action is unknown. Our results suggest that  $\text{SCN}^-$  acts by combining with  $\text{H}^+$  in the mucosal unstirred layer (secretory pits) and diffusing back into the cells as HSCN, thus dissipating the proton gradient across the secretory membrane. A similar mechanism of action is proposed for some other inhibitors of gastric acid secretion, e.g., nitrite ( $\text{NO}_2^-$ ), cyanate ( $\text{CNO}^-$ ) and  $\text{NH}_4^+$ .

Supported by NIH grants GM 28844 and ES 02289.

**T-AM-Po37** ACIDS AND BASES AS VERY SMALL NONELECTROLYTE PERMEANTS OF LIPID BILAYER MEMBRANES.

Anne Walter and John Gutknecht. Dept. Physiol., Duke Univ. Marine Laboratory, Beaufort, N.C. 28516.

Water permeability of lipid bilayer membranes appears to be anomalously high when compared to other nonelectrolyte solutes by correlating relative hydrophobicity with permeability coefficients. We hypothesized that the apparently high permeability of water is a function of its small size and not a function of its chemical characteristics (dipole moment, ability to form hydrogen bonds) or its presence in uniquely high concentrations (55 M). We established a correlation between the permeability coefficient (P) and hexadecane/water partition coefficient (Kp) for nonelectrolyte solutes with molecular weights (MW) from 50-300 and used this correlation to compare P's of solutes with MW less than 50. The small solutes included water, HCl, HF, methylamine and formic acid. P's were determined from tracer fluxes or net  $\text{H}^+$  fluxes across egg phosphatidylcholine-decane planar bilayer membranes. Kp's were determined for the unionized forms of the solutes using tracer or chemical methods to determine solute concentrations. The correlation between P and Kp for the larger solutes is described by the line,  $\log P = 1.0 + 1.0 \log Kp$  ( $r=0.98$ ). The observed P's for the small solutes are 4 to 10-fold higher than predicted by the regression line established for the larger solutes. The Kp's for the smaller solutes ranged from  $2.4 \times 10^{-6}$  (water) to  $6.0 \times 10^{-2}$  (HCl) indicating that "high" permeability is not a function of a solute's chemical nature but is a characteristic of small size. Higher permeabilities are predicted for very small solutes by the diffusion characteristics of liquid hydrocarbon solvents and polymers, and by the partition characteristics of the hydrocarbon core of the bilayer membrane. (Supported in part by NIH grant HL12157)

**T-AM-Po38** RATE OF TRANSFER OF SPHINGOMYELIN BETWEEN PHOSPHOLIPID BILAYERS. A. Frank, Y. Barenholz, D. Lichtenberg and T.E. Thompson, introduced by J. Ogilvie, Dept. of Biochemistry, University of Virginia, Charlottesville, VA 22908.

The rate of excimer/monomer decay of sphingomyelin, labelled with pyrene in the  $\omega$  position of the acyl chain, was used to determine the half-time of transfer of this molecule between unilamellar phospholipid vesicles. The half-time of transfer of this molecule from bilayers comprised of either sphingomyelin or 1-palmitoyl-2-oleyl phosphatidylcholine at  $20^\circ\text{C}$  was found to be greater than 7 days. At  $50^\circ\text{C}$  the rate of transfer of this molecule from either lipid was found to be about 12 hrs. These results have been confirmed by measuring the half-time of equilibration of  $[\text{3H}]$ -sphingomyelin in similar vesicle systems. The data strongly suggest that at  $20^\circ\text{C}$  in the concentration range of 5 mole % sphingomyelin in 1-palmitoyl-2-oleyl phosphatidylcholine bilayers, a sphingomyelin gel phase coexists with a liquid crystalline phase composed primarily of dioleyl phosphatidylcholine. (This work was supported by USPHS grants GM-14628, HL-17576 and GM-23573.

**T-AM-Po39** EOSIN Y-SENSITIZED PHOTODYNAMIC EFFECTS ON LIPOSOMES. J.E. Clark\* and G.E. Cohn, Physics Dept., Illinois Institute of Technology, Chicago, IL 60616.

Spin labeling ESR spectroscopy has been applied to study the modification of lipid bilayer properties by visible light irradiation of asolectin liposomes in the presence of molecular oxygen and the photosensitizing dye eosin Y. The spin labels 12NSme and 2N19 localized in the liposomal wall both before and after photodynamic irradiation. The probe 2N19 appeared to localize near the membrane surface and 12NSme near the membrane interior. Column chromatography indicated that eosin Y remained outside the liposomes following 180 minutes of photodynamic irradiation, indicating that any damage to the liposomes was sensitized either from the outside or at the membrane surface. Destruction of the liposomes was detected from changes in relative optical density for a variety of irradiation environments, but the maximum change occurred under photodynamic conditions. Significant changes in spin label rotational correlation times and hyperfine couplings occurred for photodynamic irradiation but not in the absence of eosin Y or molecular oxygen, indicating that the maximum loss of membrane integrity is due to photodynamic action. (Supported by Research Corporation Cottrell Research Grant No. 7250 and by U.S. Department of Energy Contract EY-76-02-2217). [Current Addresses: A.B. Dick Company, Advanced Development Center, Skokie, IL 60076 (JEC); Abbott Laboratories, D-93C, North Chicago, IL 60064 (GEC)].

**T-AM-Po40** PERMEABILITY OF BILAYERS COMPOSED OF PHOSPHOLIPID MIXTURES. Michael Singer, Dept. of Medicine, Queen's University, Kingston, Ontario, Canada. K7L 3N6

Liposomes composed of an equimolar binary mixture of phospholipids were formed from a series of saturated phosphatidylcholines (PC) and phosphatidylethanolamines (PE). Mixtures were chosen such that the two phospholipids differed in terms of head group alone, chain length alone, or head group plus chain length. Cation permeability, both with and without ionophores, was measured over a wide temperature range. The temperature region over which phase separation occurred for these lipid mixtures was determined either from known phase diagrams or changes in optical density. These vesicles display broad permeability maxima, the onset of which begin about 5 to 10° below the temperature at which phase separation occurs. For phospholipid mixtures with the same fatty acyl chain but different head groups (PC vs PE), the PC group "controls" permeability. For mixtures of PC's differing in chain length, the short chain lipid dominates the permeability pattern provided the chain lengths are sufficiently different. Lipids differing in both head group and chain length give rise to complex patterns. In liposomes composed of saturated phospholipids, permeability is determined by the structure and number of defects occurring at mismatch zones between different phases. The results of the present study are interpreted in terms of one or the other of the lipid components of the mixture specifically congregating at the defect regions and thus "regulating" permeability.

**T-AM-Po41** pH-SENSITIVE LIPOSOMES - IN VITRO STUDIES, Milton B. Yatvin, Theodore C. Cree, Inga-Mai Tegmo-Larsson, Jerry J. Gipp, Radiobiology Research Laboratory and Department of Human Oncology, University of Wisconsin, Madison, WI 53792.

We have previously described pH-sensitive liposomes which have potential clinical application in the treatment of cancer metastasis. The release of the ionic dye carboxyfluorescein (CF) from liposomes as a function of pH and temperature was followed in vitro. Those studies have been extended to compare the effect of pH on the release of a non-ionic dye, calcein. The release of calcein from liposomes composed of diheptadecanoylphosphatidylcholine; palmitoylhomocysteine (88:12; w/w) as a function of pH and temperature is qualitatively the same as that for CF in 25% calf serum. Similar results were obtained for the release of calcein in the absence of serum except that a greater release was observed. Dual radio-labeled liposomes composed of <sup>14</sup>C-labeled phospholipid and <sup>3</sup>H-labeled PHC were prepared and subjected to exclusion chromatography after being cycled from pH 7.4 to 6.0 then back to 7.4. Both radiolabels co-elute as a single peak (on both Sephadex-G-50 and Sepharose 4B) suggesting that the PHC remains associated with the liposome. Comparison of pH trigger mediated release of CF with pH dependent release of CF from phosphatidylcholine vesicles (Szoka et al, BBA 551, 295 (1979)) shows that PHC mediated release is three orders of magnitude greater than that obtained from a non-specific pH dependent release.

This work was supported by PHS grant No. 5T32 CA 09206CT and NIH grant No. GM 91846.

**T-AM-Po42** PROTON/HYDROXYL PERMEABILITY OF LIPOSOME MEMBRANES. D.W. Deamer, Dept. of Zoology, University of California, Davis CA, and J.W. Nichols, Dept. of Embryology, Carnegie Institute of Washington, Baltimore MD

There is a large variance in reported values of proton/hydroxyl permeability coefficients in liposomes, which range from  $10^{-4}$  to  $10^{-9}$  cm/sec. We have compared two liposome systems which produced extreme values, those of Nichols and Deamer (PNAS 77:2038, 1980) and Nozaki and Tanford (PNAS 78:4324, 1981). The former study prepared internally buffered liposomes (pH 7) in  $K_2SO_4$  by ether vaporization and used acid/base pulses to produce small pH gradients. The latter study prepared aspartate buffered liposomes (pH 4) in  $NaNO_3$  and NaCl by octyl glucoside dialysis and produced pH gradients by adjusting the external pH to near 7. Both methods estimated proton/hydroxyl permeability by measuring the decay kinetics of the pH gradients. In repeating the latter study, we found that: 1) Counterion flux limits proton/hydroxyl flux, since decay rates were significantly increased in the presence of valinomycin and  $K^+$ ; 2) It cannot be assumed that the major proton flux occurs in association with anions, because proton/hydroxyl flux is readily measured solutions of sulfate, a strongly dissociated anion; 3) Because of proton/hydroxyl flux in the initial period of decay, internal pH cannot be assumed to be that of the original buffer in calculating permeability coefficients. When we measured proton/hydroxyl permeability of octyl glucoside dialysis liposomes in  $K_2SO_4$  by the acid/base pulse method, permitting counterion flux with valinomycin, we obtain values in the range of  $10^{-4}$  cm/sec. We conclude that liposomes formed by octyl glucoside dialysis are similar to those prepared by ether vaporization in having an anomalously high proton/hydroxyl permeability.

**T-AM-Po43** MECHANISM OF THE SPONTANEOUS TRANSFER OF PHOSPHOLIPIDS. J.B. Massey, D. Hickson, S. She, A.M. Gotto, Jr., and H.J. Pownall. (Intr. by J.R. Brainard). Baylor College of Medicine and The Methodist Hospital, 6565 Fannin, Houston, Texas 77030.

The kinetics of transfer of fluorescent phospholipids (PL) between apolipoprotein-phospholipid recombinants was measured to establish the mechanism and to identify the rate controlling factors. Phosphatidylcholines (PC) were synthesized with 9-(3-pyrenyl)nonanoic acid in the SN-2 position and 12:0, 14:0, 16:0, 18:0, 18:1, or 18:2 fatty acids in the SN-1 position. Phosphatidylserine (PS), phosphatidylglycerol (PG), phosphatidylethanolamine (PE), phosphatidic acid (PA), and a diacylglycerol (DG), all of which were 1-myristoyl-2[9(3-pyrenyl)nonanoyl] glycerides, were also synthesized. The transfer of these lipids is a first order process which is independent of the acceptor concentration. The addition of a methylene unit to the acyl chains decreased the rate of transfer by a factor of 4 to 5, whereas the addition of a double bond increased the rate by a factor of 4 to 10. Changes in the polar headgroup had little effect on the rate with PE (slowest) having a halftime four times that of PC (fastest). DG transfer is 20 times slower than PC transfer. Activation energies ranged between 20 and 26 kcal/mole. The kinetic data are consistent with a mechanism in which these lipids transfer as monomers via the aqueous phase. The results suggest that the rate and activation energy for the spontaneous transfer of PLs can be predicted, to a first approximation, on the basis of their hydrophobic content, irrespective of the identity of the polar headgroup. (Supported by a Grant from the American Heart Association, Texas Affiliate, Inc. and by grants from The National Institutes of Health, HL26250 and HL17269.

**T-AM-Po44** KINETICS AND THERMODYNAMICS OF PAH TRANSFER: RELATION TO AQUEOUS CAVITY FORMATION.

Anne L. Plant. Baylor College of Medicine and The Methodist Hospital, Houston, TX 77030.

Pyrene, chrysene, triphenylene, 1,1'-binaphthyl, 2,2'-binaphthyl, 1,2-benzanthracene, 9-phenylanthracene, 3,4-benzophenanthrene, m-quaterphenyl and 1,3,5-triphenylbenzene are polycyclic aromatic hydrocarbons (PAH), each of which have 4 six-membered rings but differ in molecular surface areas. Transfer kinetics between single-walled 1-palmitoyl-2-oleoylphosphatidylcholine vesicles were studied to identify the relationship of transition state energetics and the aqueous cavity formed by rate-limiting desorption of PAH into the aqueous phase. Transfer was monitored by time dependent decreases in the fluorescence intensity of individual PAH when donor vesicles were mixed with a 10-fold excess of acceptor vesicles which contained only a non-exchangeable quencher, N(2,4-dinitrophenyl)-N,N-diocetylamine. In 40 mM Tris, pH 7.4, and 0.15 M NaCl, pyrene transferred with a halftime of 10 msec at 37°C; triphenylbenzene transferred with a halftime of 3.7 sec. Other PAH gave intermediate values. Molecular surface areas were estimated from CPK space-filling molecular models. Plots of surface areas vs transfer rates gave a strong linear correlation ( $r = 0.98$ ). Retention times on HPLC were negatively correlated with transfer rates ( $r = 0.94$ ) and directly correlated with estimated surface areas ( $r = 0.95$ ). The linear correlation of  $\langle G^* \rangle$ , calculated from activation energies and rate constants, and molecular surface areas supports the hypothesis that formation of the aqueous cavity required to accomodate each PAH is the determining factor in transfer (supported by Welch, ACS, EPA, USPHS).